

**OXIDATIVE STRESS MECHANISMS OF HYDROXYUREA INDUCED
DEVELOPMENTAL TOXICITY IN THE ORGANOGENESIS STAGE MOUSE
EMBRYO**

by

Ava Schlisser

Department of Pharmacology and Therapeutics

McGill University, Montreal

February, 2014

A thesis submitted to McGill University in partial fulfillment for the requirements of the degree
of Doctor of Philosophy

© Copyright by Ava Schlisser, 2014

ABSTRACT

Hydroxyurea was used as a model teratogen to investigate the role of oxidative stress and stress-response pathways in mediating drug teratogenicity. Hydroxyurea exposure during organogenesis induced fetal death and growth retardation, as well as external and skeletal malformations. Many of these malformations were concentrated in the caudal region, specifically affecting the hindlimbs, lumbosacral vertebrae, and tail. In utero exposure to hydroxyurea caused a depletion of glutathione, a major cellular antioxidant, and increased lipid peroxidation as assessed by the production of 4-hydroxynonenal protein adducts; interestingly, 4-hydroxynonenal protein adducts were enhanced within regions of high susceptibility to hydroxyurea-induced malformations. One of the major proteins modified by 4-hydroxynonenal adducts, glyceraldehyde-3-phosphate dehydrogenase (GAPDH), is involved in energy metabolism; the formation of 4-hydroxynonenal-GAPDH-protein adducts led to a decrease in the enzymatic activity of GAPDH and a reduction in lactate formation. Under non-stress conditions, GAPDH was found in the cytoplasm; however, GAPDH was translocated into the nucleus following hydroxyurea exposure. Pharmacological inhibition of the nuclear translocation of GAPDH with deprenyl led to an enhancement of malformations, specifically those of the hindlimbs, lumbosacral vertebrae, and tail, without further depleting glutathione. Thus, GAPDH plays a protective role in the nucleus following oxidative stress-induced insult.

In utero exposure to hydroxyurea led to a disruption in redox homeostasis in the embryo, oxidizing critical oxidoreductases, such as thioredoxin (TRX1) and GAPDH. The dysregulation in redox status stimulated the expression of nuclear factor (erythroid-derived 2)-like 2 (*Nrf2*) and its target gene peroxiredoxin 1 (*Prdx1*). Thioredoxin interacting protein (*Txnip*), an endogenous inhibitor of TRX1 was also upregulated. The major pathways activated following hydroxyurea exposure were apoptosis and cell cycle arrest. Many genes involved in these pathways are redox-sensitive, including mitogen-activated protein kinases (MAPKs) and components of AP-1 signaling such as C-JUN. Cleaved PARP1 and cleaved caspase-3 immunoreactivity, markers of apoptosis, were dramatically enhanced following hydroxyurea treatment. Thus, the dysregulation in redox homeostasis and changes in embryonic gene expression contribute to hydroxyurea-induced developmental toxicity.

RÉSUMÉ

L'hydroxyurée a été utilisée comme modèle tératogène afin d'étudier le rôle du stress oxydatif et les cascades moléculaires activées par ce stress, pouvant expliquer l'effet tératogène de médicament. Une exposition à l'hydroxyurée pendant l'organogenèse a entraîné la mort fœtale et un retard de croissance, ainsi que des malformations externes et squelettiques. Plusieurs de ces malformations étaient concentrées dans la région caudale, affectant particulièrement les membres postérieurs, les vertèbres lombo-sacrées et la queue. L'exposition in utero à l'hydroxyurée a causé une réduction du glutathion, un antioxydant cellulaire majeur, et l'augmentation de la peroxydation lipidique tel qu'évalué par la création de produits agglomérés de protéines 4 - hydroxynonéal. De plus, les agglomérations de la protéine 4 - hydroxynonéal ont augmenté dans les régions sensibles aux malformations par l'hydroxyurée. L'une des principales protéines modifiées par ces accumulations de 4 - hydroxynonéal, la glycéraldéhyde-3-phosphate déshydrogénase (GAPDH), est impliquée dans le métabolisme de l'énergie. La formation des agglomérations de la protéine 4 - hydroxynonéal-GAPDH a mené à une diminution de l'activité enzymatique de GAPDH et une réduction de la formation de d'acide lactique. Sous des conditions non stressantes, GAPDH a été trouvé dans le cytoplasme mais suite à une exposition à l'hydroxyurée, GAPDH a été déplacé dans le noyau. L'inhibition pharmacologique de la translocation nucléaire de GAPDH avec déprényl a augmenté les malformations, plus spécifiquement celles des membres postérieurs, des vertèbres lombo-sacrée et la queue, sans réduire d'avantage la glutathion. Ainsi, GAPDH joue un rôle protecteur dans le noyau suivant un stress oxydatif.

L'exposition in utéro à l'hydroxyurée a conduit à une perturbation de l'homéostasie d'oxydoréduction de l'embryon, en oxygénant d'importantes oxydoréductases, tels que la thiorédoxine (TRX1) et GAPDH. Le dysfonctionnement de l'état d'oxydoréduction a stimulé l'expression du facteur nucléaire tel que le dérivé des érythroïdes 2 (*Nrf2*) et son gène cible la peroxyredoxine 1 (*Prdx1*). La protéine de thiorédoxine (*Txnip*), un inhibiteur interne de la TRX1 a également été augmenté. Suite à une exposition à l'hydroxyurée, les principales cascades moléculaires activées étaient liées à l'apoptose et l'arrêt du cycle cellulaire. Plusieurs gènes impliqués dans ces mécanismes sont sensibles à l'oxydoréduction, incluant les kinases activées par les mitogènes (MAPKs) et les composants de la signalisation AP-1, tel que le C-JUN.

L'immunoréactivité des formes actives de PARP1 et de caspase-3, des marqueurs d'apoptose, ont été considérablement augmentées après le traitement d'hydroxyurée. Ainsi, le dérèglement de l'homéostasie de l'oxydoréduction et les changements d'expression des gènes embryonnaires contribuent à la toxicité induite par l'hydroxyurée.

TABLE OF CONTENTS

Abstract.....	ii
Resumé.....	iii
Table of Contents.....	v
List of Figures.....	ix
List of Tables.....	xiii
Abbreviations.....	xiv
Acknowledgements.....	xvii
Preface.....	xx
Contributions of Authors.....	xxi

Chapter I: Introduction

1.1 Statement of the problem and purpose of the investigation.....	2
1.2 Hydroxyurea.....	3
1.2.1 Mechanism of action.....	4
1.2.2 Pharmacokinetics.....	5
1.2.3 Hydroxyurea developmental toxicity in experimental animal models.....	5
1.3 Embryogenesis.....	6
1.3.1 Organogenesis.....	6
1.3.2 Energy requirements.....	7
1.3.3 Susceptibility to oxidative stress.....	7
1.4 Oxidative stress.....	8

1.4.1 The generation of reactive oxygen species and the antioxidant defense system	9
1.4.2 Mammalian redox-homeostasis and developmental consequences of redox disruption	12
1.5 Glutathione and thioredoxin	15
1.6 Lipid peroxidation product 4-hydroxynonenal (4-HNE)	17
1.6.1 The chemical reaction producing 4-HNE and its detoxification	18
1.6.2 Protein modifications by 4-HNE	18
1.6.3 Stress responses to 4-HNE toxicity	22
1.7 Glyceraldehyde-3-phosphate dehydrogenase (GAPDH)	26
1.7.1 GAPDH in glycolysis	27
1.7.2 GAPDH activity and localization	27
1.7.3 GAPDH as a target of 4-HNE	28
1.8 Deprenyl	28
1.8.1 Mechanism of action	29
1.8.2 Pharmacokinetics	30
1.8.3 Pharmacological inhibition of nuclear GAPDH	30
Research objectives	32

Chapter II: Teratogen-induced oxidative stress targets glyceraldehyde-3-phosphate dehydrogenase in the organogenesis stage mouse embryo

Abstract	34
Introduction	35
Materials and Methods	37

Results.....	42
Discussion.....	62
Acknowledgements.....	66
References.....	67
Connecting Text from Chapter II to III.....	72

Chapter III: Deprenyl enhances the teratogenicity of hydroxyurea in organogenesis stage mouse embryos

Abstract.....	74
Introduction.....	75
Materials and Methods.....	78
Results.....	82
Discussion.....	105
References.....	110
Connecting Text from Chapter III to IV.....	115

Chapter IV: The effects of hydroxyurea on redox status and gene expression in organogenesis stage mouse embryos

Abstract.....	117
Introduction.....	119
Materials and Methods.....	121

Results.....	126
Discussion.....	147
Acknowledgements.....	155
References.....	156

Chapter V: Discussion

5.1 Summary.....	162
5.2 The role of oxidative stress in hydroxyurea-induced developmental toxicity	162
5.3 The role of GAPDH in hydroxyurea-induced developmental toxicity.....	164
5.4 The role of the embryonic stress response.....	166
5.5 The role of apoptotic gene regulation.....	167
5.6 The role of cell cycle gene regulation.....	168
5.7 The role of DNA repair pathways.....	169
5.8 Conclusions.....	170
Original Contributions.....	172
References.....	173

LIST OF FIGURES

Fig. 1.1	ROS generation and detoxification.....	10
Fig. 1.2	Redox switching during proliferation, differentiation, and cell death..	13
Fig. 1.3	4-HNE formation from arachidonic acid and 4-HNE reactions with amino acid side chains.....	20
Fig. 1.4	4-HNE-induced modulation of different cell signaling pathways.....	24
Fig. 2.1	Illustration of the separation of the mouse embryo. Analysis of 4-HNE- protein adducts in three parts of the embryo treated with saline, 400 or 600 mg/kg hydroxyurea.....	43
Fig. 2.2	2D gel electrophoresis of the tail samples obtained from embryos treated with saline or 600 mg/kg hydroxyurea, and the corresponding 2D Western blots illustrating immunoreactive 4-HNE-protein adducts	46
Fig. 2.3	2D gel electrophoresis of the tail samples obtained from embryos treated with saline or 600 mg/kg hydroxyurea, and the corresponding 2D	

	Western blots illustrating GAPDH immunoreactive protein spots.....	49
Fig. 2.4	Spectrophotometric analysis of NADH as a measure of GAPDH activity following saline, 400 or 600 mg/kg hydroxyurea. Lactate measurements of embryos treated with saline, 400 or 600 mg/kg hydroxyurea.....	53
Fig. 2.5	Confocal microscopy images of embryos treated with saline or 600 mg/kg hydroxyurea. Green fluorescence represents GAPDH immunoreactivity.....	56
Fig. 2.6	IMARIS 3D-image analysis of nuclear GAPDH and DAPI immunoreactivity in embryos exposed to saline or 600 mg/kg hydroxyurea.....	58
Fig. 2.7	Intensity mean analysis of nuclear GAPDH in embryos exposed to saline or 600 mg/kg hydroxyurea.....	60
Suppl. Fig. 2.1	GAPDH protein expression in head, body, and tail regions of the embryo following hydroxyurea exposure.....	64

Fig. 3.1	IMARIS 3D-image analysis of nuclear GAPDH in embryos exposed to saline, 400 or 600 mg/kg hydroxyurea with or without deprenyl pretreatment.....	84
Fig. 3.2	Incidence of external malformations from litters of dams treated with saline, deprenyl and/or hydroxyurea (400 or 600 mg/kg).....	89
Fig. 3.3	Illustrations of some of the skeletal defects observed in GD 18 fetuses after exposure to saline or 600 mg/kg hydroxyurea.....	94
Fig. 3.4	Lactate measurements in embryos exposed to saline, deprenyl and/or hydroxyurea (400 or 600 mg/kg).....	97
Fig. 3.5	Glutathione status of embryos exposed to saline, deprenyl and/or hydroxyurea (400 or 600 mg/kg).....	100
Fig. 3.6	Analysis of cleaved capase-3 immunoreactivty in embryos exposed to saline, deprenyl and/or hydroxyurea (400 or 600 mg/kg).....	103
Suppl. Fig. 3.1	4-HNE-tagged proteins and GAPDH in gestation day 9 whole embryos following treatment with deprenyl and hydroxyurea.....	108

Fig. 4.1	Redox status of TRX1 and GAPDH in embryos exposed to saline, 400 or 600 mg/kg hydroxyurea.....	127
Fig. 4.2	Number of probe sets and genes that significantly altered by hydroxyurea. Venn diagram and principle component analysis of probe sets and genes expressed in control and treated embryos.....	130
Fig. 4.3	Microarray analysis and real-time qRT-PCR of genes involved in oxidative stress.....	137
Fig. 4.4	Pathway analysis of apoptotic genes following hydroxyurea exposure.....	143
Fig. 4.5	Analysis of cleaved PARP1 immunoreactivity in embryos exposed to saline, 400 or 600 mg/kg hydroxyurea.....	145
Suppl. Fig. 4.1	The effects of hydroxyurea exposure on the expression of glutathione genes in the embryo.....	152
Suppl. Fig. 4.2	The effects of hydroxyurea exposure on the expression of thioredoxin genes in the embryo.....	152

LIST OF TABLES

Table 2.1	Identification of proteins conjugated with 4-HNE in the tail regions of the embryo.....	52
Table 3.1	Fetal observations in dams treated with saline, deprenyl and/or hydroxyurea (400 or 600 mg/kg).....	87
Table 3.2	Fetal axial skeletal defects following maternal treatment with saline, deprenyl and/or hydroxyurea (400 or 600 mg/kg).....	92
Table 4.1	Up- and downregulated genes in embryos exposed to saline or 400 mg/kg hydroxyurea.....	132
Table 4.2	Functional grouping of genes up- or downregulated following hydroxyurea exposure.....	135
Table 4.3	Pathway analysis of genes that were significantly altered by hydroxyurea.....	140
Table 4.4	Upregulated genes involved in apoptosis following hydroxyurea exposure.....	142

ABBREVIATIONS

ALB	Albumin
ALDOA1	Aldolase 1, A isoform
AP-1	Activator protein-1
APE1	Apurinic/aprimidinic endonuclease 1
BAX	Bcl2-associated X protein
BCL-2	B-cell lymphoma 2
BSO	Buthionine sulfoxamine
CAT	Catalase
CBP	CREB-binding complex
D	Deprenyl
DNTP	Deoxyribonucleotide triphosphate
ERK	Extracellular signal-regulated protein kinase
FAS	TNF receptor superfamily, member 6
HIF	Hypoxia-inducible factor 1
4-HNE	4-Hydroxynonenal
GAPDH	Glyceraldehyde-3-phosphate dehydrogenase
γ -GCL	Gamma-glutamylcysteine ligase
γ -GCLC	Gamma-glutamylcysteine ligase, catalytic subunit
γ -GCLM	Gamma-glutamylcysteine ligase, modulator subunit
GD	Gestational day
GOT2	Glutamic-oxaloacetic transaminase 2

GR	Glutathione reductase
GSH	Reduced glutathione
GSH-Px	Glutathione peroxidase
GSS	Glutathione synthetase
GSSG	Oxidized glutathione
GST	Glutathione transferase
H	Hour
HNRNPA1A	Heterogeneous nuclear ribonucleoprotein isoform A1-A
HR	Homologous repair
HSP60	Heat shock protein 60 kDa
HU	Hydroxyurea
IP	Intraperitoneal injection
JNK	c-Jun N-terminal protein kinase
KG	Kilogram
MAOI	Monoamine oxidase inhibitor
MAPK	Mitogen-activated protein kinase
MAP3K	Mitogen-activated protein kinase kinase kinase
MG	Milligram
MM	Millimolar
MV	Millivolt
NAC	N-acetylcysteine
NADH	Nicotinamide adenine dinucleotide
NADPH	Nicotinamide adenine dinucleotide phosphate

NHEJ	Non-homologous end-joining
NDP	Ribonucleotide diphosphates
NF- κ B	Nuclear factor kappa B
NM	Nanometer
NRF2	Nuclear factor (erythroid-derived 2)-like 2
PAR	Poly ADP-ribosylation
PARP1	Poly (ADP-ribose) polymerase family, member 1
PRX	Peroxiredoxin
qRT-PCR	Quantitative real-time polymerase chain reaction
RNR	Ribonucleotide diphosphate reductase
REF-1	Redox factor-1
RFU	Relative fluorescence unit
ROS	Reactive oxygen species
RNS	Reactive nitrogen species
SOD	Superoxide dismutase
TR	Thioredoxin reductase
TRX1	Thioredoxin 1
TXNIP	Thioredoxin interacting protein
V	Volt
WNT	Wingless-related integration site

ACKNOWLEDGEMENTS

I am very thankful for having an outstanding mentor and supervisor, **Dr. Barbara Hales**, who gave me the opportunity to pursue my passion in teratology and for her positive support and guidance, constructive criticism, and endless patience. I would also like to thank **Dr. Bernard Robaire**, for his profound insight, support, and valuable discussions throughout the years.

I would like to thank the members of my committee, my advisors, **Dr. Daniel Bernard**, for being an excellent mentor, providing important guidance in my project, and for those hard questions, and **Dr. Anne McKinney**, for her critical suggestions and expertise with confocal microscopy. **To Dr. Greg Miller**, thank you for your expertise in crystallography and advice on better understanding the molecular functions of GAPDH, and to **Dr. Jason Tanny**, thank you for your constructive comments and suggestions on how to improve my research.

A heartfelt thanks goes to the staff of the Department of Pharmacology and Therapeutics, **Tina Tremblay, H el ene Duplessis, Chantal Gagnon, and David Kalant**, for all your support related to the program and the time and effort you spent helping with the events I have organized throughout the years. I will never forget it.

A very special thank you goes to **Dr. Chunwei Huang**, for always having everything running smoothly in the lab and for your thoughtfulness and caring nature. You were an important part of my success in the lab.

I am grateful to **Eugene Galdones**, for being my first mentor and teacher in the lab. You taught me good lab etiquette and helped me get started on my 599 project that led me into the master's/PhD program.

A warm thank you to **Ghalib Bardai** for conducting the lactate measurements at the Royal Victoria Hospital, in chapter II.

To my dearest friends, **Dr. Lisanne Grenier**, thank you for being my best buddy in the lab and in my life, you made the doctoral experience the best I could ever ask for. Thank you for all those in-depth discussions about science and memorable times we spent together in- and outside the lab. To **Dr. Michelle Carroll**, thank you for your incredible positivity and fun personality that made my time in the lab a fun place to be. To **Caroline Dayan**, thank you for your wonderful friendship in the lab and in my life, working with you side-by-side on the microarray made the experience so much more enjoyable. You are one of the most loving and caring people I know and I look forward to a lifetime of kids parties and sharing great times together. To **Tina Scardochio**, your friendship throughout the years starting in Vanier is one I hold close to my heart. I will never forget all the great times we've spent together in- and outside the McIntyre. I will greatly miss our meetings for lunch but I look forward to all the new experiences we will be creating together.

I am grateful to **Dr. Claudia Lalancette**, for your expertise, help, and patience with the microarray protocol and analysis. Thank you for being great company and a great colleague to learn from.

To **Elise Boivin-Ford, Jennifer Maselli, France Paradis, and Dr. Sheila Ernest**, thank you for keeping the lab an enjoyable and friendly place to go to everyday, for your laughter, advice, and helpful discussions throughout the years.

Finally, a deep gratitude goes to my parents and my husband. For my parents who raised me with a love of science and supported me in all my years of pursuits and to my patient and devotedly supportive husband, thank you so much. For your unconditional love and support, I dedicate this thesis to you.

PREFACE

Format of the Thesis

This is a manuscript-based thesis in accordance with the Thesis Preparation and Submission Guidelines outlined by the Faculty of Graduate and Postdoctoral Studies at McGill University. This thesis entails five chapters. Chapter I, the introduction, provides the foundation for the studies presented in this dissertation. The model teratogen, hydroxyurea and its biochemistry in producing oxidative stress are briefly reviewed. A lipid peroxidation product, 4-hydroxynonenal (4-HNE), the multifunctional protein glyceraldehyde-3-phosphate dehydrogenase (GAPDH), and its inhibitor deprenyl are also reviewed. The hypothesis and the research objectives are also presented in Chapter I.

Three data chapters, Chapter II, Chapter III, and Chapter IV, are included in this thesis. Chapter II is published in *Toxicological Sciences* (118, 686-695, 2010) as well as Chapter III (134, 391-399, 2013). Chapter IV is a manuscript in preparation. Each data chapter is preceded by a connecting text providing continuity to the development of the research.

Chapter V, the final conclusions, presents a detailed and concise discussion of the results and their relevance to the field of developmental toxicology and future studies, followed by a list of Original Contributions. References are provided at the end of the thesis.

Contribution of Authors

All the experiments presented in this thesis were performed by the candidate with the exception of the 4-HNE-protein adduct quantification and 2D gel electrophoresis done by Dr. Jin Yan and lactate measurements done by Ghalib Bardai in Chapter II.

Chapter I

Introduction

1.1 Statement of the problem and purpose of the investigation

Every year an estimated 8 million children – 6% of total births worldwide – are born with a serious birth defect due to gene defects, infections, and/or maternal exposure to environmental agents (March of Dimes, 2006). Of these, 270 000 newborns die during the first few months of life every year from congenital anomalies. The diverse symptoms associated with birth defects adversely impact quality of life, which can manifest in extensive physical and psychosocial burden (March of Dimes, 2006). There is also associated economic responsibility incurred, including substantial medical treatment costs and direct nonmedical costs (such as special education and developmental costs). Globally, the annual cost for one major birth defect (neural tube defects) alone is estimated at 168 billion dollars (CDC, 2011).

Approximately 70% of birth defects have unknown etiologies and 3% are due to harmful environmental exposures, including drugs and radiation. For many women, pregnancy is unintentional and some expose their unborn children to harmful agents before they even know they are pregnant. Another major concern is the use of medication that is sometimes inevitable in the treatment of women of reproductive age and during pregnancy. Over the last 40 years, approximately 2,500 chemicals have been identified to be developmental toxicants in humans and their exact mechanisms of teratogenesis are generally unknown (Hansen, 2006). Some of these human teratogens include thalidomide, valproic acid, heavy metals, alcohol, cigarette smoke, and irradiation (Kim and Scialli, 2011; Ornoy, 2007; Tung and Winn, 2011; Paniagua-Castro *et al.*, 2008). Interestingly, many of these compounds are capable of generating reactive oxygen species (ROS) and oxidative stress. Since so many potential teratogens cause oxidative stress it is suggested that oxidative-induced misregulation of redox-sensitive elements may be a general teratogenic mechanism (Hansen, 2006). Cellular homeostasis of oxidizing and reducing equivalents is maintained by antioxidant systems; however, the embryo has a limited capacity to control ROS (Ozolins and Hales, 1999). The imbalance of reducing and oxidizing equivalents, where the latter predominates, leads to oxidative stress-induced cellular damage, changes in signal transduction, and alterations in gene expression. Investigating the role of oxidative stress in mediating teratogenesis induced by exposure to toxicants is of major concern and our ultimate question.

To address this question, we utilized hydroxyurea as a model developmental toxicant. Hydroxyurea is an inhibitor of ribonucleotide reductase, inhibiting *de novo* synthesis of DNA,

and is commonly used for myeloproliferative blood disorders, such as primary polycythemia as well as sickle cell anemia (Liebelt *et al.*, 2007). Studies on hydroxyurea have demonstrated an early cell death response. Antioxidant preadministration revealed a significant attenuation in the development of malformations (DeSesso and Goeringer, 1990a). We hypothesized that oxidative stress is fundamental in hydroxyurea teratogenicity. CD1 mice were chosen as our animal model. CD1 mice are an outbred strain that carry genetic variability; this strain is an appropriate model for studies on developmental toxicants. Timed pregnant CD1 mice were treated on gestational day 9 (GD 9), during organogenesis, when the embryo is most susceptible to malformations by toxicant exposures. Defining the mechanisms of oxidative stress and the response of the conceptus at the protein and gene level will help to elucidate the role of hydroxyurea developmental toxicity.

Having a healthy pregnancy is more than just eating a balanced diet and receiving adequate prenatal care. Understanding the environmental factors that put a pregnancy at risk is the goal of these studies. Thus, elucidating the mechanisms of oxidative stress in developmental toxicity will advance education of birth defect prevention.

1.2 Hydroxyurea

Hydroxyurea is a nonalkylating antiproliferative and antiviral agent that is used for a variety of neoplastic and non-neoplastic conditions. Hydroxyurea was first synthesized in 1869 in Germany by Dressler and Stein. It was FDA approved in 1967 and is a staple in the management of chronic myeloproliferative disorders (MPDs), including chronic myelogenous leukemia, essential thrombocythemia, polycythemia vera, and primary myelofibrosis (Spivak and Hasselbalch, 2011). Hydroxyurea is also widely used to treat sickle cell anemia (SCA) and more recently was approved for hydroxyurea-based regimens for patients with HIV (Lori *et al.*, 2004). Hydroxyurea use during pregnancy and in nursing women is contraindicated and labeled to pregnancy category D by the FDA. There is a large body of evidence for its teratogenicity in many species, including the mouse, rat, hamster, rabbit, and guinea pig at doses 1-3.3 times the human therapeutic dose (Bailey *et al.*, 2005). Animal studies have revealed that hydroxyurea crosses the placenta and exposure to the conceptus is associated with embryotoxicity, malformations, growth retardation, and impaired learning ability (FDA, 2013). There are no controlled studies in human pregnancy; however, several case studies are documented. One case

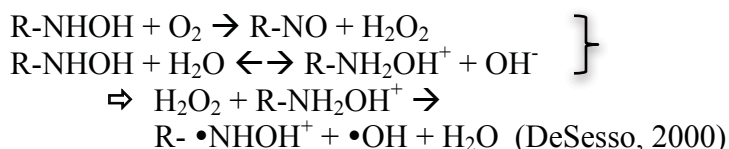
study with 31 pregnancies with hydroxyurea exposure ended in 24 liveborn infants (one pregnancy had twins), five induced abortions, one spontaneous abortion and two *in utero* fetal deaths. Among the 24 liveborn infants, nine were premature, three had minor malformations, and five displayed neonatal respiratory distress (Thauvin-Robinet *et al.*, 2001). The potential of hydroxyurea exposure during pregnancy as a carcinogen and a mutagen has not been evaluated. Unintentional exposure of hydroxyurea during pregnancy or advised treatment in women suffering from MPDs or SCA is very controversial and is still being practiced.

1.2.1 Mechanism of Action

Hydroxyurea acts primarily to inhibit DNA synthesis, inactivating ribonucleotide reductase (RNR), the enzyme that catalyzes the conversion of ribonucleotides to deoxyribonucleotides during *de novo* DNA synthesis and repair, the rate-limiting step in this process (Gwilt and Tracewell, 1998). RNR consists of 2 protein dimers, M1 and M2. Dimer M1 contains binding sites for the ribonucleotide substrates. The M2 dimer is the catalytic subunit and includes a tyrosine free radical stabilized by a non-haem iron complex. Hydroxyurea transfers an electron to the enzyme-bound tyrosine radical quenching and inhibiting RNR enzyme activity (Gwilt and Tracewell, 1998). Hydroxyurea depletes deoxyribonucleotide triphosphate (dNTP) pools resulting in S-phase cell cycle arrest. The dNTP depletion also leads to replication fork arrests causing double strand DNA breaks (DeSesso *et al.*, 2000; Spivak and Hasselbalch, 2011).

Early developmental toxicology studies on hydroxyurea in white rabbits during organogenesis have demonstrated a rapid onset of cell death, beginning at 2 hours after treatment. After 3-4 hours of treatment a profound inhibition of DNA synthesis, measured by 3H-thymidine incorporation, occurred (DeSesso and Goeringer, 1990b). The early cell death episode was suggested to be responsible for the development of malformations after hydroxyurea exposure. A variety of antioxidants, D-mannitol, propyl gallate, ethoxyquin, and nordihydroguaiaretic acid, delayed the onset of hydroxyurea-induced cell death in embryos. Furthermore, antioxidants ameliorated hydroxyurea-induced developmental toxicity (DeSesso and Goeringer, 1990a; DeSesso *et al.*, 1994). Supporting the hypothesis that early onset cell death is due to the rapid generation of reactive oxygen species, the hydroxylamine moiety (-

NHOH) can react with oxygen and water to produce hydrogen peroxide (H₂O₂) and the hydroxyl radical (OH[•]). The reaction is summarized as follows:



It has been strongly suggested that the developmental toxicity of hydroxyurea is not attributed to its ability to inhibit DNA synthesis, but rather to the capacity of the hydroxylamine moiety to generate reactive oxygen species, leading to oxidative stress and cell death in embryos.

1.2.2 Pharmacokinetics

Hydroxyurea is water-soluble and well absorbed. Hydroxyurea enters cells via passive diffusion and crosses the blood brain-barrier (Morgan *et al.*, 1986; Ware *et al.*, 2011). Based on human studies, after intraperitoneal injection (IP) there is an initial distribution phase of ~0.63 hours within a volume similar to that of total body water and the drug is concentrated in erythrocytes and leukocytes (Bristol-Myers-Squibb, 2002). In human studies, the half-life of hydroxyurea is ~3.36 h; in rat embryos, it is estimated to have a half-life of 2-3 h (Rodriguez *et al.*, 2013; Wilson *et al.*, 1975).

1.2.3 Hydroxyurea developmental toxicity in experimental animal models

In utero exposure to hydroxyurea at different times throughout gestation produces a variety of malformations. Rodent studies in which embryos were exposed to hydroxyurea during organogenesis present with low fetal weight, high rate of resorptions, hindlimb and tail malformations and a variety of skeletal defects (Schlisser and Hales, 2013; Campion *et al.*, 2012). Necrosis and apoptosis are two major events in hydroxyurea teratogenicity and occur within 2 hours of *in utero* exposure (DeSesso and Goeringer, 1990a). A profound inhibition of DNA synthesis and cell cycle arrest at G1-S phase were also observed (Vogel *et al.*, 1978). Furthermore, protein modifications and gene expression changes leading to cell death were also reported, including increased phospho-p53, phospho-p38 immunoreactivity, and increased transcript levels of pro-apoptotic genes, *p21*, *bax* and *cyclin G* (Woo *et al.*, 2003; Banh and Hales, 2013). The rapid cell death observed subsequent to hydroxyurea exposure occurs in

regions of high susceptibility to malformations, specifically the limb buds (DeSesso and Goeringer, 1990a; Woo *et al.*, 2003). The cell death observed in fetal tissues is associated with the generation of ROS (DeSesso, 1981a; DeSesso and Goeringer, 1990b; DeSesso *et al.*, 1994). Moreover, maternal superoxide dismutase 1 (hSOD1) overexpression in dams has been shown to protect fetuses against malformations induced by hydroxyurea (Larouche and Hales, 2009). The evidence provided strongly suggests that oxidative stress plays an important role in the developmental toxicity of hydroxyurea. The effects of oxidative stress on proteins, nucleic acids, and lipids, may be, at least in part, underlying the mechanisms of hydroxyurea teratogenicity.

1.3 Embryogenesis

During mammalian embryogenesis, an intricate series of morphological and molecular changes occur to establish the body plan. Development from zygote to blastocyst commences in the oviduct and cleavage divisions occur as the zygote progresses to the uterus. Once it attaches to the uterus it has become a cluster of small cells called a morula. The morula develops into a sphere of cells surrounding a fluid filled cavity and is now termed a blastocyst. The blastocyst segregates into a two-layered disk; one layer of cells, called the epiblast, is associated with the development of the amniotic cavity and the other layer, the hypoblast, is associated with the developing yolk sac cavity. The epiblast rearranges during gastrulation into three primary germ layers (ectoderm, mesoderm, and endoderm), as well as the notochord. Specific tissues of the body are derived from each germ layer. The ectoderm will give rise to the nervous system, skin, and adnexal dermal organs, including teeth, nails, hair, and both the sweat and mammary glands. The derivatives of the mesoderm include cartilage, bone, muscle, tendons, connective tissue, kidneys, gonads, and blood. The endoderm gives rise to the linings of the alimentary, respiratory, and lower urinary tracts. At this stage in development, the conceptus is less susceptible to malformations from toxicant insult (Moore and Persaud, 1998).

1.3.1 Organogenesis

Organogenesis in the human occurs between GD 17-52 and in the mouse embryo between GD 8-15 and is a period of dynamic change (DeSesso, 2011). The embryo develops in a cranial-caudal sequence and is characterized by the development of the internal organs and limbs. Pattern formation, specification of positional information, induction, morphogenesis and cellular

differentiation direct the development of the embryo into the fetal stage. Limb development is controlled by homeobox genes that are expressed in the lateral mesoderm and are involved in specifying the position and type of limb. For example, the induction of fibroblast growth factor family proteins and transcription factors, such as T-Box proteins, is involved in specific development of the hindlimb and not the forelimb (Rancourt *et al.*, 1995). During organogenesis, the embryo is highly susceptible to developmental toxicants, especially those that produce oxidative stress and can develop an array of malformations (Hansen and Harris, 2013). Sensitivity of the limbs to an oxidative stress-inducing teratogen, for example thalidomide, occurs between day 27-33 in the human, by directly inhibiting fibroblast growth factor 8, an essential regulator of limb development, causing apoptosis (Knobloch *et al.*, 2011). Thalidomide also prevents angiogenic outgrowth during this period; such vessel loss occurs upstream of changes in limb morphogenesis and gene expression, resulting in limb defects, in addition to other developmental defects or embryonic death (Therapontos *et al.*, 2009).

1.3.2 Energy requirements

During mid-organogenesis, about GD 8 in the mouse, when the major organs are forming and the embryo is undergoing rapid morphological changes, the embryo relies heavily on glycolysis and lactate metabolism for its ATP production (Neubert, 1970). Anaerobic glycolysis coincides with delamellated cristae of the mitochondria during which the terminal electron transport phosphorylation is very low (Mackler *et al.*, 1973). Exposure to carbon monoxide, which inhibits the terminal electron transport system, has no adverse effects on GD 9 mouse embryos (Robkin, 1997). Supporting this hypothesis, oxygen exposure beyond 10% is toxic to GD 9 mouse embryos. Between GD 9-10 in the mouse embryo, the mitochondria approach maturity with the development of numerous cristae and the majority are lamellated, concurrent with the activation of oxidative respiration (Shepard *et al.*, 1998). During the switch between anaerobic to aerobic metabolism, the cardiovascular system is established and the chorioallantoic circulation is developed (Choe *et al.*, 2001). At this developmental stage, the embryo is exposed to significantly more reactive oxygen species generated by the mother as well as its own mitochondrial end-products of oxidative respiration, namely hydrogen peroxide, superoxide, and hydroxyl radicals.

1.3.3 Susceptibility to oxidative stress

During gastrulation and organogenesis, oxygen supply to the embryo is tightly controlled and the embryo is normally in a state of hypoxia. Disturbances in the oxygen status can easily lead to oxidative stress and abnormal development. Prior to the anaerobic to aerobic metabolic switch, the control of oxygen is mainly regulated by hypoxia-inducible factor (HIF) and accumulates in response to oxygen concentrations (Webster and Abela, 2007). As embryonic requirements for O₂ increase, the probability for ROS formation also increases and the embryo must adapt, removing ROS and preventing cell damage and death. Glutathione (GSH) is the most abundant endogenous intracellular thiol (0.2-10 mM), found in most mammalian and many prokaryotic cells. It is well known for its cellular protective roles against ROS by acting as a radical scavenger and intracellular antioxidant (Meister and Anderson, 1983). Glutathione peroxidase (GSH-PX) and glutathione disulfide reductase (GSSG-RD) are directly involved in the regulation of GSH and intracellular redox status (Choe *et al.*, 2001). In the rat embryo, during early developmental periods (GD 9-13), GSH-PX and GSSG-RD activities do not change but increase in the visceral yolk sac. SOD increases over early gestational times (GD 9-12); however, it does not appear to respond to the shift in metabolic activity occurring between GD 9 and 11 (Choe *et al.*, 2001). GSH is found in the embryo and in the visceral yolk sac; however, levels in the embryo are significantly less than those in the mother (Yan and Hales, 2005). Treatment with L-buthionine-S,R-sulfoxamine (BSO) a drug that depletes GSH by inhibiting γ -glutamylcysteine synthetase, on GD 10 in the rat embryo revealed that the embryo is unable to quickly respond to GSH depletion and resynthesize GSH, most likely due to the lack of amino acid precursors (Hansen *et al.*, 2004). The susceptibility to oxidative stress during the metabolic switch may be defined by the capacity of the embryo to control ROS by antioxidant regulation.

1.4 Oxidative stress

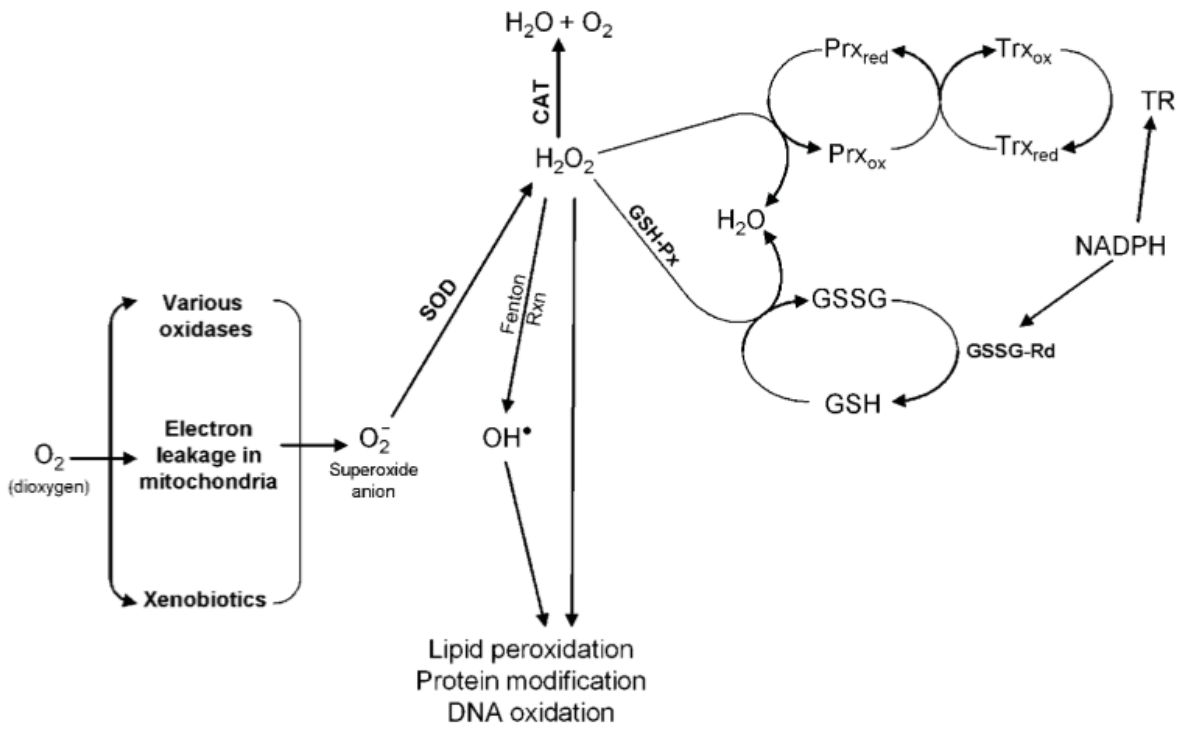
The classic definition of oxidative stress describes a disturbance in the pro-oxidant-antioxidant balance in favor of the former (Sies and Cadenas, 1985). The accumulation of data on redox signaling pathways, antioxidant preadministration, and oxidative stress markers, indicates that a contemporary definition should be adopted, based on a disruption of redox signaling and control (Jones, 2006). Oxidative stress and redox disturbances has been strongly associated with several conditions, such as Alzheimer's disease and diabetes, and is proposed to

be a leading teratogenic mechanism for many drugs, such as thalidomide, phenytoin, ethanol, hydroxyurea, isotretinoin, and valproic acid (Dennerly, 2007; Hansen, 2006).

1.4.1. The generation of reactive oxygen species and the antioxidant defense system

Mid-organogenesis (GD 9 in the mouse or GD 10 in the rat) concurrent with the metabolic switch to aerobic respiration, there is an oxygen surge emerging from the electron transport chain in the mitochondria and the development of the uteroplacental circulation. Free radicals, such as oxygen free radicals and superoxide anions that are generated in the embryo or enter the embryo from the maternal circulation can be metabolized into hydrogen peroxide (H_2O_2) by SOD. H_2O_2 can react with cellular components or can form the hydroxyl radical (OH^\cdot) via the Fenton reaction and/or the Haber-Weiss reaction (Kruszewski and Iwanenko, 2003) (Fig 1.1). OH^\cdot is a highly reactive and toxic oxygen species with a half-life of 10^{-9} s where the reaction with its target takes place at the site of generation (Sies, 1993). Specific antioxidant systems have evolved to counter the effects of ROS, such as GSH, glutathione peroxidase, catalase, peroxiredoxin, and thioredoxin systems (Hansen, 2006). Exogenous antioxidants, including essential nutrients (vitamin c, vitamin e, selenium) and dietary compounds (bioflavonoids, proanthocyanidans) along with the endogenous antioxidant molecules, regulate redox homeostasis (Saha, 2011).

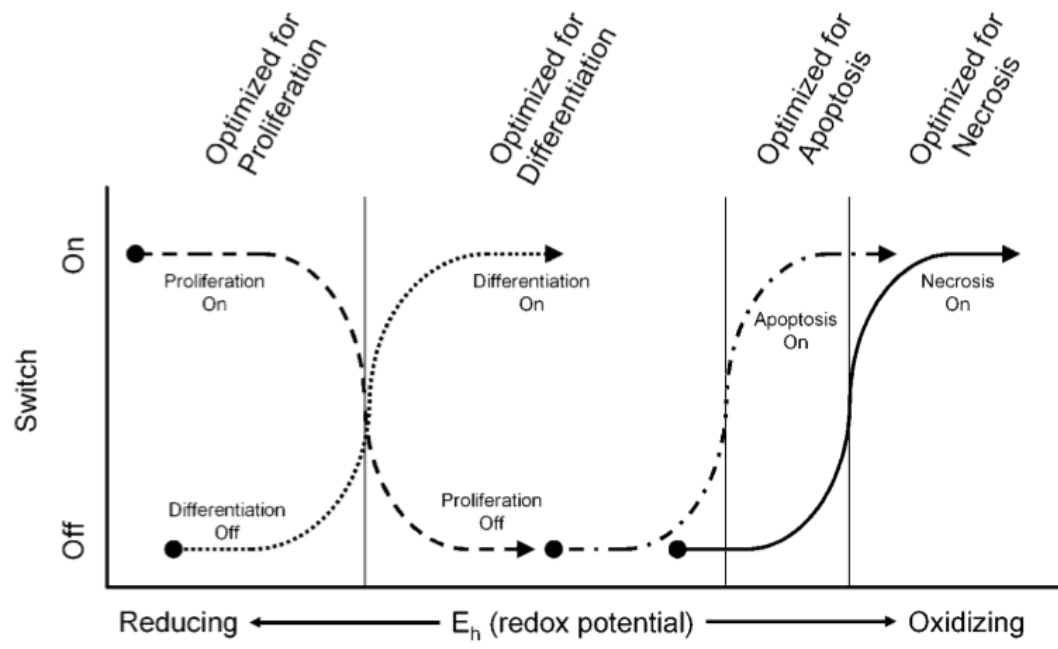
Fig. 1.1 ROS generation and detoxification. Superoxide anion ($\bullet\text{O}_2$) is mainly generated from the mitochondria but other sources, such as xanthine and NADPH oxidases, as well as xenobiotics, can generate $\bullet\text{O}_2$. The metabolism of H_2O_2 can occur through interaction with GSH through GSH-PX to form GSSG and H_2O . GSSG can be reduced back to GSH by GSSG-RD using NADPH as a cofactor. H_2O_2 can also be reduced by the TRX/PRX system. Oxidized PRX can be reduced by TRX. Oxidized TRX can be reduced through TR using NADPH as a cofactor. CAT, catalase; GSH, glutathione; GSSG, glutathione disulfide; GSSG-RD, glutathione disulfide reductase; GSH-PX, glutathione peroxidase; PRX, peroxiredoxin; SOD, superoxide dismutase; TRX, thioredoxin; TR, thioredoxin reductase. Modified from (Hansen, 2006).



1.4.2. Mammalian redox-homeostasis and developmental consequences of redox disruption

Redox homeostasis is defined by the balance between pro- and anti-oxidative processes. Pro-oxidative reactions generate ROS and/or reactive nitrogen species (RNS); when produced in excess ROS/RNS are toxic to the cell. In contrast, antioxidant reactions detoxify ROS/RNS in attempt to maintain redox balance and are of major biological importance. Redox status has been proposed to regulate proliferation, differentiation, and apoptosis by the GSH/GSSG, Cys/CySS, and TRX1_{red}/TRX1_{ox} redox couples (Schafer and Buettner, 2001) (Fig. 1.2). GSH potential (E_h) favoring a more reduced state supports proliferation whereas a more oxidized state supports differentiation and apoptosis.

Fig. 1.2 Redox switching during proliferation, differentiation, and cell death. Proliferation appears to be supported by very reducing GSH *Eh* (-250 mV). Oxidation to approximately -220 mV correlates with differentiation and further oxidation (less than -190 mV) promotes cell death. Proliferation switches are “on” in a reducing environment, but when cells become increasingly oxidized these switches are turned “off.” Differentiation switches that are “off” at highly reducing redox potentials are turned “on” as cells move to a more oxidizing, less proliferative state. Cell death switches that are kept “off” can be turned “on” by a more oxidizing redox potential. These switches are naturally occurring and a critical component to normal development. Introduction to a chemical that could alter the action of these switches, either directly or indirectly, could have serious, long-standing effects on normal developmental pathways (Schafer and Buettner, 2001).



The high reactivity of ROS/RNS inevitably has a countless number of targets, including lipids, proteins, nucleic acids, and carbohydrates (Ufer and Wang, 2011). Modifications to these targets often lead to cellular dysfunction. ROS can induce protein sulfhydryl oxidation and disulphide formation. With oxidative stress, the rates of disulphide bonds and mixed disulphide formations increase within the cell. As a consequence, inactivation of enzymes such as glyceraldehyde-3-phosphate dehydrogenase can occur and have detrimental effects on development (Halliwell and Gutteridge, 1989). The consequences of redox alterations are rather complex but have clear effects on energy homeostasis and gene expression. Metabolic consequences will be addressed in chapter II and V. Regulation of gene expression can be at the level of epigenetics, transcriptional, and posttranslational mechanisms. Redox-sensitive transcription factors that have a significant role in embryonic development include hypoxia-inducible factor 1 (HIF-1), nuclear factor kappa-light-chain-enhancer of activated B cells (NF- κ B), activator protein-1 (AP-1), nuclear factor (erythroid derived-2) like-2 (NRF2), and wingless-related integration site (WNT). Oxidative stress induced AP-1 response may alter gene expression profiles, leading to malformations, altered development and apoptosis (Ozolins and Hales, 1997). During mid-organogenesis (GD 9 in the mouse), specific regions are undergoing rapid proliferation, such as the caudal region. Proliferation is associated with reduced redox potential and reflects the time of organogenesis. As cells exit the cell cycle and become more oxidized, differentiation is supported and would constitute a period of embryonic development that may be most susceptible to oxidants (Hansen and Harris, 2013). Reactive oxygen species generated by teratogens may target areas of highly reduced states because the potential for oxidation is greater.

1.5 Glutathione and thioredoxin

GSH (L- γ -glutamyl-L-cysteinylglycine) is the major cellular non-protein sulfhydryl compound that plays a prominent role in detoxification of exogenous and endogenous compounds, anti-oxidative defense as well as maintaining the intracellular redox status. Glutathione exists in its reduced (GSH) and oxidized (GSSG) form and plays a central role in regulating ROS concentrations, directly as a free-radical scavenger and indirectly as a substrate with NADPH for detoxifying ROS (Guerin *et al.*, 2001). GSSG can be recycled back to GSH by the highly conserved glutathione reductase enzyme, maintaining GSH in high concentrations; the

molar ratio of GSH/GSSG in a mammalian cell is typically between 10:1 – 1000:1, however under oxidative stress, this ratio decreases (McDermott *et al.*, 2011).

The synthesis of GSH from its constituent amino acids involves two ATP-requiring enzymatic steps: formation of γ -glutamylcysteine from glutamate and cysteine and formation of GSH from γ -glutamylcysteine and glycine (Yang *et al.*, 2005). The first step of GSH biosynthesis is rate limiting and catalyzed by glutamate cysteine ligase (GCL), which is composed of a catalytic (GCLC) and a modifier (GCLM) subunit. *De novo* synthesis of GSH is regulated by the expression of GCLM that is controlled by NRF2, AP-1, and NF- κ B; its expression is induced by oxidative stress (Lu, 2013).

Many teratogens have been described to act through the disruption of redox couples: these include thalidomide, phenytoin, ethanol, methyl mercury, cocaine, and glucose (Hansen *et al.*, 1999; Wong and Wells, 1988; Dreosti, 1987; Thompson *et al.*, 2000; Lipton *et al.*, 2003). Phenytoin-induced birth defects (cleft lip/palate, microcephaly) are significantly decreased by pretreatment with the glutathione synthesis precursor, N-acetylcysteine (NAC). Conversely, pretreatment with GSH depleting agent diethyl maleate, exacerbated phenytoin-induced defects (Wong and Wells, 1988). Treatment with a glutathione precursor or an antioxidant can prevent, partially or completely, the developmental toxicity of these developmental toxicants by increasing reduced GSH concentrations.

The thioredoxin (TRX) system plays critical roles in providing reducing equivalents for DNA synthesis, maintaining cellular thiol-redox homeostasis, defending against oxidative stress, controlling protein folding and regulating cell growth/apoptosis (Zhang *et al.*, 2013). TRX_{ox} can be reduced back to TRX_{red} with TRX reductase (TR), providing electrons from NADPH to a very large number of critical cellular proteins, and thus is involved in a wide range of cellular functions. TRX was discovered to be the electron donor for RNR from *Escherichia coli* (Holmgren, 1985). TRX reduces the disulfide in the C-terminus of R1 subunit of RNR after a cycle of catalytic reactions (Holmgren and Lu, 2010).

TRX homeostasis is essential for both normal embryo development and defense against toxicant insult. TRX1 is a central redox regulator that mediates the activation of many transcription factors which are involved in cell growth, apoptosis, and inflammation, such as NF- κ B, AP-1, P53, HIF-1, and redox factor 1 (REF-1) (Lillig and Holmgren, 2007). Under oxidative stress conditions, TRX1 translocates from the cytosol to the nucleus maintaining the redox status

of the Cys residues in the DNA binding site of these transcription factors, promoting the DNA binding activities of NF- κ B and AP-1 (Hirota *et al.*, 1999). TRX1 can directly prevent apoptosis by associating with apoptosis signal regulating kinase 1 (ASK1) and MAP3K (Saitoh *et al.*, 1998). MAP3K activates C-JUN N-terminal kinase and P38 MAP kinase pathways and is required for tumor necrosis factor (TNF)- α -induced apoptosis (Lu and Holmgren, 2012). It is not surprising that TRX1 also induces apoptosis; it interacts with thioredoxin interacting protein (TXNIP), an endogenous inhibitor of TRX1 that forms a complex with reduced TRX1, but not with oxidized TRX1 (Lu and Holmgren, 2012). TRX1 and TRX2 knock-out (KO) mice are not viable, while TRX1 KO embryos die prior to implantation and TRX2 embryos die around gestational day 10.5 (Matsui *et al.*, 1996). During organogenesis and when the shift from anaerobic to aerobic metabolism takes place, the embryo increasingly depends upon oxidative phosphorylation to meet its energy needs. TRX2 (mitochondrial specific) was found to maintain redox homeostasis as these processes are initiated. TRX2 mutant embryos have an open anterior neuropore and suffer massive apoptosis (Hansen and Harris, 2013).

TRX and GSH act together to maintain redox homeostasis and are suggested to function in a compartmentalized fashion. For example, NRF2 can be activated through the oxidative modification of KEAP1 that occurs in the cytoplasm and is primarily regulated by GSH (Hansen *et al.*, 2004). The DNA binding activity of NRF2 takes place in the nucleus and is predominantly regulated by TRX1 (Hansen *et al.*, 2004). Teratogen induced alterations in redox homeostasis in each respective compartment would ultimately affect the functions of the NRF2 pathway.

1.6. Lipid peroxidation product 4-hydroxynonenal (4-HNE)

Lipid peroxidation is an important process to study, as it is a marker of oxidative stress in many diseases, drug toxicities, traumatic or ischemic injuries (Uchida and Stadtman, 2000). Among the many different aldehydes that can be formed during lipid peroxidation, the most intensively studied are malonaldehyde (MDA) and 4-hydroxyalkenals, in particular 4-hydroxy-2-nonenal (4-HNE). 4-HNE is a stable mediator of oxidative stress and can be easily detected by antibodies developed against 4-HNE modified epitopes on proteins. Immunohistochemical and immunofluorescent analysis can detect 4-HNE-protein adducts in the embryo after exposure to developmental toxicants (Yan and Hales, 2006). Proteins modified by 4-HNE can be identified

with immunoblotting and mass spectrometry, providing insight into the molecular changes occurring with oxidant insult.

1.6.1. The chemical reaction producing 4-HNE and its detoxification

Free radical chain reactions with Ω -3-polyunsaturated fatty acids generate α , β -unsaturated aldehydes (Esterbauer and Cheeseman, 1990). 4-HNE is reported to be formed from linoleic acid and arachidonic acid (Fig. 1.3A) (Esterbauer *et al.*, 1982) and can accumulate in membranes up to 5mM (Uchida, 2003). There are several theoretical mechanisms of 4-HNE formation but the precise route of the transformation from polyunsaturated fatty acids to aldehydes *in vivo* has not been elucidated. It is generally agreed that it is a non-enzymatic free radical process, yielding hydroperoxides that decompose to 4-HNE by fragmentation as primary products (Poli and Schaur, 2000).

The mechanisms proposed for the metabolism of 4-HNE are reduction of the carbonyl group to an alcohol, oxidation to the corresponding carbonic acid and conjugation to GSH via Michael addition of the thiol group by glutathione-s-transferases (GSTs) (Poli and Schaur, 2000). The proteasome pathway is also activated to detoxify 4-HNE-protein adducts (Okada *et al.*, 1999). Aldehyde and alcohol dehydrogenases also play a prominent role in 4-HNE metabolism; 4-HNE metabolites may be excreted as a weak acid or alcohol, respectively. Furthermore, 4-HNE can positively regulate its own metabolism by activating NRF2 (Dalleau *et al.*, 2013).

1.6.2. Protein modifications by 4-HNE

The facile reactivity of 4-HNE is a consequence of the C=C double bond, the C=O carbonyl, and the hydroxyl group, which can participate alone or in sequence in chemical reactions with other molecules. 4-HNE-protein adducts do not occur randomly, rather 4-HNE reacts specifically to sulfhydryl groups and ϵ -amino group of lysine and histidine in proteins, and to lipids and nucleic acids (Esterbauer and Cheeseman, 1990; Uchida and Stadtman, 1992; Schaur, 2003). Reactions of the C=C double bond occur by Michael addition, where a nucleophile, e.g. cysteine or GSH, is added to the C=C double bond. The reaction of the carbonyl group of 4-HNE with thiols lead to the formation of an acetal and the hydroxyl group at carbon 4 can undergo a hemi-acetal formation as a secondary reaction after a Michael addition (Schaur, 2003). Schiff-base formation with primary amines (cysteine, lysine, and histidine) is a

competitive reaction to the Michael addition; this reaction contributes frequently to the crosslinking of proteins by 4-HNE (Uchida and Stadtman, 1992) (Fig. 1.3B). 4-HNE is moderately hydrophobic compared to the more hydrophobic aldehyde 4-hydroxydodecadienal (4-HDDE). Higher hydrophobicity increases the amount of adducts that are made (Bacot, *et al.*, 2003). Mass spectrometry and first-order kinetic measurements of reactivity of amino acids towards 4-HNE have the following order: cysteine >> histidine > lysine (Doorn and Petersen, 2002).

Fig. 1.3 A. Arachidonic acid reaction with free-radicals to form a free-radical intermediate, which further reacts with molecular oxygen to generate two aldehyde fragments, 9-oxo-nanonic acid and 4-HNE (Modified from Schneider *et al.*, 2005). B. 4-HNE reactions with amino acid side chains. Reaction of 4-HNE with proteins occurs primarily by Michael addition to cysteine, histidine and lysine. However, 4-HNE also reacts with lysine to form Schiff base, but this is quantitatively less significant than Michael addition. In a highly oxidizing cellular environment, protein cross-linking reactions involving histidine or lysine residues has also been demonstrated to arise from the bi-functional generation of both Michael and Schiff base adducts (Modified from Jacobs and Marnett, 2009).

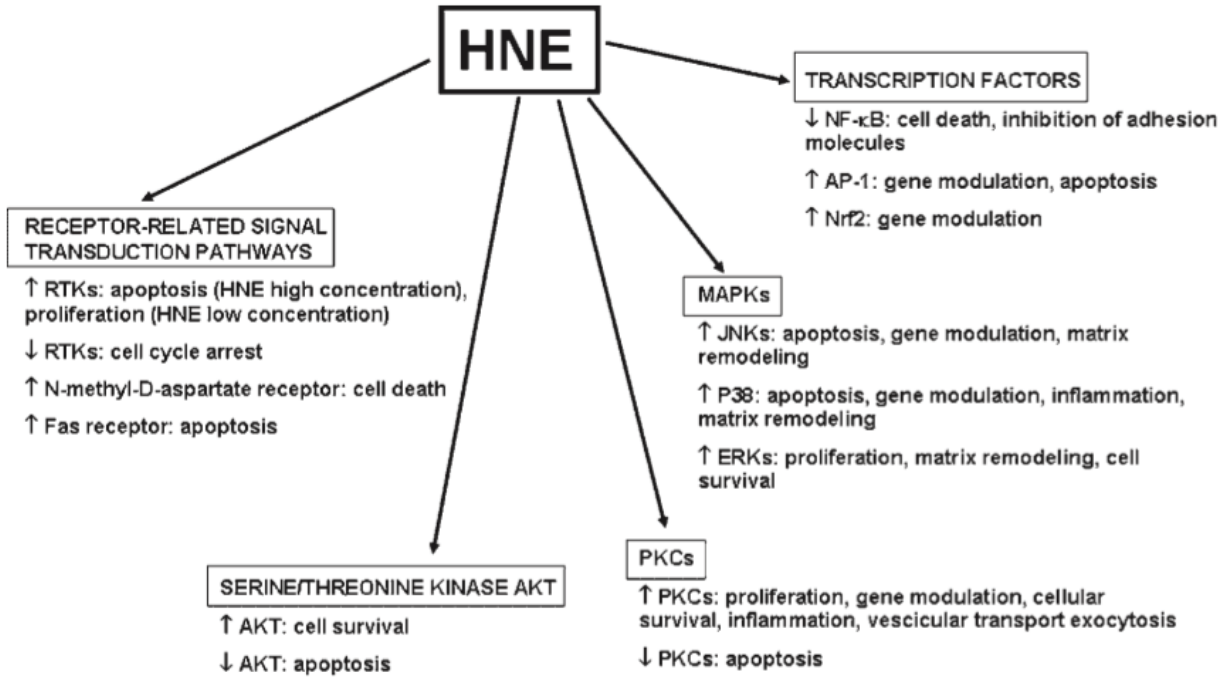
represents one of the main mechanisms by which 4-HNE can influence physiological as well as pathological processes (Petersen and Doorn, 2004). Numerous targets are identified to be adducted by 4-HNE; however, proteins and peptides represent the most important group for 4-HNE targeted biomolecules. The main detoxification peptide of 4-HNE, GSH, will react with 4-HNE via Michael addition spontaneously; however, the conjugation is also catalyzed via GSTs (Petersen and Doorn, 2004). Several other targets of 4-HNE include oxidoreductases (e.g., glutathione reductase, aldose reductase, thioredoxin reductase, alcohol dehydrogenase, Cyp P450), hydrolases (e.g., caspase 3, 20s, 26s-proteasome), protein kinases (e.g., phosphoinositide-specific protein kinase C, C-JUN N-terminal kinase), carriers, receptors, ion channels and transport proteins (e.g., albumin, myoglobin), cytoskeletal proteins (e.g., albumin, tubulin), and energy metabolism enzymes (e.g., glyceraldehyde-3-phosphate dehydrogenase (GAPDH), aldolase A) (Aldini *et al.*, 2006; Carbone *et al.*, 2004; Ferrington and Kapphahn, 2004; Yu *et al.*, 2004; Srivastava *et al.*, 1998; Chiarpotto *et al.*, 1999; Buko *et al.*, 1999; Finkelstein *et al.*, 2005; Hussain *et al.*, 2006; Alderton *et al.*, 2003; Uchida and Stadtman, 1993; Ozeki *et al.*, 2005; Neely *et al.*, 1999). Adduction by 4-HNE usually leads to the inhibition or decrease in protein function, either by modification of the critical or active sites required for normal function or by preventing proper protein folding. For instance, 4-HNE adducts to cysteine 149 of GAPDH, which is at the catalytic site competing with NAD⁺ binding and inhibits the enzymatic functions of the enzyme (Uchida and Stadtman, 1993). In contrast, 4-HNE-protein adducts can activate several targets, such as epidermal growth factor receptor (EGFR), extracellular signal regulated kinases (ERKs) and C-JUN N-terminal kinases (JNKs), contributing to pathogenesis and inducing apoptosis (Liu *et al.*, 1999).

1.6.3. Stress responses to 4-HNE toxicity

4-HNE is both a signaling molecule and a mediator of oxidative stress. By modulating the expression of different genes, it may play a role in growth, differentiation and apoptosis. At physiological concentrations, 4-HNE can activate stress response mechanisms, such as MAPKs, detoxification mechanisms, and inflammatory response, contributing to cell survival against insult. The interaction with a variety of kinases, oxidoreductases, and transferases, all involved in cell signaling, strongly suggests that 4-HNE acts as a second messenger in stress conditions.

The signaling pathways modulated by 4-HNE are diverse; however, the majority are involved in stress responses. They include receptor-related signal transduction pathways (e.g., receptor tyrosine kinases (RTKs), N-methyl-D-aspartate receptor, and Fas receptor), serine/threonine kinase (e.g., AKT), protein kinase C, MAPKs (e.g., JNK, P38, ERK), and transcription factors (e.g., NF- κ B, AP-1, NRF2) (Poli *et al.*, 2008). The consequences of 4-HNE adduction are summarized in Fig. 1.4. Many *in vitro* cell culture experiments have shown that addition of 4-HNE negatively affects cell proliferation by downregulating the expression of genes encoding for C-MYB, CYCLINS D1, D2, and A, and, on the contrary, upregulating P21 (Calonghi, 2002; Barrera, 2004). In addition, differentiation (Barrera *et al.*, 1991), and apoptosis (Deavall, 2012) are also affected by 4-HNE, depending on the intracellular concentration (Poli, 2000). During oxidative stress, 4-HNE mainly induces apoptosis despite the direct induction of GCL through the JNK pathway in cell lines (Dickinson *et al.*, 2002). Addition of increasing concentrations of 4-HNE to cell culture medium induces apoptosis in many cells of diverse origin (Awasthi *et al.*, 2008).

Fig. 1.4. 4-HNE-induced modulation of different cell signaling pathways. (Poli *et al.*, 2008).



1.7 Glyceraldehyde-3-phosphate dehydrogenase (GAPDH)

Glycolytic enzymes are of particular interest as sensitive targets of ROS within the developing embryo because they are critically required for ATP production before and during the metabolic switch (Dumollard *et al.*, 2009). GAPDH is inactivated during periods of oxidative stress and is modified by 4-HNE in several experimental models (Botzen and Grune, 2007; Schutt *et al.*, 2003; Uchida and Stadtman, 1993). Over 200 isoforms of GAPDH exist and although it was once thought to be involved only in cellular maintenance, it is now recognized as an important multifunctional entity (Arcari *et al.*, 1989; Butterfield *et al.*, 2010). The functional avenues that deviate from glycolysis under normal or stress conditions are diverse. GAPDH participates in membrane trafficking, facilitating vesicular tubular clusters (VTCs) shuttling from the endoplasmic reticulum and the Golgi complex by associating with the complex. Tyrosine phosphorylation of GAPDH by protein kinase C, facilitated by RAB 2, increases phospho-GAPDH recruitment to VTCs (Tisdale, 2001). In the presence of nitrosative stress, posttranslational modifications of *S*-nitrosylation commit GAPDH to an irreversible signaling cascade promoting the binding with Siah1, a nuclear localization signal containing U3 ubiquitin ligase, which leads to the nuclear translocation of GAPDH (Sen *et al.*, 2009). The nuclear localization of GAPDH is suggested to control gene transcription by modulating P300/CBP activity (Sen *et al.*, 2008). GAPDH is also involved in a number of different pro-apoptotic mechanisms and been described to a contributing factor in the progression of several degenerative diseases. GAPDH can localize to the mitochondria and induce pro-apoptotic mitochondrial membrane permeabilization via the association with voltage-dependent anion channel 1 (VDAC1) in HeLa, HT29, HEK293, and MCF7 cells (Tarze *et al.*, 2007). In addition to gene modulation through P300/CBP, GAPDH can also be acetylated at Lys-160 by P300/CBP through direct protein interaction, in turn promoting P53-induced apoptosis (Sen *et al.*, 2008). Posttranslational modifications of GAPDH during normal or stress conditions are thought to be responsible for its multiple cellular functions. The diverse roles of GAPDH are described in many cell lines, under different types of stressors and the exact roles in the mammalian system are not clear. Since GAPDH is pharmacologically targeted by selegiline (deprenyl®) in degenerative diseases and this approach is widely used in the clinic, it is critical to better understand its diverse roles in the aging human as well as in the embryo of pregnant women suffering from cognitive decline.

1.7.1. GAPDH in glycolysis

Glycolysis takes place in the cytoplasm and has two stages. GAPDH catalyzes the sixth reaction in glycolysis and represents the beginning of what is referred to as the second stage of glycolysis. Stage one of glycolysis starts with glucose, which is the ubiquitous hexose that is converted to the molar equivalent of two triose-phosphates (i.e. D-glyceraldehyde-3-phosphate (G3P) and dihydroxyacetone phosphate). In stage two G3P is converted to pyruvate, the first reaction of which requires GAPDH and produces 1,3-bisphosphoglycerate (BPG) using NAD^+ as a cofactor. There are 2 net moles of NADH made that are made specifically in the reaction catalyzed by GAPDH (Seidler, 2013).

1.7.2. GAPDH activity and localization

GAPDH exists as a homotetramer (~150 kDa), monomer, and dimer. The tetrameric form is located mainly in the cytoplasm and is comprised of four chemically identical subunits, each approximately 37 kDa, with three asymmetric interfaces between subunits. The monomeric form is localized to the nucleus, mainly during cell proliferation (Cool and Sirover, 1989). Each GAPDH monomer contains two binding domains: an N-terminal NAD^+ -binding domain and a C-terminal catalytic domain (Butterfield *et al.*, 2010). The NAD^+ -binding domain contains amino acid residues 1-151, forming the main-chain, while the catalytic domain consists of residues 315-335, forming the C-terminal helix. The NAD^+ -binding domain is known as the Rossmann fold and is essential to the dehydrogenase activity of GAPDH (Butterfield *et al.*, 2010). The reversible phosphorylation of G3P to BPG, using NAD^+ as a cofactor, involves the nucleophilic attack by the sulfhydryl group of Cys-152 on the carbonyl of G3P to form a hemiacetal. The hemiacetal intermediate is oxidized to a thioester, by hybrid transfer to NAD^+ , in the catalytic domain (Soukri *et al.*, 1989). During oxidative stress, GAPDH activity is inhibited by the oxidation of Cys-152 and it localizes to the nucleus. Several roles have been proposed for nuclear GAPDH subsequent to oxidative insult. In HEK293 cells, following exposure to H_2O_2 , GAPDH enhanced the activity of topoisomerase I by associating with 54 kDa nuclear RNA-binding protein (P54NRB), suggesting a role in regulating transcription and replication (Hwang *et al.*, 2009). Nuclear GAPDH interacts with the transforming growth factor- β -inducible early gene 2 and increases MAO B transactivation, enhancing cell damage in neuronal cells in oxidative stress conditions (Ou *et al.*, 2010). Knockdown of the expression of GAPDH or

treatment with a GAPDH inhibitor, deprenyl, blocked the apoptotic cascade induced by nuclear GAPDH (Ou *et al.*, 2010; Nakajima *et al.*, 2009; Bar-Am *et al.*, 2010). The accumulation of nuclear GAPDH results in protein aggregates leading to the formation of abnormal oligomers and amyloid fibrils, similar to A β and α -synuclein aggregates (Nakajima *et al.*, 2009). On the contrary, GAPDH also participates in DNA repair and cellular protection following genotoxic-induced oxidative stress. GAPDH directly interacts with apurinic/aprimidinic endonuclease 1 (APE1), an essential enzyme that functions in the base excision DNA repair pathway to process spontaneous and drug-induced abasic or apurinic/aprimidinic (AP) sites, to maintain the redox state of the protein, in human colon carcinoma (HTC116) and lung fibroblast (LF1) cell lines (Azam *et al.*, 2008).

1.7.3. GAPDH as a target of 4-HNE

The high sensitivity of GAPDH to oxidative inactivation is attributable to the oxidation of Cys-149 and 152, which is at the catalytic site of the enzyme (Uchida and Stadtman, 1992; Nakajima *et al.*, 2009). However, later studies show that 4-HNE inactivation of GAPDH is not only due to the modification of Cys-149 in the catalytic site but also to several other selective modifications of the amino acids primarily located on the surface of the GAPDH molecule (Ishii *et al.*, 2003). Five amino acid residues were identified to be covalently modified by 4-HNE; His-164, Cys-244, Cys-281, His-327, and Lys-331. Cys-281 and His-164 were very rapidly modified within 5 min, followed by modification of the other amino acids within 30 min in rabbit muscle GAPDH (Ishii *et al.*, 2003). It is suggested that different animal species have shown that the amino acid sequence of covalent attachment ranges over 12 amino acids, including Cys-149 (Allison, 1968). The covalent formation of 4-HNE-GAPDH protein adducts occurs by a Michael addition reaction followed by a significant decline in the enzyme activity (Uchida and Stadtman, 1993; Ishii *et al.*, 2003).

1.8 Deprenyl

In 1935, amphetamine was introduced as a stimulant to treat narcolepsy and for hyperactivity in children. It was also noticed that amphetamines produce certain beneficial effects in parkinsonian patients, improving sleep, muscle strength and rigidity, and elevating mood. In 1968, monoamine oxidase B (MAO-B) inhibitors and methamphetamine derivatives

led to the discovery that deprenyl ((R)-(-)-N,2-dimethyl-N-2-propynylphenethylamine hydrochloride) possessed high potency as an inhibitor of MAO without the “cheese effect” (Knoll, 1983). The “cheese effect” is an adverse drug reaction referring to the increase in dietary amines triggered by MAO inhibitors (MAOIs) that can lead to hypertensive crisis in individuals that ingest foods containing tyramine (Grady and Stahl, 2012). Structurally, deprenyl is a propargylamine derivate; the propargyl moiety is attached to the amino group of methamphetamine. The potent MAOI activity is a result of replacing the phenyl ring of methamphetamine with a furan or an indenyl group resulting in potent inhibition of MAO-B (Knoll, 1986). Deprenyl is widely used as a monotherapy in early Parkinson’s disease or as adjunctive therapy with dopamine replacement as the disease progresses. It is also unconventionally prescribed to treat attention deficit hyperactivity disorder (ADHD) in children (Akhondzadeh *et al.*, 2003).

Deprenyl is labeled a pregnancy category C drug, where no teratogenic effects were observed in pregnant Sprague-Dawley rats at oral doses of 4, 12, and 36 mg/kg or 4, 12 and 25X the human therapeutic dose (based on mg/m²). However, there was a decrease in fetal body weight at the highest dose tested (Somerset Pharmaceuticals, 2009). In rabbits treated with very high doses of 50 mg/kg, an increase in resorptions and a decrease in the number of pups surviving were observed (Hagell *et al.*, 1998). There are no controlled developmental toxicity studies in pregnant women. Several case studies describe women of child bearing age suffering from early onset Parkinson’s disease, progressive bilateral tremor, hypokinesia/bradykinesia, and/or rigidity that were taking deprenyl and who when they became pregnant were advised to discontinue the drug (Hagell *et al.*, 1998). Unintentional exposure of the embryo to deprenyl is a risk and pregnancy should be monitored closely under those circumstances since animal data indicate that the use of deprenyl should be avoided during pregnancy.

1.8.1 Mechanism of action

Deprenyl is a potent irreversible MAO inhibitor with preferred selectivity to MAO B rather than A with a ratio of selectivity (IC₅₀ MAO A/MAO B) of ~ 500. MAOs have substrate specificity, where MAO A selectively catabolizes serotonin, both MAO A and B catabolize dopamine, noradrenaline, and tyramine, and MAO B selectively catabolizes β-phenylethylamine (Magyar, 2011). Deprenyl increases the concentration of dopamine in the CNS, reduces

oxidative stress by lowering H₂O₂ overproduction, which is a byproduct of MAO activity, as well as diminishes the overall amount of ROS and RNS produced (Hornykiewicz, 2001; Tipton *et al.*, 2004). Neuroprotective effects of deprenyl not related to its MAO B inhibition include the inhibition of the activation of MPTP (1-methyl-4-phenyl-1,2,3,6-tetrahydro-pyridine) to MPP⁺ (1-methyl-4-phenyl-piperidine), a toxin, selectively taken up by the dopaminergic system, damaging dopamine-producing neurons (Glover *et al.*, 1986; Langston, 1990). Deprenyl also alters the levels of other proteins linked to apoptosis signaling, like C-JUN, C-FOS, heat shock protein 70 and GAPDH. GAPDH may mediate deprenyl-induced neuroprotection (Tatton *et al.*, 2003). A number of studies using antisense oligonucleotides showed that GAPDH is essential to the progression of some forms of neuronal apoptosis (Tatton *et al.*, 2000). GAPDH mRNA and protein levels increase in neurons at the beginning of apoptosis signaling and are associated with the dense nuclear accumulation of GAPDH, which can serve as a marker of those forms of apoptosis involving GAPDH. Studies with green fluorescent protein tagged GAPDH indicate that GAPDH translocates from the cytosol to the nucleus in some forms of neuronal apoptosis (Shashidharan *et al.*, 1999).

1.8.2 Pharmacokinetics

Deprenyl is a highly lipid-soluble compound, absorbed completely ($t_{max} = 25$ min) and rapidly. In human testing, oral administration resulted in 4% biological bioavailability, maximum plasma concentrations were reached within 0.5 and 1.5 h, and elimination half-life was 70 min (Magyar *et al.*, 2010). Transdermal application provided about 50-fold higher plasma concentration compared to oral drug administration (Barrett *et al.*, 1996). The majority of deprenyl was excreted in the urine and the main metabolite was (R)-methamphetamine (accounting for ~37% of the dose). Other metabolites found in the urine were amphetamine and desmethylselegiline.

1.8.3. Pharmacological inhibition of nuclear GAPDH

The inhibition of the nuclear translocation of GAPDH by deprenyl is unrelated to its MAOI activity, rather it is due to the propargylamine moiety. The propargylamine binds to GAPDH, dissociating the tetrameric form of the protein, maintaining GAPDH as a dimer in the cytosol. GAPDH is stabilized as a dimer and cannot bind to Siah1, thereby preventing its

translocation and upregulation of anti-apoptotic proteins or aggregation (Hara *et al.*, 2006). Other propargylamine-containing compounds prevent the nuclear translocation of GAPDH, allowing neurons to upregulate the levels of anti-apoptotic molecules such as Bcl-2, SOD, GSH, and HSP 70, preventing oxidative stress, maintaining mitochondrial membrane potential, and blocking apoptosis (Tatton *et al.*, 2003). Furthermore, deprenyl-GAPDH binding is associated with decreased synthesis of pro-apoptotic proteins like BAX, C-JUN, and GAPDH (Carlile *et al.*, 2000; Youdim *et al.*, 2006; Maruyama *et al.*, 2001; Olanow, 2006; Tatton *et al.*, 2003). The neuroprotective action of deprenyl appears to be a result of the prevention of GAPDH nuclear translocation rather than the effects of MAO inhibition.

There are very few data on the roles of GAPDH in the embryo, let alone any studies of deprenyl in the embryo. One published study using iodoacetate, an inhibitor of all cysteine peptidases, including the catalytic cysteine residues in proteins such as GAPDH, demonstrated a decrease in glycolytic metabolism and an increase in malformations in embryos at the 3-6 somite stage (Hunter and Tugman, 1995). Unfortunately, cysteine proteases belong to 14 superfamilies plus several unassigned families each containing many sub-families, and thus iodoacetate is not a specific tool to understand the roles of GAPDH.

During organogenesis and fetal stages of development, MAO-B expression is low (Nicotra *et al.*, 2004), only increasing to adult levels postnatally (Diez and Maderdrut, 1977; Nicotra *et al.*, 2004). Furthermore, MAO-B deficient transgenic mice show no overt abnormalities or altered levels of dopamine, norepinephrine or serotonin in the cerebral cortex, substantia nigra or hippocampus (Nicotra *et al.*, 2004). Thus, deprenyl is a good tool to use in the developing embryo to study the roles of GAPDH since it blocks the nuclear translocation of GAPDH without an effect as an MAOI.

Elucidating the roles of GAPDH in the embryo and how GAPDH may promote or prevent apoptosis during developmental toxicant-induced oxidative stress is critical to understanding embryonic development and will help provide strategies to prevent or ameliorate developmental defects.

The objectives of these studies are first to evaluate the impact of oxidative stress-induced by hydroxyurea on specific proteins during important developmental events such as

organogenesis, second to assess the roles of oxidative stress-targeted proteins during insult, and third to determine changes in redox homeostasis that may drive redox-sensitive gene expression. We hypothesize that maternal exposure to hydroxyurea during organogenesis will generate oxidative stress that elicits disruption of critical protein functions, activates stress responses that causes changes in normal gene expression and detrimental events leading to malformations in the embryo.

Research objectives

- (1) To identify the proteins modified by oxidative stress in the conceptus and their roles in mediating the developmental toxicity of HU.
- (2) To determine the effects of manipulating the proteins targeted by oxidative stress and their role during a teratogenic insult.
- (3) To assess the impact of oxidative stress on redox homeostasis and dysregulation of normal gene expression.

Our ultimate goal is to use our understanding of how embryos respond to stress to devise means of protecting the conceptus. These studies will elucidate molecular events in the stress response pathways that are triggered in early embryos by teratogen exposure. Elucidating the consequences of selectively modifying components of the embryonic response to insult will move us towards our goal of decreasing the incidence of birth defects in the population.

Chapter II

Teratogen-induced Oxidative Stress Targets Glyceraldehyde-3-phosphate Dehydrogenase in the Organogenesis Stage Mouse Embryo

Ava Schlisser, Jin Yan, and Barbara F. Hales

Toxicological Sciences (2010) 118(2):686-695.

ABSTRACT

Exposure during the organogenesis stage of the mouse embryo to the model teratogen, hydroxyurea (HU), induces curly tail and limb malformations. Oxidative stress contributes to the developmental toxicity of HU. Reactive oxygen species (ROS) interact with polyunsaturated bilipid membranes to form α,β -unsaturated reactive aldehydes; 4-hydroxy-2-nonenal (4-HNE), one of the most cytotoxic of these aldehydes, covalently adducts with proteins, lipids, and nucleic acids. The goal of the current study is to determine if HU exposure of CD1 mice on gestation day 9 generates region-specific 4-HNE-protein adducts in the embryo and to identify the proteins targeted. The formation of 4-HNE-protein adducts was elevated in the caudal region of control embryos; HU exposure further increased 4-HNE-protein adduct formation in this area. Interestingly, three of the 4-HNE-modified proteins, glyceraldehyde-3-phosphate dehydrogenase (GAPDH), glutamate oxaloacetate transaminase 2, and aldolase 1, A isoform, are involved in energy metabolism. The formation of 4-HNE-GAPDH protein adducts reduced GAPDH enzymatic activity by 20% and attenuated lactate production by 40%. Furthermore, HU exposure induced the nuclear translocation of GAPDH in the caudal region of exposed embryos; this nuclear translocation may be associated with the reactivation of oxidized proteins involved in DNA repair, such as apurinic/apyrimidinic endonuclease-1, and the stimulation of E1A-associated P300 protein/creb-binding protein (P300/CBP) activity, initiating cell death in a P53-dependent pathway. We propose that GAPDH is a redox-sensitive target in the embryo and may play a role in a stress response during development.

INTRODUCTION

Reactive oxygen species (ROS) play a significant role in embryonic development. ROS modulate signaling pathways that promote differentiation, proliferation, and apoptosis (Dennery, 2007). Excess ROS lead to oxidative stress and the perturbation of redox-sensitive signaling pathways, some of which are associated with dysmorphogenesis (Ozolins and Hales, 1997). During midorganogenesis, a period when the embryo is undergoing rapid cellular growth and differentiation leading to major structural changes, ROS may play an important role in mediating teratogenic insult. The mechanisms by which oxidative stress leads to embryotoxicity and teratogenesis are still not fully understood.

ROS contribute to embryonic maldevelopment by modifying redox-sensitive signaling pathways critical to development. During organogenesis, oxidative stress posttranslationally modifies redox-regulated transcription factors with subsequent changes in gene expression in the embryo (Dennery, 2007). A caudal isoform of Wnt, Wnt8c, important for body patterning and organogenesis (Geetha-Loganathan, 2008), is perturbed by H₂O₂, inducing rapid stabilization of b-catenin and increasing the expression of Wnt target genes (Korswagen, 2006). Activator protein-1 (AP-1) is a redox sensitive early response transcription factor composed of Jun and Fos families of nuclear proteins whose gene products are associated with antioxidant defense, cell cycle control, and apoptosis. Hydroxyurea (HU), a free-radical producing teratogen, induces oxidative stress during organogenesis, enhancing the formation of c-Fos heterodimers and leading to increased AP-1 DNA-binding activity (Yan and Hales, 2005). Transgenic overexpression of superoxide dismutase (hSOD1) in dams treated with HU lowers the incidence of malformations (Larouche and Hales, 2009). It is clear that oxidative stress plays a critical role in HU-induced developmental defects.

ROS may also cause embryotoxicity by inducing lipid peroxidation. Free-radical chain oxidation reactions with polyunsaturated fatty acids within cellular membranes produce electrophilic aldehydes (Sayre *et al.*, 2006). 4-Hydroxy-2-nonenal (4-HNE) is one of the most widely recognized and most studied cytotoxic products of lipid peroxidation (Uchida, 2003). 4-HNE is diffusible; it may act locally or be distributed to other tissues through the circulation (Sayre *et al.*, 2006). Michael addition reactions with the side chain of cysteine are highly susceptible to covalent modifications by 4-HNE (Grimsrud *et al.*, 2008). Covalent adducts of 4-HNE are key regulators of the stress response. A number of the protein targets of 4-HNE affect

energy production. Glycolytic enzymes, namely, glyceraldehyde-3-phosphate dehydrogenase (GAPDH), phosphofructokinase, aldolase, and lactate dehydrogenase, are redox sensitive and form covalent modifications with 4-HNE (Novotny *et al.*, 1994). Previous studies from our laboratory have revealed the formation of region-specific 4-HNE adducts in teratogen exposed organogenesis stage mouse embryos.

Glycolytic enzymes are of particular interest as sensitive targets of ROS within the developing embryo because they are critically required for ATP production (Dumollard *et al.*, 2009; Grant, 2008; Neubert, 1970). GAPDH is inactivated during periods of oxidative stress and is modified by 4-HNE in several experimental models (Botzen and Grune, 2007; Schutt *et al.*, 2003; Uchida and Stadtman, 1993). GAPDH, once thought to be involved only in cellular maintenance, is now recognized as an important multifunctional entity. There is compelling evidence that GAPDH is a developmentally critical enzyme that protects the embryo from endogenous and xenobiotic-initiated oxidative stress and DNA damage that results in a broad range of embryopathies. Posttranslational modifications of GAPDH during oxidative stress are thought to be responsible for its multiple cellular functions, including P53-dependent cell death (Hwang *et al.*, 2009; Sen *et al.*, 2008). HU, a model teratogen, is used as an anticancer agent and for the treatment of sickle cell disease. HU is a potent inhibitor of class I ribonucleotide reductase, quenching the tyrosyl free radical within its catalytic center, resulting in inhibition of DNA replication and the induction of oxidative stress. HU exposure on gestation day 9 (GD 9) causes a dose-dependent increase in caudal defects, mainly hindlimb and lumbosacral vertebral column defects. Pretreatment with antioxidants ameliorates HU-induced malformations and impedes the onset of apoptosis (DeSesso, 1981; DeSesso *et al.*, 1994). We have shown previously that HU causes a dose-dependent increase in 4-HNE-protein adduct immunoreactivity in the caudal tissues in organogenesis stage embryos; HU-induced malformations and 4-HNE adducts were increased by treatment with L-buthionine-S, R-sulfoxamine, an irreversible inhibitor of ϵ -glutamylcysteine synthetase that results in the depletion of glutathione and an increase in oxidative stress (Yan and Hales, 2006). The role of 4-HNE-protein adducts in oxidative stress-induced teratogenesis and the region-specific effects and pathways abrogated by 4-HNE that have a potential impact on caudal malformations have yet to be defined. The goal of this study is to determine if HU exposure generates 4-HNE-protein adducts in malformation-

sensitive regions of the embryo, identify the proteins targeted, assess the effects on protein function, and localize 4-HNE-adducted targets.

MATERIALS AND METHODS

Timed-pregnant CD1 mice were purchased from Charles River Canada Ltd (St. Constant, Quebec, Canada) and housed in the McIntyre Animal Resource Centre (McGill University, Montreal, Quebec, Canada). Animal protocols were conducted in accordance with the guidelines outlined in the Guide to the Care and Use of Experimental Animals. CD1 mice mated between 8:00 and 10:00 A.M. (GD 0) were treated with saline (control) or HU (Aldrich Chemical Co., Madison, WI) at 400 or 600 mg/kg by ip injection at 9:00 A.M. on GD 9. Female mice were euthanized by CO₂ and cervical dislocation on GD 9 at 3 h after treatment; each treatment group consisted of 7–12 litters. On GD 9, the uteri were removed and embryos were explanted to Hanks' balanced salt solution (Invitrogen Canada, Inc., Ontario, Canada). Embryos were cut into head, body, and tail sections (Fig. 1). Protein extracts were obtained immediately for assessment of 4-HNE-protein adducts by Western blotting or the analysis of GAPDH enzymatic activity. For two-dimensional (2D) gel electrophoresis, the tail parts from four litters of embryos exposed to vehicle or HU600 were pooled and subjected to protein extraction immediately. Embryos were left whole for lactate assays and immunofluorescence.

1D and 2D gel electrophoresis and Western blot analysis of 4-HNE-protein adducts

For 4-HNE-protein adduct determination using 1D gel electrophoresis, 7.5 µg of protein from each sample was separated by 10% SDS-polyacrylamide gel electrophoresis (PAGE) (15 wells) and then transferred onto equilibrated polyvinylidene difluoride membranes (PVDF) (Amersham Biosciences, Buckinghamshire, U.K.) by electroblotting. Protein concentrations were determined using the Bio-Rad Bradford protein assay (Bio-Rad Laboratories, Ontario, Canada). To analyze GAPDH using Western blotting of proteins from fractionated (head, body, and tail) embryos, 20 µg of protein from each sample was separated by 8% SDS-PAGE and then transferred onto PVDF membranes (Invitrogen Corporation). Membranes were blocked using 10% nonfat milk and then probed with primary antibodies against 4-HNE-protein adducts (1:500; OXIS International, Inc., Foster City, CA), GAPDH (1:1000; Abcam, Inc., Cambridge, MA), and β-actin (1:5000; Santa Cruz Biotechnology, Inc., Santa Cruz, CA) overnight at 4°C.

Membranes were incubated with horseradish peroxidase–conjugated secondary antibodies (1:10,000; GE Healthcare, Buckinghamshire, U.K.) for 2 h at room temperature, and proteins were detected by enhanced chemiluminescence (GE Healthcare). Protein bands were quantified by densitometric analysis using a ChemiImager 400 Imaging system (Alpha Innotech, San Leandro, CA); the peak area represents the intensity of the signal.

For 2D gel electrophoresis, protein determination, separation, and mass spectrometry were conducted by the Genome Quebec Innovation Centre (Montreal, Quebec, Canada). Protein concentration was determined with use of 2D Quant Kit (Amersham, Baie D'Urfe, Quebec, Canada). Fifty micrograms of protein in 155 μ l of Destreak rehydration buffer supplemented with 1% IPG Buffer (3–10 NL, Amersham) were placed in each of four chambers of ZOOM IPGRunner Cassette (Invitrogen). ZOOM Dry Strips (7 cm, pH range 3–10 NL, Invitrogen) were placed in the chambers that were then sealed and left for rehydration for 16 h. The cassette was inserted in ZOOM IPGRunner (Invitrogen Canada, Inc.) and voltage gradient (200–2000 V) was applied as recommended by the manufacturer. A total of 2000 Vh was applied. After isoelectric focusing was completed, strips were equilibrated with SDS using NuPAGE LDS Sample Buffer (1X, Invitrogen Canada, Inc.), reduced with 2% dithiothreitol (DTT, Amersham), and alkylated with iodacetamide (IAA, Sigma). Both steps (DTT and IAA) were done at room temperature for 15 min. Electrophoresis in the second dimension (SDS-PAGE) was done on gradient 4–12% BisTris precast minigels (Invitrogen) immobilized with 1% agarose in XCell SureLock (Invitrogen). The upper and lower chambers were filled with MOPS Running Buffer (Invitrogen); molecular weight standards (Broad Range Protein Molecular Weight Markers, Amersham, 0.9 μ g/gel) were placed in the marker wells, and 200 V were applied for 50 min. After completion of the run, one of every pair of gels was fixed overnight in 50% methanol/10% acetic acid fixation solution and stained with silver nitrate by modified Shevchenko's protocol (Yan et al., 2000). Gel images were acquired on an ImageScanner (Amersham) in TIF format.

Immediately after SDS-PAGE, the second gel was covered with a nitrocellulose membrane, placed between two sheets of Whatman paper and two sponges, and inserted into an XCell II Blot Module (Invitrogen). The module was then placed in XCell SureLock. Transfer Buffer (Invitrogen) supplemented with 10% methanol was added in the module, and protein transfer was carried out at 30 V for 1 h. The quality of the protein transfer was controlled by staining with Ponceau S. The membranes were blocked with 5% skim milk for 1 h at room

temperature after washing off the Ponceau S stain and then probed with primary antibodies against 4-HNE–modified proteins (1:500, OXIS International, Inc.) overnight at 4°C. After incubation with horseradish peroxidase–conjugated secondary antibodies (1:10,000) for 2 h at room temperature, proteins were detected with the same method as 1D gels.

Mass spectrometry

Protein spots on the silver-stained 2D gels that correspond to those detected by immunoblotting of 4-HNE–modified proteins were excised from the gel and subjected to trypsin digestion. Sample injection and high-performance liquid chromatography (HPLC) separation were done using an Agilent 1100 series system (Agilent Technologies, Ontario, Canada). Twenty microliters of digest solution were loaded onto a Zorbax 300SB-C18 5 x 0.3 mm trapping column and washed for 5 min at 15 µl/min with 3% acetonitrile (ACN):0.1% formic acid (FA). Nano-HPLC peptide separation was done using a New Objective (Woburn, MA) Biobasic C18 10 3 0.075 mm picofrit analytical column. The gradient was 10% ACN:0.1% FA to 95% ACN:0.1% FA in 15 min at 200 nl/min.

Mass spectrometry was done with a QTRAP 4000 from Sciex-Applied Biosystems (Concord, Ontario, Canada). Information-dependent mass spectrometry/mass spectrometry (MS/MS) analysis was done on the three most intense ions selected from each full scan MS with dynamic exclusion for 90 s. The survey scan used was an enhanced MS scan from 3500 to 1600 m/z at 4000 amu/s using dynamic fill time. MS/MS data were acquired for three scans from 70 to 1700 m/z using a fixed 25 ms trap fill time and with Q0 trapping activated. Peaklists were generated with Mascot Distiller 1.1 from Matrixscience (Boston, MA). Searches of sequences from NCBI nr database using a rodent taxonomy filter (157,986 sequences) were done with Mascot 1.9 using trypsin as digestion enzyme, carboxyamidomethylation of cysteines as fixed modification, and methionine oxidation as variable modification and 1.5 Da precursor and 0.8 fragment search tolerances.

2D Western blot analysis of GAPDH

Membranes obtained from 2D Western blot of 4-HNE–modified proteins were stripped once with stripping buffer (2% SDS; 62.5mM Tris, pH 6.7; 100mM β-mercaptoethanol). After washing three times with tris-buffered saline tween-20 (0.1% Tween-20) for 10 min each,

membranes were blocked with 5% skim milk for 1 h at room temperature, probed with a primary antibody against GAPDH (1:2000, rabbit polyclonal immunoglobulin G [IgG], Abcam, Inc.) at 4°C overnight, and incubated with horseradish peroxidase–conjugated secondary antibody (1:10,000, GE Healthcare) for 2 h at room temperature. Proteins were detected and quantified with the same protocol as 1D gels.

GAPDH enzyme assay

GD 9 embryos were separated into head, body, and tail and pooled from three litters for each treatment group, homogenized in lysis buffer containing protease cocktail inhibitor, and used for the two-step enzymatic reaction in the production of reduced nicotinamide adenine dinucleotide (NADH). The enzyme assay mixture contained 100mM triethanolamine buffer, pH 7.6, 100mM 3-phosphoglyceric acid, 200mM L-cysteine HCL, 100mM magnesium sulfate, 7.0mM b-nicotinamide adenine dinucleotide, 34mM adenosine triphosphate, and 200 units/ml 3-phosphoglyceric phosphokinase (3-PGK); all reagents were dissolved in deionized water. 3-PGK was added last to start the reaction; all reagents were mixed by inversion and equilibrated to 25°C. Spectrophotometric absorbance was measured for NADH production at 340 nm for approximately 5 min, and the DA340/min was measured using the maximum linear rate for both test and blank.

Lactate assay

GD 9 whole embryos were pooled from three litters from each treatment group, homogenized in lysis buffer, flash frozen, and stored at -80°C. Reaction ingredients, including 700 units/l of lactate oxidase, 508 units/l of peroxidase, 2.0 mmol/l of dichlorobenzenesulfonic acid (DCBSA), and 1.16 mmol/l of 4-aminoantipyrine (4-AAP), were added to the homogenized sample (Policy and Procedure Central Laboratory, Biochemistry, McGill University Health Centre). In the reaction, lactate oxidase converts lactate into pyruvate with the simultaneous generation of hydrogen peroxide (H₂O₂). The H₂O₂ reacts with DCBSA and 4-AAP to form a chromophore, catalyzed by peroxidase. The lactic acid concentration is determined by measuring the change in absorbance at 520 nm.

Immunofluorescence

Three hours after the treatment of dams with HU or vehicle on GD 9, embryos were explanted and immersed in 4% paraformaldehyde for 4 h at 4°C. Embryos were then dehydrated in ethanol, embedded in paraffin, and serially sectioned (5- μ m sections) along the sagittal plane. Tissues were deparaffinized and rehydrated with PBS for 5 min and then incubated for 30 min in blocking serum (0.1% bovine serum albumin, 0.1% Triton X-100, and PBS). Blocking serum was gently tipped off the slides, and then the sections were incubated with GAPDH primary antibody (1:100; Abcam, Inc., diluted in blocking serum) overnight at 4°C in a humidified chamber. Sections were rinsed three times for 5 min in PBS and then incubated with secondary anti-rabbit IgG (1:200; Vector Laboratories, Inc.) diluted in blocking serum for 1 h at room temperature. After washing three times for 5 min in PBS, tissues were counterstained with 4',6-diamidino-2-phenylindole (DAPI) for 5 min and then washed again with PBS for 5 min. Slides were mounted with Vectashield for fluorescence (Vector Laboratories, Inc.). As a negative control, only the secondary antibody was added.

Confocal microscopy and quantitative analysis

A Zeiss LSM 510 Axiovert 100 M confocal microscope with a Plan-Apochromat 363/1.4 oil digital image correlation objective was used to visualize the fluorescent GAPDH stained sagittal sections of embryos treated with vehicle and HU. Optimal settings for laser scanning fluorescence imaging were determined experimentally for both GAPDH antibody and DAPI. All embryos were scanned at a 1.28- μ s pixel time speed with an optical slice of approximately 0.6 μ m, zoom factor equal to one, and a pinhole setting of 82 lm for GAPDH and 1000 lm for DAPI. Z-stack images of six independent vehicle-treated and seven independent HU600-treated embryos were acquired, and quantitative analysis was done with IMARIS Software (Bitplane AG, Zurich, Switzerland). 3D iso-surfaces of vehicle- and HU600-treated embryos were generated. Only lumbosacral somites were analyzed in this study. 3D surface-rendered GAPDH was isolated from the 3D surface-rendered DAPI. The software enabled GAPDH to be subtracted from the cytoplasm, isolating the colocalized DAPI and GAPDH surfaces to be analyzed by intensity mean.

Statistical analyses

Statistical analyses were done by a one-way or a two-way ANOVA on ranks, as appropriate, using the SigmaStat computer program, followed by a post hoc Holm-Sidak or Dunn's analysis of the 1D and 2D gel electrophoresis. A one-way ANOVA, followed by the Bonferroni correction for multiple testing, was done for the GAPDH enzymatic analysis and lactate measurements. A Student's t-test was performed using GraphPrism to test for intensity mean differences. The a priori level of significance was $p < 0.05$.

RESULTS

4-HNE Is Differentially Localized in the Embryo

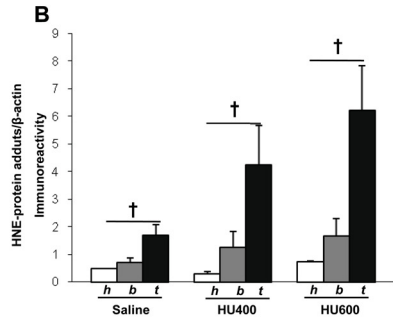
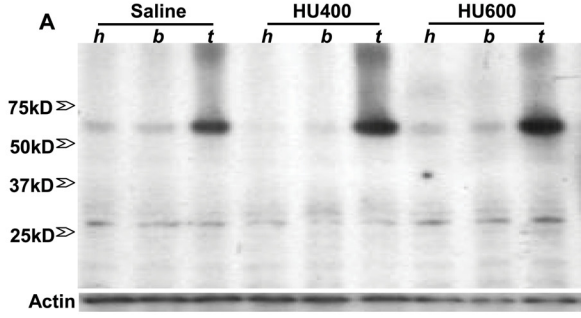
Proteins extracted from head, body, and tail of control and HU-exposed embryos were analyzed by Western blot analysis to determine the relative distribution of 4-HNE-protein adducts. A major 4-HNE immunoreactive band was observed in the 65 kDa molecular weight range (Fig. 2.1A). Interestingly, a higher content of the 65 kDa 4-HNE-protein adducts was found in the tail than in the head or body region of both control embryos and those treated with HU (400 or 600 mg/kg) (Fig. 2.1B). Multiple low intensity bands of 4-HNE-protein adducts were detected below 50kDa (Fig. 2.2A), but none were greater in content in any of the three body regions of the embryo in any treatment group (Fig. 2.1B).

The Identification of 4-HNE-Conjugated Proteins

To identify the 4-HNE-protein adducts enriched in the embryonic tail region, after exposure to vehicle or 600 mg/kg HU, embryo tails were excised and subjected to 2D gel electrophoresis (Fig. 2.2). 4-HNE-modified protein immunoreactivity revealed eight protein spots in both control and HU-treated embryos. According to the molecular weight range, spots 7 and 8 may be the 4-HNE-protein adducts concentrated in the tail part, whereas spots 1–6 may be more evenly distributed throughout the three embryo regions.

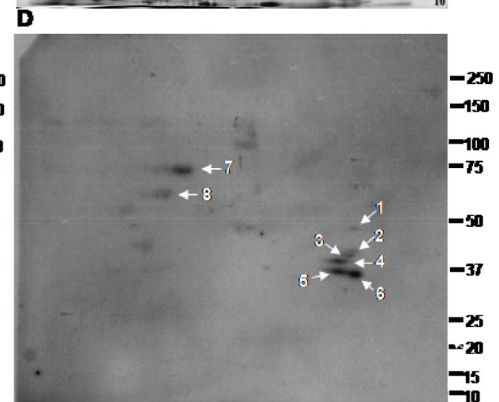
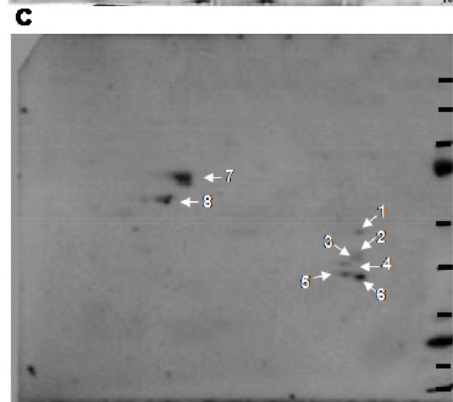
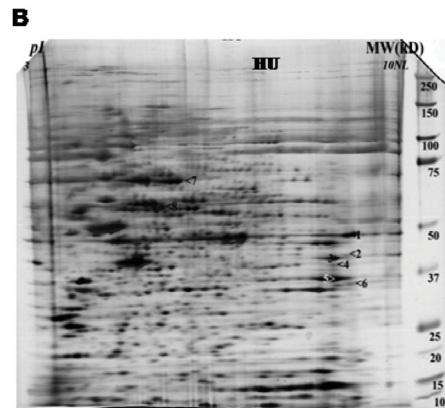
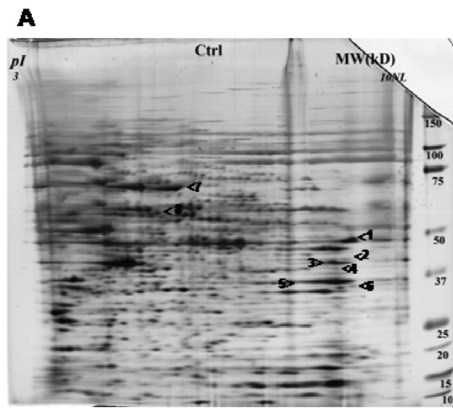
Using MS, identifications were assigned to seven spots (2–8), as summarized in Table 1. The tail-localized 4-HNE-modified proteins were identified as albumin (spot 7), chaperonin subunit theta, and possibly heat shock 60 kDa protein 1 (HSPD1, spot 8). 2D Western blots did not detect a consistent change in the intensity of these three protein adducts when control

Fig. 2.1 Illustration of the separation of the mouse embryo. Head part (h), from the cranial end (top) of the embryo to the caudal end of the first branchial arch; body part (b), the region between the head and the tail part; tail part (t), from the cranial border of the third somites (counted from the caudal end) to the caudal end of the embryo. (A) Western blot analysis of 4-HNE-protein adducts in the three parts of embryos exposed to vehicle (saline) or HU (HU400, 400 mg/kg or HU600, 600 mg/kg). All 4-HNE-protein adducts were quantified by scan densitometric analysis, as indicated in (B). Each bar (mean \pm SEM) represents three litters. “Dagger” denotes a significant difference between different parts of the embryo within the same treatment group ($\dagger p < 0.05$).



embryos were compared with HU-exposed embryos. Interestingly, among the lower molecular weight protein adducts (perhaps not tail specific), three of the identified proteins are involved in energy metabolism. These include glutamate oxaloacetate transaminase 2 (GOT2, spot 2); aldolase 1, A isoform (ALDOA1, spot 3); and GAPDH (spot 5). HU exposure resulted in increases in 4-HNE–conjugated GOT2 (1.6-fold), ALDOA1 (1.6-fold), and GAPDH (1.8-fold) compared with controls. The two remaining 4-HNE–modified proteins that were identified are inducible small cytokine subfamily E member 1 (SCYE1, spot 4) and heterogeneous nuclear ribonucleotide protein A1 isoform a (HNRNP A1A, spot 6). HU exposure increased the amounts of both SCYE1 (1.8-fold) and HNRNP A1A (2.1-fold) compared with control.

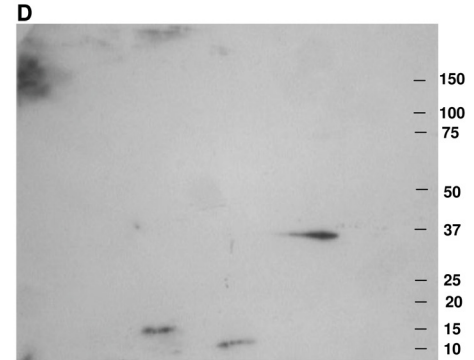
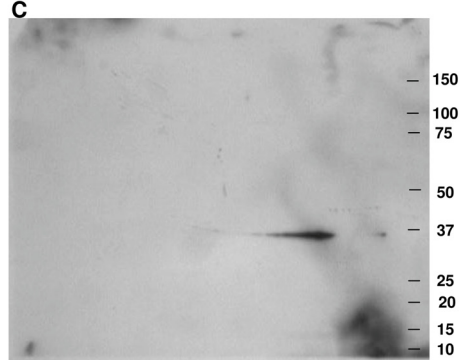
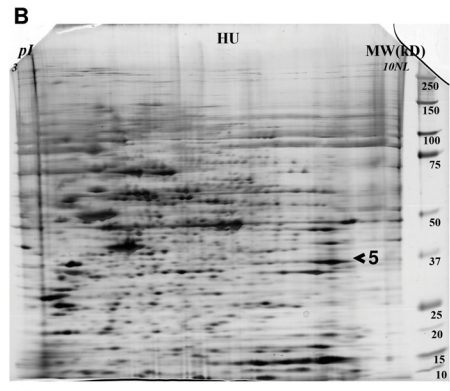
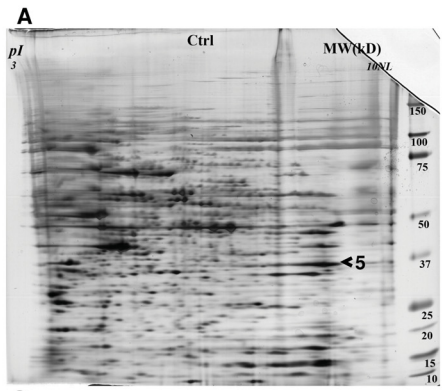
Fig. 2.2. 2D gel electrophoresis of the tail samples obtained from embryos treated with saline (controls, A) or HU (600 mg/kg, B) and the corresponding 2D Western blots illustrating immunoreactive 4-HNE-protein adducts (C, control; D, HU 600 mg/kg treated). Spots 1–8 were analyzed by MS (see Table 1); (n = 2).



4-HNE Modifications Alter GAPDH Protein

Because glycolysis is a critical energy pathway during organogenesis, we further investigated the importance of GAPDH as a 4-HNE-protein target in the malformation-sensitive tail region of HU-exposed embryos using 2D Western blot analysis (Fig. 2.3). Western blots of the tail parts of the embryo exposed to saline or HU600 resulted in an immunoreactive spot that matched that of the spot corresponding to the silver-stained gel identified by MS (Figs. 3C and 3D). At 3 h, HU treatment not only increased 4-HNE-protein adducts with GAPDH but also decreased the amount of GAPDH detected and altered the protein conformation of GAPDH, as reflected by a shortened protein migration tail toward the lower isoelectric point.

Fig. 2.3. 2D gel electrophoresis of the tail samples obtained from embryos treated with saline (control, A) or HU (600 mg/kg, HU600) (B) and the corresponding 2D Western blots illustrating GAPDH immunoreactive protein spots (control, C; HU600, D); (n = 2).



Effects of HU Exposure on GAPDH Enzymatic Activity and Lactate Production

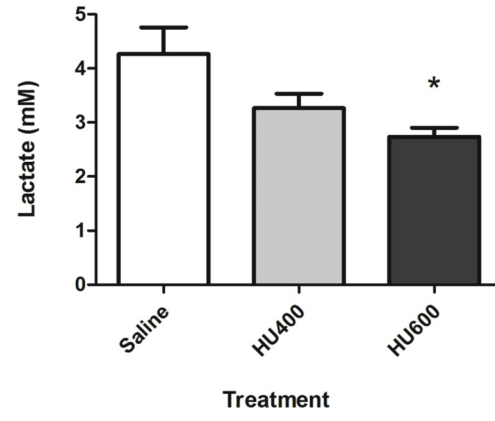
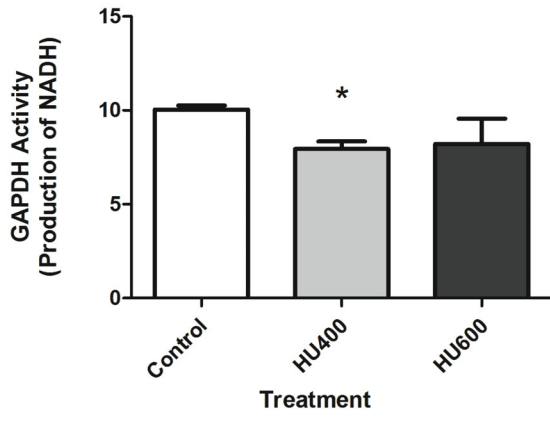
To determine if the formation of GAPDH-4-HNE adducts affected the catalytic activity of GAPDH, we measured its enzymatic activity in the embryo 3 h after exposure of the dams to vehicle or HU. Although GAPDH immunoreactivity in the head, body, and tail were not significantly affected (Supplementary fig. 1), GAPDH activity was significantly decreased in the HU400-treated group (20%), but not the HU600 group, compared with saline (Fig. 2.4A). The appearance of lactate was measured in whole embryos exposed to HU as a measure of the entire glycolytic pathway because lactate is produced predominantly in anaerobic glycolysis and is an important source of ATP production in the embryo. A 20% decrease in lactate production was observed in embryos exposed to HU400, whereas a 40% decrease occurred in embryos exposed to HU600 (Fig. 2.4B).

Table 2.1 The identification of proteins conjugated with 4-HNE in the tail regions of embryos.

Spot No.	Protein name	Function	MW	pI	Sequence Coverage (%)
#1	Unnamed protein	-	50.4	9.1	24
#2	GOT2	Amino acid metabolism, Krebs's cycle	47.8	9.13	28
#3	ALDOA	Glycolysis	39.8	8.31	49
#4	SCYE1	Protein translation, apoptosis	35.5	8.75	40
#5	GAPDH	Glycolysis	36.1	8.44	44
#6	HNRNPA1A	RNA processing	34.3	9.27	23
#7	ALB	Transport protein in serum	70.7	5.75	41
#8	CCT8 HSPD1 (possible)	Chaperone Chaperone	60.1 61.1	5.44 5.91	47 10

MW, molecular weight; pI isoelectric point

Fig. 2.4. (A) Spectrophotometric analysis of NADH as a measure of GAPDH activity in whole embryo samples after treatment with saline (control), low-dose HU (400 mg/kg, HU400), or high-dose HU (600 mg/kg, HU600); (n = 7). (B) Lactate measurements of whole embryo samples treated with saline (control), low-dose HU (400 mg/kg, HU400), or high-dose HU (600 mg/kg, HU600); (n = 3). Asterisk denotes a significant difference between control and treated group (*p < 0.05).



HU Promotes the Nuclear Translocation of GAPDH

In cell cultures, oxidative stress has been reported to induce the nuclear translocation of GAPDH (Nakajima *et al.*, 2007; Oritz-Oritz *et al.*, 2010); thus, we focused on image analysis to localize GAPDH. Initially, confocal microscopy presented discreet homogeneous spots of immunoreactive GAPDH in both vehicle- and HU-treated embryos, and it was challenging to accurately measure nuclear versus cytoplasmic localization in both treatment groups (Fig. 2.5). Consequently, we quantified the subcellular localization of GAPDH with z-stack imaging coupled with IMARIS, an advanced 3D imaging software. The lumbosacral somites, the caudal area with the most significant malformations, were the focus of this analysis. A 3D surface render of GAPDH revealed the subcellular localization of GAPDH. In both vehicle- and HU-treated groups, GAPDH immunoreactivity was unevenly distributed within the 3D projection of a given cell; although GAPDH was present both in the cytoplasm and nucleus, its density increased toward the nuclear membrane (Figs. 2.6A and 2.6B). A masking technique in IMARIS was applied that subtracted the cytoplasmic from the nuclear staining using DAPI as the nuclear border to quantify nuclear GAPDH (Fig. 2.6D). Interestingly, although GAPDH was present within the nucleus of nontreated groups, in agreement with the literature, a twofold increase in the nuclear localization of GAPDH was observed in embryos exposed to HU600 compared with saline-treated embryos (Fig. 2.7).

Fig. 2.5. Confocal microscopy images of saline (control, A) or HU (600 mg/kg, HU600, B)-treated embryos. Green fluorescence represents GAPDH immunoreactivity; (n = 5).

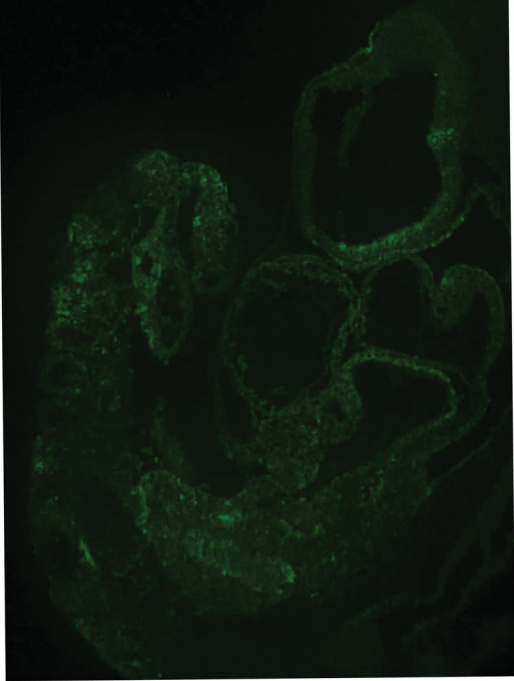
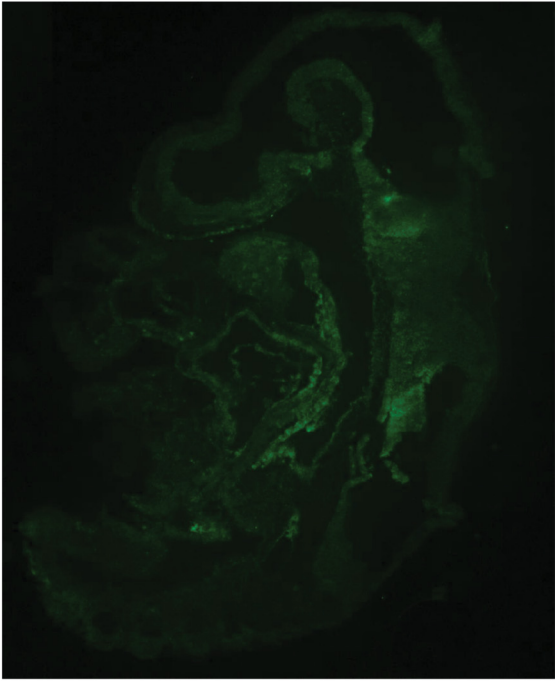


Fig. 2.6. IMARIS 3D-rendered surface of lumbosacral somites (control sample) to show technique. (top left) Raw data, blue: DAPI, green: GAPDH; (top right) 3D-rendered surface of GAPDH and DAPI combined; (bottom left) 3D-rendered surface of DAPI; (bottom right) 3D surface of DAPI removed leaving nuclear GAPDH; (control n = 6, HU600 n = 7).

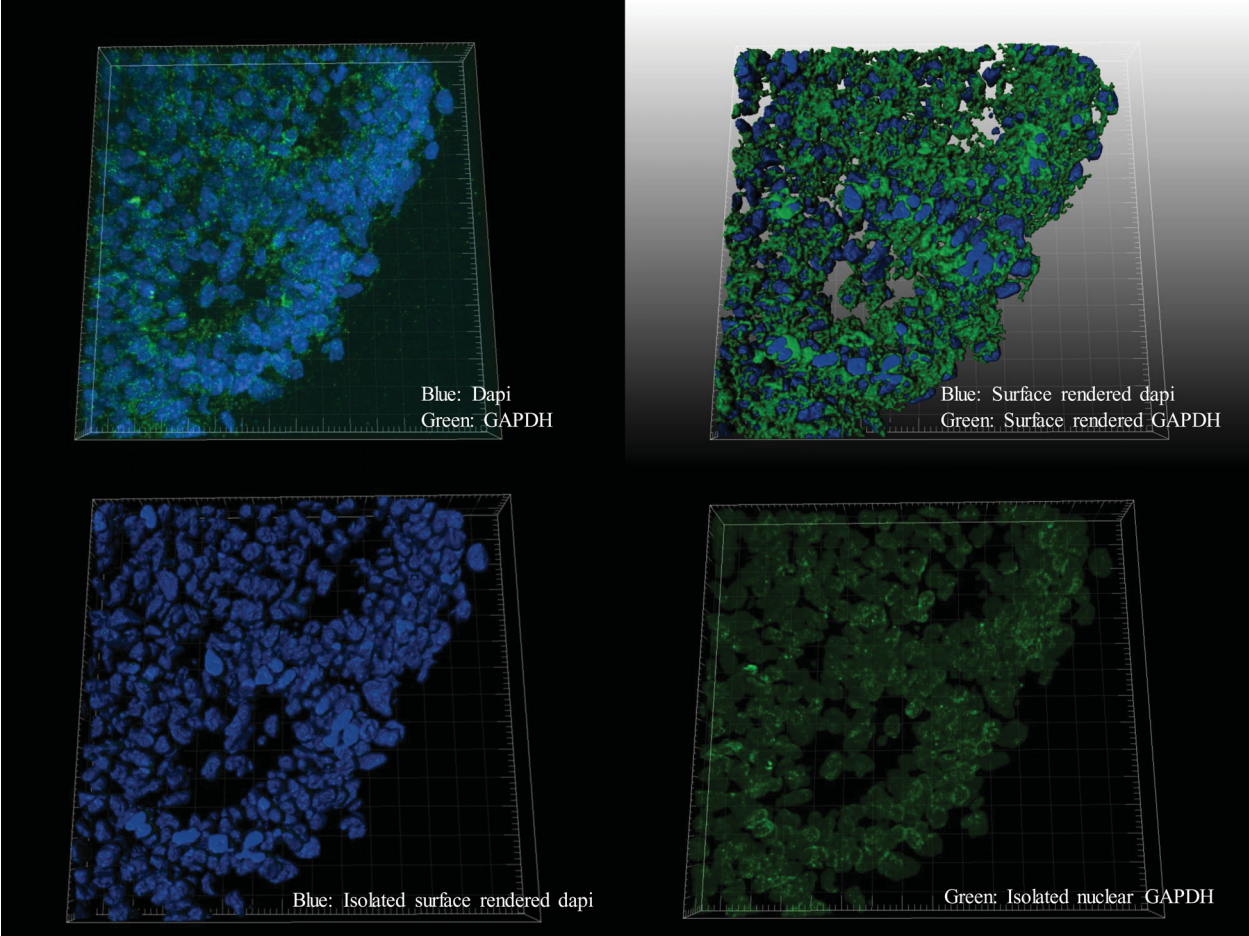
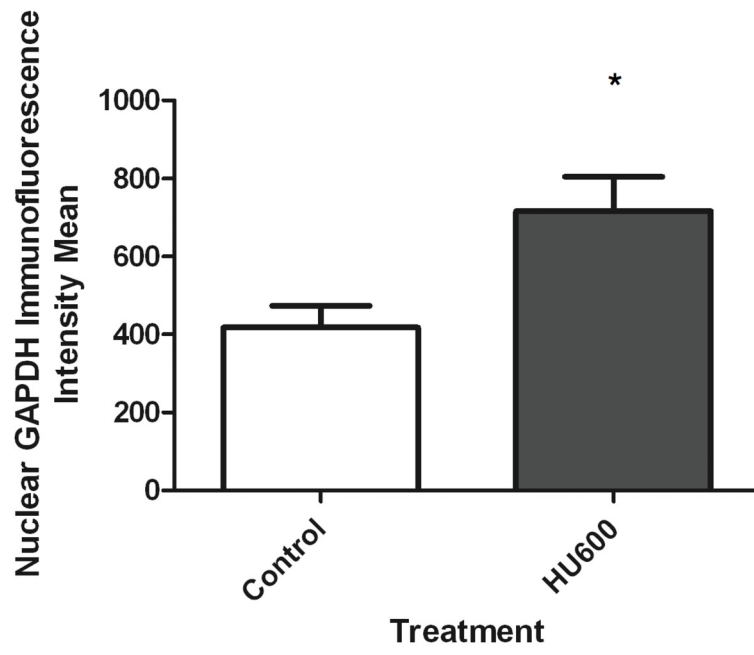


Fig. 2.7 Intensity mean analysis of nuclear GAPDH, provided by IMARIS software, of embryos treated with saline (control) or HU (600 mg/kg, HU600). Asterisk denotes a significant difference between control and treated group (*p < 0.05).



DISCUSSION

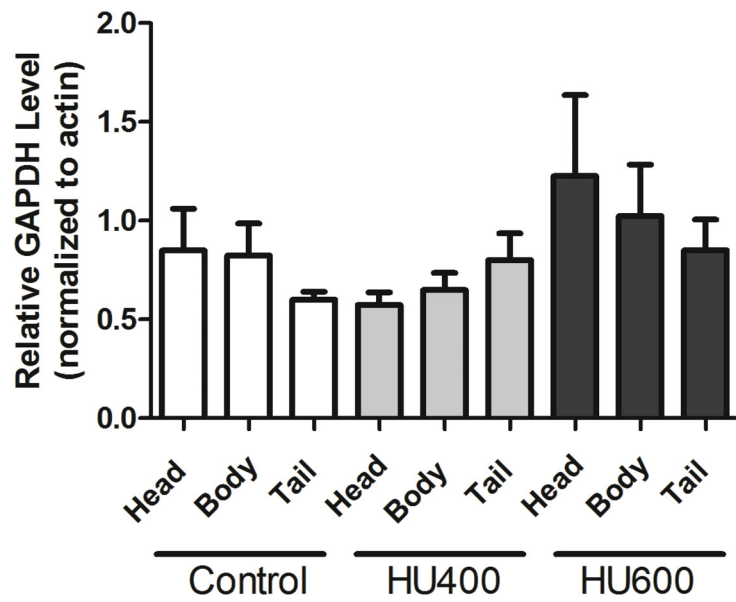
The reactive hydroxylamine group of HU induces ROS, promoting the formation of reactive aldehydes such as 4-HNE through lipid peroxidation (Grimsrud *et al.*, 2008; LoPachin *et al.*, 2009). In previous studies, we reported that 4-HNE-protein adduct immunoreactivity was enhanced in the caudal, malformation-sensitive tissues of embryos exposed to HU. In this study, we identify protein targets of 4-HNE in the tail region of teratogen-exposed embryos. Covalent modifications of 4-HNE to proteins involved in energy metabolism, including GAPDH, were detected. Interestingly, GAPDH, a protein that is critical in glycolysis in the developing embryo, is susceptible to 4-HNE-protein adduct formation. Furthermore, glycolytic metabolism is reduced in treated embryos. During mid-organogenesis (GD 8.5–9.5), the embryo undergoes a metabolic switch from anaerobic to aerobic respiration, coincident with mitochondrial maturation, vascular development, and chorioallantoic coupling (Alcolea *et al.*, 2007; Shepard *et al.*, 1998). At this stage, oxidative phosphorylation has yet to become an important source of energy; indeed, inhibition of the electron transport chain with carbon monoxide on GD 9 does not produce an adverse reaction (Robkin, 1997). Prior to this switch, lactate is the major molecule used in the synthesis of ATP; once this switch has taken place, the reaction equilibrium to pyruvate for transfer into the mitochondria becomes dominant and decreases lactate production. Lactate levels measured in the embryo in this study reflect those of anaerobic glycolysis at GD 9 (4.3 ± 0.8 mmol/l); this is expected to drop (to 2.9 ± 0.3 mmol/l) once the embryo reaches GD 10 (Neubert, 1970). During anaerobic glycolysis, lactate produces only 2 mol of ATP/unit time as compared with aerobic glycolysis, which produces ATP 183x faster. This difference in rate outlines the limitation of anaerobic glycolysis, 2 versus 38 mol of ATP for oxidative phosphorylation. The decrease in glycolytic activity of GAPDH and the subsequent decrease in lactate at this critically susceptible respiratory period suggest that ATP may be deficient during this crucial stage of development. It has been suggested that the reduction of ATP below a critical threshold causes teratogenesis (Ritter *et al.*, 1975). Another glycolytic target of 4-HNE-protein adducts that has been identified within the caudal region of the embryo is fructose-bisphosphate ALDOA1. There are three ALDO isozymes (A, B, and C); ALDOA1 is mainly produced by the developing embryo and is responsible for the conversion of fructose 1,6-diphosphate into dihydroxyacetone phosphate and glyceraldehyde-3-phosphate in the glycolytic pathway. 4-HNE-protein targets in Parkinson's disease were identified to be ALDOA1 and

GAPDH contributing to the metabolic dysfunction of the frontal lobe in the brain (Gómez and Ferrer, 2009); however, there is limited literature reporting that 4-HNE forms protein adducts with ALDOA1. This is the first identification of GAPDH-4-HNE and ALDOA1-4-HNE-protein adducts within the caudal, malformation-sensitive tissue of the developing embryo. Other glycolytic enzymes in muscle, such as enolase, which are a target of 4-HNE-protein adducts, have been shown to have altered enzymatic activity, akin to the enzymatic activity of GAPDH (Hussain *et al.*, 2006). We propose that HU-induced caudal malformations may in part be caused by the aberrant regulation of energy metabolism resulting in cell arrest and death. In response to the decrease in metabolic function of GAPDH, its nuclear translocation is enhanced. Nuclear translocation of GAPDH is hypothesized to be a stress response during exposure to free radicals and to play a role in the initiation of apoptosis in damaged cells. 2D gel electrophoresis reveals that 4-HNE modifies GAPDH. We hypothesize that GAPDH is primarily modified in the cytoplasm where it comes in direct contact with 4-HNE. Once 4-HNE modifies GAPDH, it is then translocated into the nucleus, whereby it may form new complexes with nuclear proteins, such as P300/CBP and P53, to initiate a cell death signaling cascade. Modifications of GAPDH in the cytoplasm in response to oxidative stress are assumed to be the primary event leading to nuclear localization. 4-HNE-conjugated GAPDH has altered electrophoretic mobility, indicating a conformational change. Accumulating evidence suggests that modifications to GAPDH render it an apoptosis executor during oxidative stress (Chuang *et al.*, 2005). In RAW264.7 cell lines, a murine macrophage-like cell line, GAPDH is S-nitrosylated on cysteine 150, abolishing its enzymatic activity (Sen *et al.*, 2008). Upon S-nitrosylation, GAPDH interacts with SIAH1, a protein containing a nuclear localization signal that permits the nuclear translocation of GAPDH because it lacks this sequence. GAPDH becomes acetylated by P300/CBP and mediates apoptosis. The hydroxylamine group of HU has been reported to produce nitric oxide in vivo (Lou *et al.*, 2009); however, whether GAPDH is S-nitrosylated in the fetal embryo at GD 9 and its possible role in mediating the nuclear translocation of GAPDH has yet to be elucidated. In addition to 4-HNE and S-nitrosylation modifications of GAPDH, poly(adenosine diphosphate-ribose) (ADP-ribose) polymerase (PARP) plays an important role in the embryo upon stress. PARP becomes cleaved and activated in response to DNA damage and/or oxidative stress, modifying many specific substrates (Koh *et al.*, 2005). Activated PARP cleaves oxidized nicotinamide adenine dinucleotide (NAD⁺) to nicotinamide and ADP-ribose and polymerizes the

latter on cytoplasmic proteins, nuclear acceptor proteins such as histones, transcription factors, and PARP itself. Poly(ADP-ribosyl) ation contributes to DNA repair and to the maintenance of genomic stability (Wang *et al.*, 1997). However, activation of PARP also depletes cellular NAD⁺, which subsequently triggers ATP depletion (Ha and Synder, 1999). Moreover, there is evidence that GAPDH is modified by poly(ADP-ribosyl)ation, causing it to become enzymatically inactivated and leading to further depletion of ATP. The decrease in energy production in the embryo as a result of the attenuation of glycolysis and the nuclear translocation of GAPDH suggest that GAPDH may serve as an intracellular sensor of oxidation and may play an early and pivotal role in the cascade leading to apoptosis. The translocation of GAPDH from the cytoplasm to the nucleus appears to be a critical step in the induction of apoptosis (Dastoor and Dreyer, 2001). Further insight into protein modifications in region-specific areas of the embryo may better our understanding of its role in oxidative stress-mediated teratogenicity.

SUPPLEMENTAL DATA

GAPDH protein expression in head, body, and tail regions of the embryo following hydroxyurea exposure presented in Supplementary Fig. S2.1. (n=4).



ACKNOWLEDGEMENTS

We thank Leonid Kriazhev, Genome Quebec, for the 2D electrophoresis and mass spectrometric analysis, Ghalib Bardai for the lactate measurements, Cory Glowinski from Bitplane for his diligent efforts and guidance using the IMARIS software, and Anne McKinney from McGill University for her important suggestions and expertise with confocal imaging.

REFERENCES

- Alcolea, M. P., Llado, I., Garcia-Palmer, F. J., and Gianotti, M. (2007). Responses of mitochondrial biogenesis and function to maternal diabetes in rat embryo during the placentation period. *Am. J. Physiol. Endocrinol. Metab.* **293**, E636–E644.
- Botzen, D., and Grune, T. (2007). Degradation of HNE-modified proteins—possible role of ubiquitin. *Redox Rep.* **12**, 63–67.
- Chuang, D. M., Hough, C., Senatorov, V. V. (2005). Glyceraldehyde-3-phosphate dehydrogenase, apoptosis, and neurodegenerative diseases. *Annu. Rev. Pharmacol. Toxicol.* **45**, 269-290.
- Dastoor, Z., and Dreyer, J. L. (2001). Potential role of nuclear translocation of glyceraldehyde-3-phosphate dehydrogenase in apoptosis and oxidative stress. *J. Cell Sci.* **114**, 1643–1653.
- Dennery, P. A. (2007). Effects of oxidative stress on embryonic development. *Birth Defects Res. C Embryo Today* **81**, 155–162.
- DeSesso, J. M. (1981). Amelioration of teratogenesis. I. Modification of hydroxyurea-induced teratogenesis by the antioxidant propyl gallate. *Teratology* **24**, 19–35.
- DeSesso, J. M., Scialli, A. R., and Goeringer, G. C. (1994). D-mannitol, a specific hydroxyl free radical scavenger, reduced the developmental toxicity of hydroxyurea in rabbits. *Teratology* **49**, 248–259.
- Dumollard, R., Carroll, J., Duchon, M. R., Campbell, K., and Swann, K. (2009). Mitochondrial function and redox state in mammalian embryos. *Semin. Cell Dev. Biol.* **20**, 346–353.
- Geetha-Loganathan, P. (2008). Wnt signaling in limb organogenesis. *Organogenesis* **4**, 109–115.

- Grant, C. M. (2008). Metabolic reconfiguration is a regulated response to oxidative stress. *J. Biol.* **7**, 1.
- Grimsrud, P. A., Xie, H., Griffin, T. J., and Bernlohr, D. A. (2008). Oxidative stress and covalent modification of protein with bioactive aldehydes. *J. Biol. Chem.* **283**, 21837–21841.
- Gómez, A., and Ferrer, I. (2009). Increased oxidation of certain glycolysis and energy metabolism enzymes in the frontal cortex in Lewy body diseases. *J. Neurosci. Res.* **87**, 1002–1013.
- Ha, H. C., and Snyder, S. H. (1999). Poly(ADP-ribose) polymerase is a mediator of necrotic cell death by ATP depletion. *Proc. Natl. Acad. Sci. U.S.A.* **96**, 13978–13982.
- Hussain, S. N., Matar, G., Barreiro, E., Florian, M., Divangahi, M., and Vassilakopoulos, T. (2006). Modifications of proteins by 4-hydroxy-2-nonenal in the ventilatory muscles of rats. *Am. J. Physiol. Lung Cell. Mol. Physiol.* **290**, L996–L1003.
- Hwang, N. R., Yim, Y. M., Jeong, J., Song, E. J., Lee, J. H., Choi, S., and Lee, K. J. (2009). Oxidative modifications of glyceraldehyde-3-phosphate dehydrogenase play a key role in its multiple cellular functions. *Biochem. J.* **423**, 253–264.
- Koh, D. W., Dawson, T. M., and Dawson, V. L. (2005). Poly(ADP-ribose)ylation regulation of life and death in the nervous system. *Cell. Mol. Life Sci.* **62**, 760–768.
- Korswagen, H. C. (2006). Regulation of the Wnt/ β -catenin pathway by redox signaling. *Dev. Cell* **10**, 687–688.
- Larouche, G., and Hales, B. F. (2009). The impact of human superoxide dismutase 1 expression in a mouse model on the embryotoxicity of hydroxyurea. *Birth Defects Res. A Clin. Mol. Teratol.* **85**, 800–807.

LoPachin, R. M., Gavin, T., Petersen, D. R., and Barber, D. S. (2009). Molecular mechanisms of 4-hydroxy-2-nonenal and acrolein toxicity: nucleophilic targets and adduct formation. *Chem. Res. Toxicol.* **22**, 1499–1508.

Lou, T. F., Singh, M., Mackie, A., Li, W., and Pace, B. S. (2009). Hydroxyurea generates nitric oxide in human erythroid cells: mechanisms for gammaglobin gene activation. *Exp. Biol. Med.* **234**, 1374–1382.

Nakajima, H., Amano, W., Fujita, A., Azuma, Y. T., Hata, F., Inui, T., and Takeuchi, T. (2007). The active site cysteine of the proapoptotic protein glyceraldehyde-3-phosphate dehydrogenase is essential in oxidative stress-induced aggregation and cell death. *J. Biol. Chem.* **282**, 26562–26574.

Neubert, D. (1970). *Aerobic glycolysis in mammalian embryos*. In *Metabolic Pathways in Mammalian Embryos during Organogenesis and Its Modifications by Drugs*, 1st ed. (R. Bass, F. Beck, H. J. Merker, D. Neubert, and B. Randhahn, Eds.), pp. 225–249. FU-Berlin, Berlin, Germany.

Novotny, M. V., Yancey, M. F., Stuart, R., Wiesler, D., and Peterson, R. G. (1994). Inhibition of glycolytic enzymes by endogenous aldehydes: a possible relation to diabetic neuropathies. *Biochim. Biophys. Acta.* **1226**, 145–150.

Oritz-Oritz, M. A., Moran, J. M., Ruiz-Mesa, L. M., Bravo-San Pedro, J. M., and Fuentes, J. M. (2010). Paraquat exposure induces nuclear translocation of glyceraldehyde-3-phosphate dehydrogenase (GAPDH) and the activation of the nitric oxide-GAPDH-Siah cell death cascade. *Toxicol. Sci.* **116**, 614–622.

Ozolins, T. R., and Hales, B. F. (1997). Oxidative stress regulates the expression and activity of transcription factor activator protein-1 in rat conceptus. *J. Pharmacol. Exp. Ther.* **280**, 1085–1093.

Ritter, E. J., Scott, W. J., and Wilson, J. G. (1975). Inhibition of ATP synthesis associated with 6-aminonicotinamide (6-AN) teratogenesis in rat embryos. *Teratology* **12**, 233–238.

Robkin, M. A. (1997). Carbon monoxide and the embryo. *Int. J. Dev. Biol.* **41**, 283–289.

Sayre, L. M., Lin, D., Yuan, Q., Zhu, X., and Tang, X. (2006). Protein adducts generated from products of lipid oxidation: focus on HNE and one. *Drug Metab. Rev.* **38**, 651–675.

Schutt, F., Bergmann, M., Holz, F. G., and Kopitz, J. (2003). Proteins modified by malondialdehyde, 4-hydroxynonenal, or advanced glycation end products in lipofuscin of human retinal pigment epithelium. *Invest. Ophthalmol. Vis. Sci.* **44**, 3663–3668.

Sen, N., Hara, M. R., Kornberg, M. D., Cascio, M. B., Bae, B. I., Shahani, N., Thomas, B., Dawson, T. M., Dawson, V. L., Snyder, S. H., et al. (2008). Nitric oxide-induced nuclear GAPDH activates p300/CBP and mediates apoptosis. *Nat. Cell. Biol.* **10**, 866–873.

Shepard, T. H., Muffley, L. A., and Smith, L. T. (1998). Ultrastructural study of mitochondria and their cristae in embryonic rats and primate (*N. nemistrina*). *Anat. Rec.* **252**, 383–392.

Uchida, K. (2003). Histidine and lysine as targets of oxidative modifications. *Amino Acids* **25**, 249–257.

Uchida, K., and Stadtman, E. R. (1993). Covalent attachment of 4-hydroxynonenal to glyceraldehyde-3-phosphate dehydrogenase. A possible involvement of intra- and intermolecular cross-linking reaction. *J. Biol. Chem.* **268**, 6388–6393.

Wang, Z. Q., Stingl, L., Morrison, C., Jantsch, M., Los, M., Schulze-Osthoff, K., and Wagner, E. F. (1997). PARP is important for genomic stability but dispensable in apoptosis. *Genes Dev.* **11**, 2347–2358.

Yan, J., and Hales, B. F. (2005). Activator protein-1 (AP-1) DNA binding activity is induced by hydroxyurea in organogenesis stage mouse embryos. *Toxicol. Sci.* **85**, 1013–1023.

CONNECTING TEXT

In chapter II, we demonstrated that exposure to hydroxyurea during organogenesis resulted in the covalent modification of several proteins by 4-HNE in the malformation-sensitive region of the embryo, the caudal area. GAPDH was one of the proteins adducted by 4-HNE. We found that it translocated from the cytoplasm to the nucleus during insult. In chapter III, we pharmacologically inhibited the nuclear translocation of GAPDH with deprenyl to better understand the roles of GAPDH in the developing embryo during oxidative stress conditions. Using confocal microscopy and 3D image analysis, performing a developmental toxicity study, and measuring GSH, we were able to demonstrate a role for GAPDH in the nucleus following hydroxyurea exposure.

Chapter III

Deprenyl Enhances the Teratogenicity of Hydroxyurea in Organogenesis Stage Mouse Embryos

Ava Schlisser, Barbara F. Hales

Toxicological Sciences (2013) 134(2): 391-399.

ABSTRACT

Hydroxyurea, an antineoplastic drug, is a model teratogen. The administration of hydroxyurea to CD1 mice on gestation day 9 induces oxidative stress, increasing the formation of 4-hydroxy-2-nonenal (4-HNE) adducts to redox-sensitive proteins such as glyceraldehyde-3-phosphate dehydrogenase (GAPDH) in the caudal region of the embryo. GAPDH catalytic activity is reduced and its translocation into the nucleus is increased. Since the nuclear translocation of GAPDH is associated with oxidative stress-induced cell death, we hypothesized that this translocation plays a role in mediating the teratogenicity of hydroxyurea. Deprenyl (also known as selegiline), a drug used as a neuroprotectant in Parkinson's disease, inhibits the nuclear translocation of GAPDH. Hence, timed pregnant CD1 mice were treated with deprenyl (10 mg/kg) on gestation day nine followed by the administration of hydroxyurea (400 or 600 mg/kg). Deprenyl treatment significantly decreased the hydroxyurea-induced nuclear translocation of GAPDH in the caudal lumbosacral somites. Deprenyl enhanced hydroxyurea-mediated caudal malformations, inducing specifically limb reduction, digit anomalies, tail defects and lumbosacral vertebral abnormalities. Deprenyl did not augment the hydroxyurea-induced inhibition of glycolysis or alter the ratio of oxidized to reduced glutathione. However, it did dramatically increase cleaved caspase 3 in embryos. These data suggest that nuclear GAPDH plays an important, region-specific, role in teratogen-exposed embryos. Deprenyl exacerbated the developmental outcome of hydroxyurea exposure by a mechanism that is independent of oxidative stress. While the administration of deprenyl alone did not affect pregnancy outcome, this drug may have adverse consequences when combined with exposures that increase the risk of malformations.

INTRODUCTION

The risk of developmental abnormalities in humans is increased by specific maternal conditions and exposure to a number of drugs and environmental chemicals (Schardein, 2000). Although some of these conditions or exposures have distinct targets and etiologies, it has been suggested that oxidative stress may represent a common effector pathway in mediating their developmental toxicity (Ornoy, 2007; Wells *et al.*, 2005). Oxidative stress is produced when reactive oxygen species are generated in amounts that exceed the antioxidant capability of the organism. Organogenesis stage embryos are particularly susceptible to oxidative stress because of their limited capacity to detoxify reactive oxygen species (Yan and Hales, 2005; Schlisser *et al.*, 2010). Exposure to a variety of teratogenic substances, including hydroxyurea, induces oxidative stress in the embryo (DeSesso *et al.*, 1994; Wells *et al.*, 2005).

Hydroxyurea, a potent teratogen in all species tested to date, inactivates ribonucleotide reductase and inhibits DNA synthesis (Kovacic, 2011). In addition to genotoxic stress, hydroxyurea treatment induces oxidative stress. Treatment with hydroxyurea during organogenesis induces malformations (DeSesso *et al.*, 2000; Yan and Hales, 2005). Exposure to hydroxyurea on gestation day nine in the mouse results predominantly in caudal malformations, of the hindlimbs, the lumbar, sacral and caudal vertebrae, and the tail (Yan and Hales, 2005). It is thought that the rapid production of hydrogen peroxide and hydroxyl radicals observed after hydroxyurea treatment contributes to its teratogenicity (DeSesso *et al.*, 2000). Hydroxyurea-induced oxidative stress increases lipid peroxidation, the radical initiated degradation of ω -6-polyunsaturated fatty acids found abundantly in mammalian cells (Esterbauer *et al.*, 1991). Previous studies have shown that 4-hydroxy-2-nonenal (4-HNE), a major product of lipid peroxidation, accumulates in the embryo in malformation-sensitive regions (Yan and Hales,

2006). This 4-HNE forms adducts with proteins, several of which are involved in glycolysis; these include glyceraldehyde-3-phosphate dehydrogenase (GAPDH), aldolase A (ALDOA), and glutamate oxaloacetate transaminase (GOT2) (Schlisser *et al.*, 2010). GAPDH metabolic activity and lactate concentrations are decreased significantly in embryos exposed to hydroxyurea. Furthermore, hydroxyurea exposure increases the translocation of GAPDH into the nucleus. The role of nuclear GAPDH as a key mediator of the action of teratogens that induce oxidative stress is not known.

Diverse functions have been attributed to nuclear GAPDH, ranging from a role in mediating cell death (Sen *et al.*, 2008) to the maintenance of genome integrity (Azam *et al.*, 2008). Indeed, nuclear GAPDH participates in apoptosis, cell cycle regulation, and DNA repair. Oxidative modifications to GAPDH, such as *S*-nitrosylation, increase binding to Siah1, a nuclear localization signal-containing protein, and mediate its nuclear translocation (Ortiz-Ortiz *et al.*, 2010). Nuclear *S*-nitrosylated GAPDH may also be important in cell signaling pathways since it transnitrosylates other nuclear proteins (Kornberg *et al.*, 2010). Modifications to GAPDH may determine its targets within the nucleus. Nuclear GAPDH is acetylated by the P300/CREB-binding complex (CBP); this interaction, in turn, stimulates the catalytic activity of P300/CBP (Sen *et al.*, 2008). Consequently, downstream targets of P300/CBP, such as P53, are activated, resulting in cell death (Sen *et al.*, 2008; Tristan *et al.*, 2011). In addition, nuclear GAPDH up-regulates the expression of pro-apoptotic proteins in the nucleus (Tristan *et al.*, 2011). GAPDH is also modified by PARP-1 catalyzed ADP-ribosylation in response to oxidative stress, inhibiting its interaction with proteins involved in DNA repair and cell cycle regulation, such as uracil-DNA glycosylase (UDG), apurinic/apyrimidinic endonuclease 1 (APE1), and the cyclin B-cdk1 regulatory protein, SET (Meyer-Siegler *et al.*, 1991; Azam *et al.*, 2008; Carujo *et al.*, 2006).

Oxidative stress induced GAPDH nucleocytoplasmic shuffling and modifications are associated with cancer and neurodegenerative diseases, such as Alzheimer's and Parkinson's diseases.

Deprenyl (also known as selegiline, Eldepryl[®]) (R-N-methyl-N-(1-phenylpropan-2-yl)prop-2-yn-1-amine), a selective monoamine oxidase (MAO) B inhibitor, has been used therapeutically in Parkinson's disease; deprenyl potentiates the effects of dopamine and slows down neuronal degradation (Magyar and Szende, 2004). During organogenesis and fetal stages of development, MAO-B expression is low (Nicotra *et al.*, 2004), only increasing to adult levels postnatally (Diez and Maderdrut, 1977; Nicotra *et al.*, 2004). Furthermore, MAO-B deficient transgenic mice showed no overt abnormalities or altered levels of dopamine, norepinephrine or serotonin in the cerebral cortex, substantia nigra or hippocampus (Nicotra *et al.*, 2004). Thus, it is unlikely that any effects of deprenyl in the organogenesis stage embryo are mediated by its effects on MAO-B activity. However, studies on the developmental toxicology of deprenyl in animals showed no teratogenic effects during gestation, although decreases in fetal body weight (at the highest dose tested in the rat study, 36 mg/kg orally) and in resorptions and post-implantation loss (at the highest dose tested in the rabbit study, 50 mg/kg orally) were noted (Human prescription drug label, Somerset Pharmaceuticals, 2009). Deprenyl binds to GAPDH and prevents its interaction with Siah1, an E3-ubiquitin ligase, which translocates GAPDH to the nucleus (Hara and Snyder, 2006).

We hypothesize that the nuclear translocation of modified GAPDH induced by teratogens that trigger oxidative stress plays a role in mediating their development toxicity. To test this hypothesis, we have determined the consequences of inhibiting the GAPDH nuclear translocation induced by hydroxyurea by co-administering deprenyl. We show that, contrary to our expectations, deprenyl treatment enhanced the teratogenicity of hydroxyurea.

MATERIALS AND METHODS

Animal experiments were approved by McGill University under protocol number 1825 and were conducted in accordance with the guidelines outlined in the Canadian Council on Animal Care Guide to the Care and Use of Experimental Animals. Timed-pregnant CD1 mice, mated between 8:00 am and 10:00 am (gestational day 0, GD 0), were purchased from Charles River Canada Ltd. (St. Constant, QC, Canada) and housed in the McIntyre Animal Resource Centre (McGill University, Montreal, QC, Canada). On GD 9 mice were randomly divided into one of six treatment groups. Dams were treated at 8:00 am with (-)-deprenyl (10 mg/kg, Sigma-Aldrich Canada Ltd., Oakville, ON, Canada) or vehicle (saline) by intraperitoneal injection. One hour later, at 9:00 am, mice were treated with hydroxyurea (400 mg/kg or 600 mg/kg, Sigma-Aldrich Canada Ltd.) or vehicle, also by intraperitoneal injection. Dams were euthanized by CO₂ overdose and cervical dislocation on GD 9 at 12:00 pm or on GD 18 at 9:00 am.

On GD 9, the uteri were removed and embryos were explanted into Hank's balanced salt solution (Life Technologies Inc., Burlington, ON, Canada). Embryos collected on GD 9 were subjected to protein extraction for western blot analysis of cleaved caspase-3 and 4-HNE immunoreactivity; alternatively, embryo homogenates were processed for the determination of lactate concentrations. Whole GD 9 embryos were fixed and prepared for immunofluorescence analysis of nuclear GAPDH. Entire litters were used for each experiment.

On GD 18, the uteri were removed and the numbers of resorption sites were recorded (8-10 litters/treatment group). Fetuses were weighed and examined for external malformations or stored in 95% ethanol and stained with alcian blue (cartilage) and alizarin red S (bone) for the assessment of skeletal malformations, as described previously (Yan and Hales, 2005).

Immunofluorescence

Dams were treated with deprenyl or vehicle and 600 mg/kg hydroxyurea or vehicle on GD 9, as described above. Three hours after treatment with hydroxyurea or vehicle, embryos were explanted and immersed in 4% paraformaldehyde for 4 h at 4°C. Embryos were then dehydrated in ethanol, embedded in paraffin and serially sectioned (5 µm sections) along the sagittal plane. Tissues were deparaffinized and re-hydrated with PBS for 5 min each, then incubated for 30 min in blocking solution (0.1% BSA, 0.1% Triton X-100, and PBS). Blocking serum was gently tipped off the slides and then GAPDH primary antibody (1:100; Cat # ab36840, Abcam Inc, MA, USA) diluted in blocking serum was added for an overnight incubation at 4°C in a humidified chamber. Sections were rinsed 3 times for 5 min in PBS and then incubated with secondary goat fluorescein 488 anti-rabbit IgG (H+L) (1:200; Cat # F1-1000, Vector Laboratories, Burlington, Ontario, Canada) diluted in blocking serum for 1 h at room temperature. After washing 3 times for 5 min in PBS, sections were mounted with VectaShield, with 4'-6-diamidino-2-phenylindole (DAPI) for nuclear staining (Vector Laboratories, Inc.). As a negative control, only the secondary antibody was added. Slides were then stored at 4°C and visualized with confocal microscopy within 2 days.

Confocal microscopy and quantitative analysis

A Zeiss LSM 510 Axiovert 100 M confocal microscope with a Plan-Apochromat x63/1.4 oil digital image correlation objective was used to visualize the green fluorescence in GAPDH-immunostained sagittal sections of embryos. Optimal settings for laser scanning fluorescence imaging were determined experimentally for both GAPDH antibody and DAPI. Z-stack images of three independent vehicle-treated and 600 mg/kg hydroxyurea-treated embryos were acquired,

as previously described (Schlisser *et al.*, 2010); quantitative analysis was done with IMARIS Software (Bitplane AG, Zurich, Switzerland). 3D iso-surfaces of vehicle- and 600 mg/kg hydroxyurea-treated embryos were generated. Only the lumbosacral somites were analyzed in this study since they were identified previously as a predominant site of 4-HNE-protein adducts and nuclear GAPDH translocation (Yan and Hales, 2006; Schlisser *et al.*, 2010).

Western blot analysis of cleaved caspase-3 and 4-HNE-protein adducts

Protein concentrations were determined using the Bio-Rad Bradford protein assay (Bio-Rad Laboratories, Hercules, CA). For cleaved caspase-3 analysis and 4-HNE protein adduct determination, proteins (20 μ g) from embryos from each treatment group were resolved by 10% sodium dodecyl sulfate (SDS)-polyacrylamide gel electrophoresis and then transferred onto equilibrated polyvinylidene difluoride membranes (PVDF) (Amersham Biosciences, Buckinghamshire, UK) by electroblotting. Membranes were blocked using 10% non-fat milk, and then probed for primary antibodies against cleaved caspase-3 (1:1000; rabbit polyclonal IgG, Cell Signaling Technology, Inc., Danvers, MA, Catalog # 9661L), 4-HNE-protein adducts (1:500; mouse monoclonal IgG, Oxis International Inc., Beverly Hills, CA, Catalog # 24327), GAPDH (1:1000; rabbit polyclonal IgG, Abcam, Inc, Catalog # ab36840), or β -actin (1:500; donkey polyclonal IgG, Santa Cruz Biotechnology, Inc., Santa Cruz, CA, Catalog # sc-2056) overnight at 4°C. Membranes were incubated with horseradish peroxidase-conjugated secondary antibodies for cleaved caspase-3, GAPDH, 4-HNE, and β -actin (1:10,000; GE Healthcare, Buckinghamshire, UK) for 2 h at room temperature and proteins were detected by enhanced chemiluminescence (Amersham Biosciences). Protein bands were quantified by densitometric

analysis using a ChemiImager 400 Imaging system (Alpha Innotech, San Leandro, CA); the peak area represented the intensity of the signal.

Assessment of skeletal malformations

Ethanol-fixed GD 18 fetuses were immersed in a water bath (70°C) for 7 s. The fetuses were skinned, eviscerated, and placed in 95% ethanol overnight. The ethanol was decanted and replaced with alcian blue solution (15 mg alcian blue; 80 ml 95% ethanol; 20 ml glacial acetic acid) for 24 h. This solution was then replaced with 95% ethanol. After 24 h, the ethanol was substituted with alizarin red S solution (25 mg/l alizarin red S in 1% potassium hydroxide) for 24 h. The dye was drained and replaced with 0.5% potassium hydroxide for 24 h. The skeletons were placed in a 2:2:1 solution (2 parts 70% ethanol: 2 parts glycerin: 1 part benzyl alcohol). After 24 h, stained skeletons were placed in 1:1 solution (1 part 70% ethanol: 1 part glycerin) for subsequent analysis of skeletal malformations, as previously described (Yan and Hales, 2005).

Lactate assay

GD 9 embryos were pooled from vehicle and drug treated dams; there were 4 samples for each group with each sample representing 2 litters. Samples were homogenized in PBS, flash frozen, and stored at -80°C. Lactate concentration was determined with the use of a Lactate Assay Kit (Biovision Research Products, Mountain View, CA). Ingredients, including lactate assay buffer, lactate probe (in anhydrous DMSO), lactate enzyme mix, and L(+)-lactate standard (100 nmol/μl), were added to the homogenized samples. Lactate concentrations were determined by measuring the change in absorbance at 570 nm. Lactate contents (nmol) were determined

from the standard curve and adjusted for protein content, assessed using the Bio-Rad Bradford protein assay.

Glutathione determinations

On GD 9, embryos were explanted into Hank's balanced salt solution, flash frozen in liquid nitrogen, and stored at -80°C . Samples were defrosted and homogenized with 5-sulfosalicylic acid (5%, w/v). Both total (GSH + GSSG) and oxidized (GSSG) glutathione were assayed using the Microplate Assay for GSH and GSSG from Oxford Biomedical Research (Cedarlane Laboratories Ltd., Burlington, ON, Canada, Product # GT40). Briefly, the reaction of GSH with Ellman's reagent (5,5'-dithiobis-2-nitrobenzoic acid (DTNB)) gives rise to a product that is quantified spectrophotometrically at 412 nm (SPECTRAMax PLUS 384, Molecular Devices, Sunnyvale, CA). A pyridine derivative is used as a thiol-scavenging reagent to assess the relative amounts of GSH and GSSG. Oxidative stress is represented as the ratio of GSSG to GSH.

Statistical analyses

Statistical analyses were done by chi-square and two-way ANOVA, as appropriate, followed by a *post hoc* Bonferroni's correction for multiple comparisons, using the GraphPad Prism computer program. The *α priori* level of significance was $p < 0.05$.

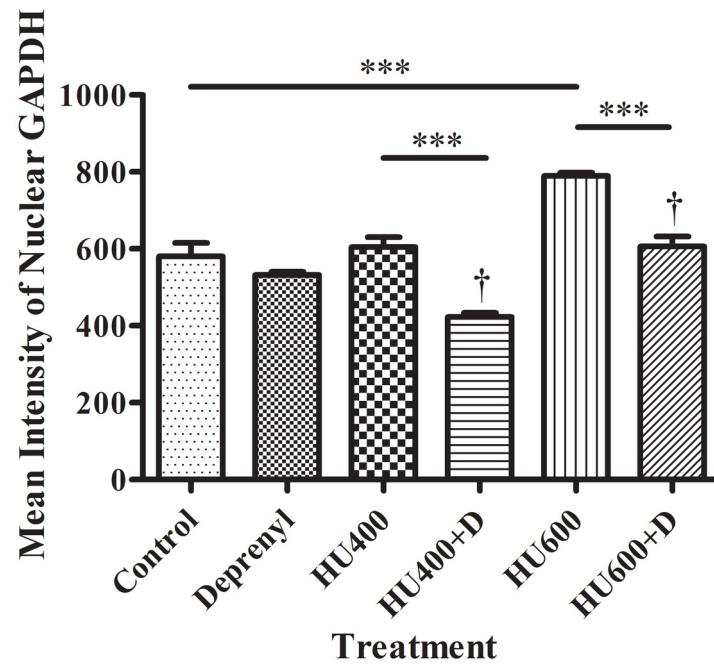
RESULTS

Deprenyl inhibited the hydroxyurea-induced nuclear translocation of GAPDH in the lumbosacral somites

Immunofluorescence confocal microscopy and IMARIS 3D image analysis were done to quantify nuclear GAPDH. Treatment with deprenyl alone did not affect the amount of GAPDH reactivity in cell nuclei in the lumbosacral somites (Fig. 3.1). While treatment with 400 mg/kg hydroxyurea did not increase the nuclear GAPDH content, exposure to 600 mg/kg hydroxyurea did significantly increase GAPDH nuclear translocation compared to control. Deprenyl co-treatment significantly reduced nuclear GAPDH content relative to the respective groups treated with hydroxyurea alone (Fig. 3.1). Thus, co-treatment with deprenyl did inhibit the nuclear translocation of GAPDH induced by hydroxyurea in organogenesis stage embryos.

Western blot analysis of 4-HNE-tagged proteins revealed that 4-HNE immunoreactivity was found predominantly in the same molecular weight range as GAPDH immunoreactivity (Supplementary data, Fig. S3.1A). Exposure to deprenyl alone, hydroxyurea alone, or the combination, did not significantly increase 4-HNE immunoreactivity in this molecular weight range, although there was a tendency towards an increase in embryos exposed to high dose hydroxyurea (600 mg/kg) (Supplementary data, Fig. S3.1B). Thus, the decrease in nuclear GAPDH in embryos exposed to deprenyl and hydroxyurea was not a consequence of an overall effect on 4-HNE-tagged GAPDH.

Fig 3.1. Analysis of the confocal images of GAPDH immunofluorescence in the lumbosacral regions of GD 9 embryos using IMARIS. The immunofluorescence intensity of isolated nuclear GAPDH is represented here. HU 400, 400mg/kg hydroxyurea; HU600, 600mg/kg hydroxyurea; D, deprenyl. Two-way ANOVA and a post hoc Bonferroni correction were done. Asterisks (***) denote a statistically significant difference ($p < 0.001$). † denotes a significant difference between the hydroxyurea-treated groups in the absence and presence of deprenyl ($p < 0.05$).



Effects of deprenyl and hydroxyurea on pregnancy outcome

Timed pregnant females were treated with deprenyl or vehicle prior to the administration of hydroxyurea to determine the effects of deprenyl co-administration on the teratogenicity of hydroxyurea. Treatment with deprenyl in the presence or absence of hydroxyurea did not affect the numbers of implantation sites per litter (Table 3.1). While treatment with 400 mg/kg hydroxyurea did not significantly affect the incidence of resorptions or the number of viable fetuses per litter, treatment with the high dose hydroxyurea (600 mg/kg) increased the number of resorptions and decreased the number of live fetuses per litter. Co-treatment with deprenyl did not alter these measures of pregnancy outcome. Treatment with deprenyl alone did result in a statistically significant but small (3%) decrease in mean fetal weights per litter. Hydroxyurea treatment produced a dose-dependent decrease in mean fetal weights per litter (Table 3.1). Treatment with deprenyl and 400 mg/kg hydroxyurea resulted in a significant reduction in fetal weights per litter; no further reduction was observed in the litters exposed to deprenyl and high dose hydroxyurea.

The administration of deprenyl alone did not significantly increase the mean number of malformed fetuses per litter (Fig. 3.2A), although one fetus with curly tail (1 of 91) was observed in this treatment group. Exposure to hydroxyurea (400 or 600 mg/kg) increased the mean number of malformed fetuses per litter in a dose dependent manner. Treatment with deprenyl in combination with hydroxyurea significantly increased the mean number of malformed fetuses per litter in both the 400 and 600 mg/kg hydroxyurea treatment groups compared to those treated with hydroxyurea alone. While some forelimb defects were observed in fetuses exposed to 400 mg/kg hydroxyurea (4.5%), 600 mg/kg hydroxyurea (9.7%), and 600 mg/kg hydroxyurea plus deprenyl (6.5%) (data not shown), the majority of the external malformations observed were in

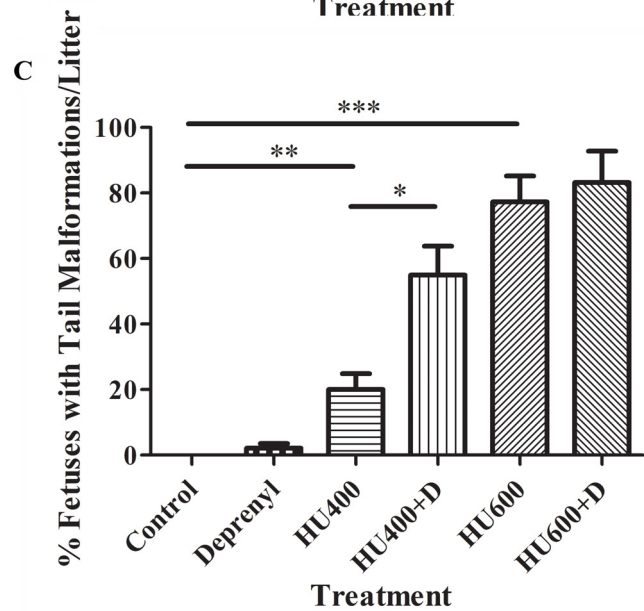
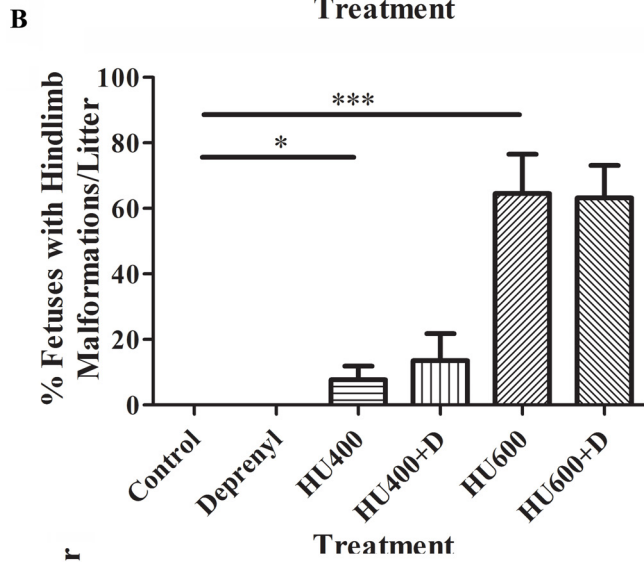
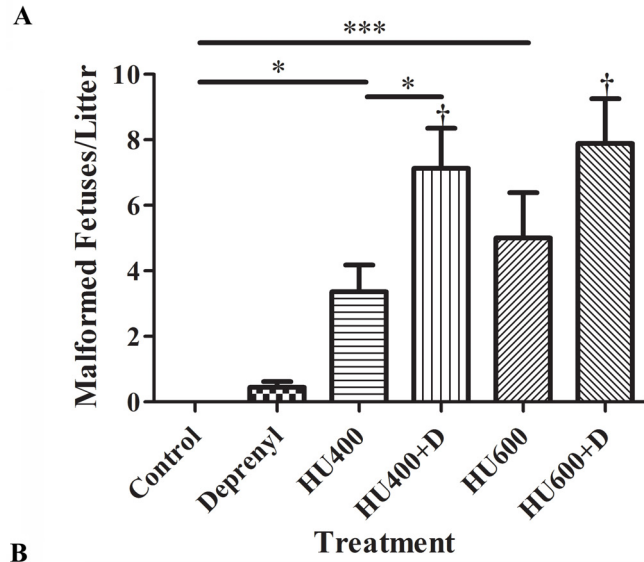
Table 3.1**Cesarean Section Observations for Dams Treated with Hydroxyurea and/or Deprenyl on Gestational Day 9**

	Saline	Deprenyl	HU (400 mg/kg)	HU (400 mg/kg) + Deprenyl	HU (600 mg/kg)	HU (600 mg/kg) + Deprenyl
Number of dams	9	9	10	8	9	9
Implantation sites	12.0 ± 2.8	10.8 ± 4.5	11.9 ± 1.9	12.6 ± 2.3	12.6 ± 2.3	12.9 ± 1.4
Late resorptions	0.3 ± 0.5	1.2 ± 2.0	1.9 ± 1.8	1.8 ± 1.6	6.1 ± 3.4***	4.1 ± 3.6*
Viable fetuses	11.7 ± 2.9	10.1 ± 4.1	10.1 ± 2.9	11.0 ± 1.6	6.1 ± 5.6*	7.6 ± 5.1
Fetal weights (g)	1.36 ± 0.05	1.32 ± 0.1*	1.27 ± 0.11*	1.16 ± 0.14*†	1.05 ± 0.07*	1.06 ± 0.07*

The data are presented as mean/ litter values ± standard errors of the mean. Two-way ANOVA and a *post-hoc* Bonferroni correction were used to determine significance. Asterisks (*) or (***) denote a statistically significant difference ($p < 0.05$) or ($p < 0.0001$), respectively, from controls; † denotes a significant difference between the HU-treated groups in the absence or presence of deprenyl ($p < 0.05$).

the caudal region. A spectrum of hindlimb defects was observed in fetuses exposed to 400 or 600 mg/kg hydroxyurea; these included agenesis, truncation of hindlimbs, showing complete absence of the phalanges and carpals, aplasia/hypoplasia of the first digit or of more than one digit, syndactyly, ectrodactyly, and polydactyly. Deprenyl co-administration did not significantly enhance the hindlimb malformations induced by 400 or 600 mg/kg hydroxyurea (Fig. 3.2B). However, deprenyl did significantly increase the tail malformations observed in litters exposed to 400 mg/kg hydroxyurea (Fig. 3.2C). Deprenyl co-administration did not result in a further increase in the already high incidence of tail malformations induced by exposure to 600 mg/kg hydroxyurea.

Fig. 3.2 The incidence of external malformations in fetuses from the litters of dams treated with saline, deprenyl, and/or hydroxyurea (HU) on GD 9. (A) The mean number of malformed fetuses per litter. (B) Fetuses presenting strictly with a hindlimb malformation were counted and are represented as a percentage of the live fetuses without a malformation. (C) Fetuses presenting strictly with a curly/hypoplastic tail were counted and are represented as a percentage of the live fetuses without a malformation. Numbers represent means \pm standard errors of the mean. The statistical analysis carried out was a two-way ANOVA followed by Dunnett's test. Asterisks (*), (**), and (***) denote a statistically significant difference ($p < 0.05$), ($p < 0.01$), and ($p < 0.001$). † denotes a significant difference between the hydroxyurea-treated groups in the presence or absence of deprenyl ($p < 0.05$).



The skeletal assessment of fetuses from the litters exposed to hydroxyurea revealed a significant increase in lumbosacral vertebral, hindlimb and tail defects, as anticipated from the external malformations that were observed (Table 3.2); examples of these defects are shown in Figure 3.3. Control and deprenyl treated fetuses appeared normal (Fig. 3.3). Fetuses exposed to 400 mg/kg hydroxyurea had shortened or kinked tails and digit hypoplasia. Fetuses exposed to 400 mg/kg hydroxyurea and deprenyl were generally more severely malformed than those treated with hydroxyurea alone; these fetuses tended to be smaller, with numerous vertebral column defects (fused, misaligned, and partial ossification of the vertebrae), missing lumbar and sacral vertebrae, tail aplasia, shortening of hindlimb long bones (tibia hypoplasia, femur hypoplasia), digit hypoplasia, neural tube defects, cranio-facial defects, partial ossification of ribs and sternum, and forelimb digit hypoplasia. Similar malformations were observed in the 600 mg/kg hydroxyurea exposed fetuses; these included fused and partial ossification of the thoracic vertebrae, partial ossification of the sacral vertebrae, hindlimb long bone malformations (femur hypoplasia, bent fibula), and hindlimb digit hypoplasia. Fetuses exposed to deprenyl and 600 mg/kg hydroxyurea displayed a variety of vertebral column defects (fused and misaligned vertebrae, partial ossification of the centra), partial ossification of the lumbar vertebrae, missing sacral vertebrae, tail aplasia, shortening of the hindlimbs (tibia and femur hypoplasia), hindlimb digit hypoplasia, shortening of the forelimbs (hypoplasia of the radius and ulna), partial ossification of the supraoccipetal bone, and partial ossification of ribs and sternum (Fig. 3.3).

A quantitative analysis of the predominant lumbosacral vertebral, hindlimb, and tail defects observed after treatment with hydroxyurea in the absence or presence of deprenyl is presented in Table 3.2. Exposure to saline or deprenyl had either no effect or a minimal effect (mild shortening of the tail with deprenyl alone) on skeletal development (Table 3.2). Fetuses from

litters exposed to hydroxyurea alone had lumbosacral vertebral malformations (400 mg/kg: 10.0%; 600 mg/kg: 53.3%), hindlimb malformations (400 mg/kg: 10.0%; 600 mg/kg: 33.3%), and tail aplasia (400 mg/kg: 40.0%; 600 mg/kg: 86.7%). The incidence of lumbosacral vertebral and hindlimb malformations was significantly increased in the group exposed to 600 mg/kg hydroxyurea and deprenyl in comparison to those treated with 600 mg/kg hydroxyurea alone (Table 3.2).

Table 3.2

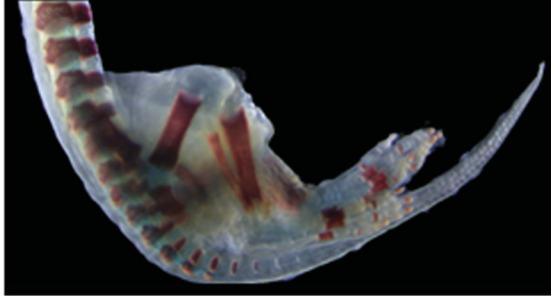
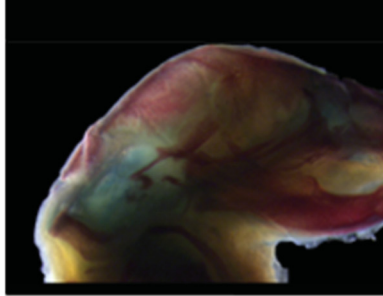
Fetal Axial Skeletal Defects

	Saline	Deprenyl	HU (400 mg/kg)	HU (400 mg/kg) + Deprenyl	HU (600 mg/kg)	HU (600 mg/kg) + Deprenyl
Fetuses (litters)	32(9)	19(9)	20(5)	16(8)	15(9)	21(8)
Abnormal supraoccipetal	-	-	1(1)	-	-	3(3)
Abnormal thoracic vertebrae	-	-	1(8)	-	-	-
Abnormal sternbrae	-	-	-	1(1)	-	1(1)
Forked ribs	-	-	-	1(1)	-	-
Abnormal forelimbs	-	-	-	2(1)	2(2)	3(3)
Abnormal lumbosacral vertebrae	-	-	2(2)	2(1)	8(6)***	15(8)*** †
Abnormal hindlimbs	-	-	2(2)	2(2)	5(5)**	13(8)***†
Amelia	-	-	-	-	-	1(1)
Femur hypoplasia	-	-	1(1)	-	1(1)	-
Tibial aplasia/hypoplasia	-	-	1(1)	-	1(1)	-
Fibula bent	-	-	-	-	1 (1)	-
Digital aplasia/hypoplasia	-	-	2(2)	2(2)	5(5) **	13(8) ***†
Tail aplasia/hypoplasia	-	2(2)	8(5)***	8(8)***	13(9) ***	18(8) ***

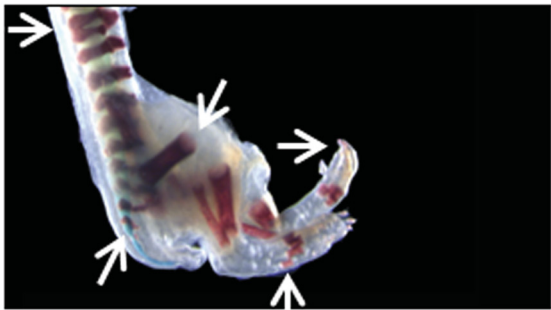
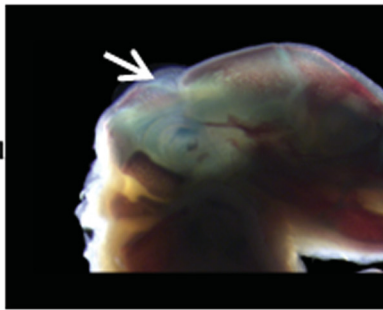
HU: hydroxyurea. The data are presented as number of fetuses (litters). Statistical analysis was done with two-way ANOVA and Dunnett's *post-hoc* test. Asterisks (**) or (***) denote a statistically significant difference ($p < 0.01$) or ($p < 0.0001$), respectively, compared to controls. † denotes a significant difference between the hydroxyurea-treated groups in the presence or absence of deprenyl ($p < 0.05$).

Fig. 3.3. Illustrations of some of the skeletal defects observed in GD 18 fetuses after exposure to saline (control) or deprenyl and 600mg/kg hydroxyurea. Bones appear red (alizarin red S); cartilage appears blue (alcian blue). Malformations are indicated by arrows and described in the text.

Control



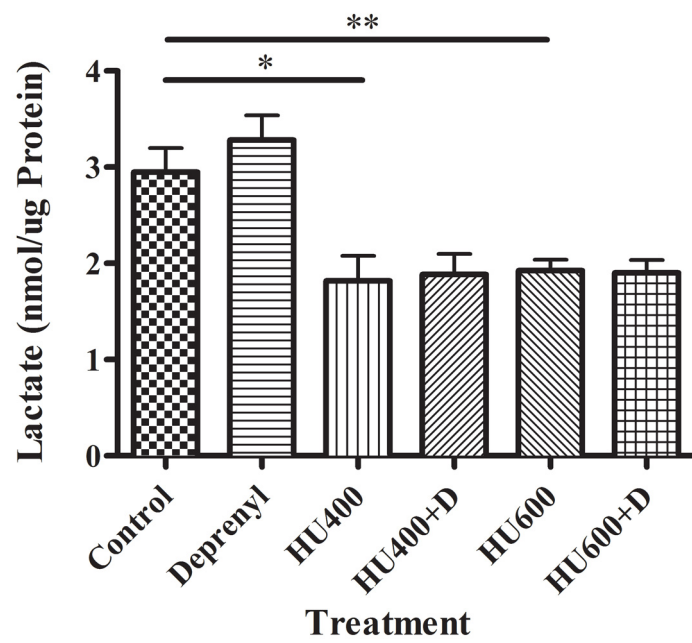
HU600 + Deprenyl



Effects of deprenyl and hydroxyurea on glycolysis

Deprenyl had no effect on glycolysis as assessed by lactate production (Fig. 3.4). As anticipated, the exposure of organogenesis stage embryos to hydroxyurea decreased lactate production, indicating that glycolysis was inhibited. Deprenyl co-administration did not affect this hydroxyurea-induced decrease in lactate production (Fig. 3.4).

Fig. 3.4 Lactate production in GD 9 embryos exposed to saline (control), deprenyl (D), and/or hydroxyurea (HU) at 400 or 600mg/kg. The data represent means \pm SEM. (n = 6 separate experiments, with 8–15 embryos per sample). Two-way ANOVA and a Dunnett's *post-hoc* were done. Asterisks (*) and (**) denote a statistically significant difference ($p < 0.05$) and ($p < 0.01$) compared with controls.

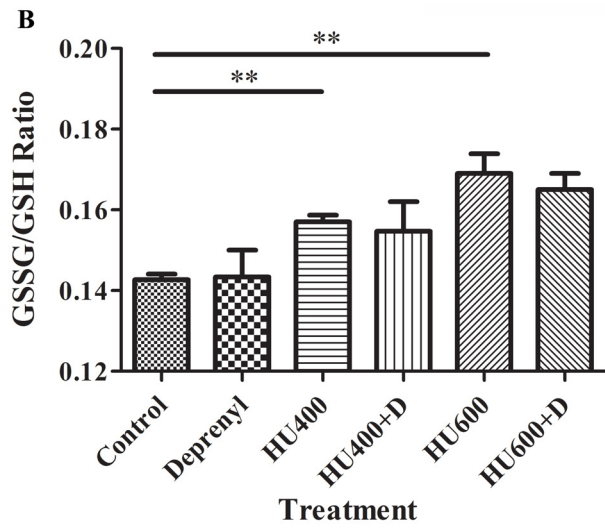
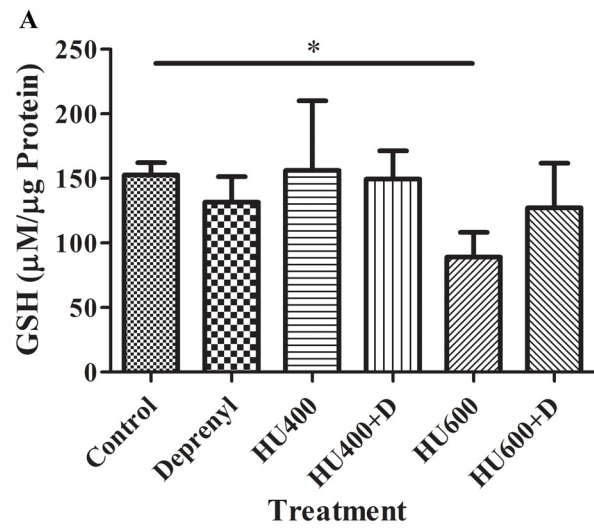


Effects of deprenyl and hydroxyurea on glutathione homeostasis

To assess the effects of deprenyl and hydroxyurea on the redox status of the embryos, we measured reduced (GSH) and oxidized (GSSG) glutathione in embryos collected 3 h after hydroxyurea treatment (Fig. 3.5). There were no significant differences in GSH content in embryos treated with deprenyl alone or with 400 mg/kg hydroxyurea in the absence or presence of deprenyl compared to control (Fig. 3.5A). Exposure to 600 mg/kg hydroxyurea resulted in a significant depletion of embryonic GSH; the GSH content of embryos in the group exposed to deprenyl in combination with this dose of hydroxyurea was not different from control.

The ratio of GSSG/GSH was computed as a measure of oxidative stress (Fig. 3.5B). Deprenyl alone did not affect the GSSG/GSH ratio. Treatment with either 400 or 600 mg/kg hydroxyurea significantly increased the GSSG/GSH ratio, indicative of oxidative stress in the hydroxyurea-exposed embryos. The presence of deprenyl in combination with 400 or 600 mg/kg hydroxyurea did not significantly affect the GSSG/GSH ratio (Fig. 3.5B).

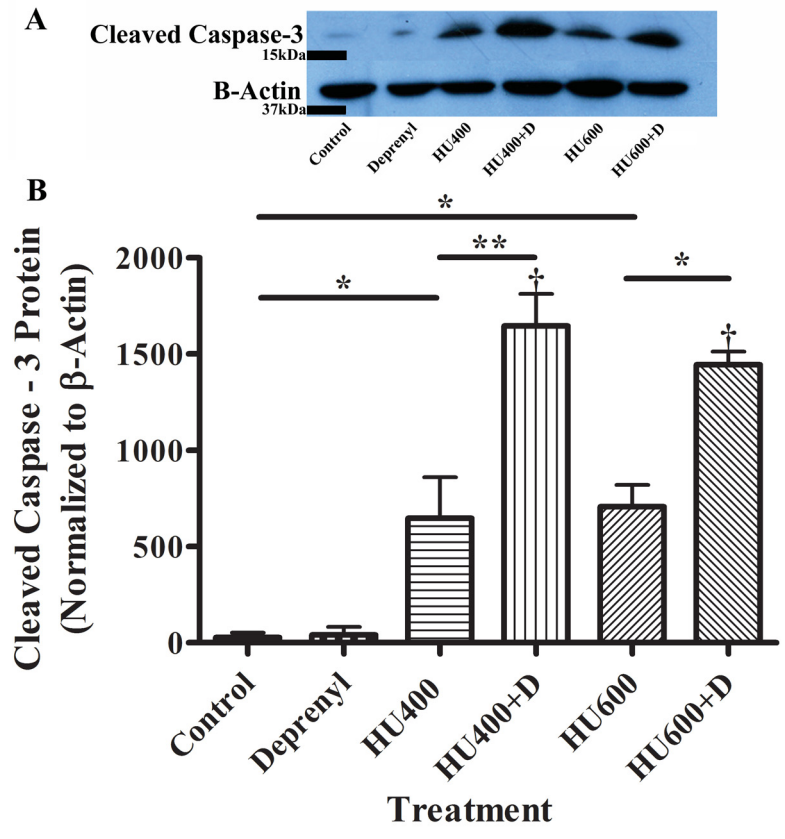
Fig. 3.5. Glutathione status of GD 9 embryos treated with saline (control), deprenyl, and/or hydroxyurea (HU) in the absence or presence of deprenyl. (A) GSH concentrations. (B) GSSG/GSH ratios. The bars indicate the means \pm SEM (n = 3 separate experiments, with 8–15 embryos per sample). Two-way ANOVA and a *post-hoc* Bonferroni or Dunnett's test were done. Asterisks (*) and (**) denote a statistically significant difference ($p < 0.05$) and ($p < 0.01$) compared with controls.



Effects of deprenyl and hydroxyurea on apoptosis

Since the nuclear translocation of GAPDH is associated with a cell death cascade of events, we examined the effects of exposure to hydroxyurea in the absence or presence of deprenyl on cleaved caspase-3 protein, a widely used marker of apoptotic cell death. Deprenyl alone did not increase the amount of cleaved caspase 3 observed in embryos (Fig. 3.6). Exposure to hydroxyurea (400 or 600 mg/kg) produced a dramatic increase in caspase-3 cleavage. Deprenyl, in combination with either 400 or 600 mg/kg hydroxyurea, significantly amplified this response, suggesting that apoptosis was dramatically enhanced in the embryos exposed to deprenyl and hydroxyurea.

Fig. 3.6 Western blot analysis of the effects of treatment with saline (control), deprenyl, and/or hydroxyurea (HU, 400 or 600mg/kg) on cleaved caspase-3 in GD 9 embryos. (A) Western blots depict cleaved caspase-3 (~17kDa), with β -actin as a loading control. (B) Quantification of Western blots. The data represent means \pm SEM (n = 4 separate experiments, with 8–15 embryos per sample). Two-way ANOVA and a *post-hoc* Bonferroni correction were done. Asterisks (*) and (**) denote a statistically significant difference ($p < 0.05$) and ($p < 0.01$), respectively. † denotes a significant difference between the hydroxyurea-treated groups in the presence or absence of deprenyl ($p < 0.05$).



DISCUSSION

The underlying mechanisms by which the maternal conditions and environmental exposures that induce oxidative stress act as developmental toxicants are not known. Using hydroxyurea as a model oxidative stress-inducing teratogen, we reported previously that teratogenic doses enhance the formation of 4-HNE adducts of GAPDH and the nuclear translocation of GAPDH (Schlisser *et al.*, 2010). GAPDH has emerged to be an important sensor of oxidative and genotoxic stress (Tristan *et al.*, 2011). Changes in GAPDH expression, glycolytic activity, nuclear accumulation, and apparent molecular size and conformation have been observed in a number of experimental paradigms (Tristan *et al.*, 2011). In this study, deprenyl was used as a tool to test the hypothesis that the nuclear translocation of GAPDH plays a role in mediating the teratogenicity of hydroxyurea. Here, we demonstrate that deprenyl co-administration inhibited the nuclear translocation of GAPDH and increased the caudal malformations induced by hydroxyurea in embryos.

In the organogenesis stage mouse embryo, gestation day 9 is a time of high susceptibility to insult. Interestingly, deprenyl co-administration increased the incidence of the malformations induced by hydroxyurea in the more caudal structures, i.e. the lumbosacral vertebrae and hindlimbs (Table 3.2). The somites that subsequently differentiate to form the axial skeleton, the muscles of the trunk, and the limbs are formed from segmentation of the paraxial mesoderm in a cranial caudal sequence. Two distinct mechanisms, replication stress and oxidative stress, have been suggested for the teratogenicity of hydroxyurea (DeSesso *et al.*, 2000). Previous studies have shown that there is a DNA damage response, as assessed by the formation of γ -H2AX foci, in hydroxyurea-exposed embryos at 3 hours in all tissues examined, including the somites; at this time, significant increases in P38 MAPK signalling were not observed in the somites (Banh and

Hales, 2013). This differential response is intriguing because the P38 family of kinases mediates responses to a wide variety of signals, including both DNA damage and oxidative stress.

Enhancement of the teratogenicity of hydroxyurea by deprenyl administration appears counterintuitive based on much of the literature. Deprenyl is used clinically to attenuate symptoms in early stage Parkinson's disease, as an adjunct therapy with carbidopa/levodopa, and for depression. Initially, it was thought that the action of deprenyl as a neuroprotectant was dependent on the inhibition of MAO B, thus reducing the production of reactive oxygen species that accompanies the metabolism of dopamine (Olanow, 1993). We now know that other mechanisms are also important since there are effects of deprenyl even in the absence of MAO B (Le *et al.*, 1997; Tatton *et al.*, 1996). Furthermore, it is now clear that deprenyl does not only have protective effects. *In vitro* exposure to high concentrations of deprenyl has been reported to enhance the apoptosis induced by the 1-methyl-4-phenylpyridium ion (MPP⁺) in a dopaminergic cell line (Le *et al.*, 1997) and by dexamethasone in thymocytes (Szende *et al.*, 2001). Deprenyl has been reported to act as an anti-oxidant by activating NRF2 nuclear translocation and thus upregulating the expression of anti-oxidant enzymes (Xiao *et al.*, 2011). However, deprenyl exposure did not enhance the oxidative stress induced by hydroxyurea since it did not affect the glutathione status of the embryos, as indicated by the GSSG/GSH ratios.

The nuclear translocation of GAPDH plays a role in the apoptotic cascade under various pathological conditions, including Parkinson's disease (Hara *et al.*, 2006; Hara and Snyder, 2006; Thangima Zannat *et al.*, 2011). Deprenyl inhibits the S-nitrosylation of GAPDH that triggers binding to SIAH1, leading to its nuclear translocation (Sen *et al.*, 2008). Inhibition of the nuclear translocation of GAPDH by deprenyl was linked to an inhibition of apoptosis in neuronal cells (Carlile *et al.*, 2000) and in retinal Müller cells (Kusner *et al.*, 2004). However, using a rat

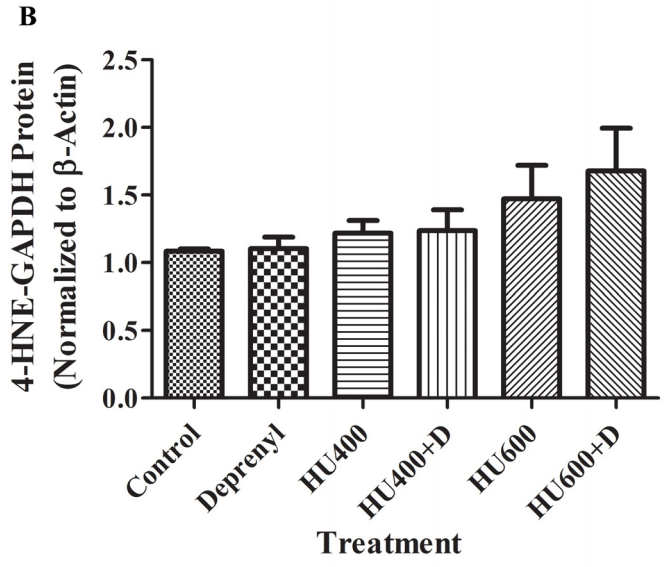
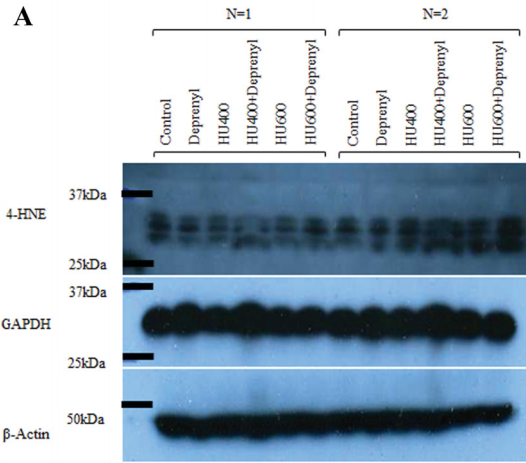
mesencephalic cell line, Ortiz-Ortiz and colleagues (Ortiz-Ortiz *et al.*, 2010) reported that even though pre-incubation with deprenyl did inhibit the nuclear translocation of GAPDH, it failed to prevent cell death triggered by paraquat. Here, we demonstrate that deprenyl augmented cell death, as assessed by caspase 3 cleavage, in hydroxyurea-exposed embryos. The mechanism by which the inhibition of GAPDH nuclear translocation triggers apoptosis is not known. One possibility is that deprenyl also inhibits the S-nitrosylation of caspase 3. Caspase 3 S-nitrosylation decreases its catalytic activity and is associated with a decrease in apoptosis in fibroblasts (Jiang *et al.*, 2009). S-nitrosylated (SNO-) GAPDH has been reported to physiologically transnitrosylate target nuclear proteins, including histone deacetylases and DNA-activated protein kinase (Kornberg *et al.*, 2010). To the best of our knowledge, this function has not been reported for cytoplasmic GAPDH. Hydroxyurea exposure may trigger transnitrosylation signaling since it is converted to nitric oxide (NO) *in vivo* and thus may serve as a source of NO (Huang *et al.*, 2006).

Since inhibition of the hydroxyurea-induced nuclear translocation of GAPDH by deprenyl was not accompanied by an effect on either glycolysis or glutathione homeostasis, it seems likely deprenyl is affecting the function of nuclear GAPDH. There is strong evidence that nuclear GAPDH plays an important role in the regulation of transcription, DNA repair and the cell cycle (Azam *et al.*, 2008; Carujo *et al.*, 2006; Zheng *et al.*, 2003). Since hydroxyurea inactivates ribonucleotide reductase, exposure leads to DNA replication stress and damage response signaling, so a role in modifying DNA repair mechanisms may be highly relevant. Elucidation of the underlying mechanisms and specific binding partners of GAPDH in the nucleus will be critical to our understanding of this response.

The enhanced developmental toxicity of hydroxyurea by deprenyl provides novel insight into its pharmacological effects. Although deprenyl is deemed to be an important neuroprotectant drug, caution should be exercised in pregnant women who may be at risk due to their exposure to maternal conditions and agents that increase oxidative stress.

SUPPLEMENTARY DATA DESCRIPTION

The western blot analyses of 4-HNE-tagged proteins and GAPDH in gestation day 9 whole embryos following treatment with deprenyl and hydroxyurea are presented in Supplementary Fig. S3.1. (n=4).



REFERENCES

- Azam, S., Jouvet, N., Jilani, A., Vongsamphanh, R., Yang, X., Yang, S., Ramotar, D. (2008). Human glyceraldehyde-3-phosphate dehydrogenase plays a direct role in reactivating oxidized forms of the DNA repair enzyme APE1. *J. Biol. Chem.* **283**, 30632-30641.
- Banh, S., Hales, B.F. (2013). Hydroxyurea exposure triggers tissue-specific activation of p38 mitogen-activated protein kinase signaling and the DNA damage response in organogenesis-stage mouse embryos. *Toxicol Sci.* **133**, 298-308.
- Carlile, G.W., Chalmers-Redman, R.M., Tatton, N.A., Pong, A., Borden, K.E, Tatton, W.G. (2000). Reduced apoptosis after nerve growth factor and serum withdrawal: conversion of tetrameric glyceraldehyde-3-phosphate dehydrogenase to a dimer. *Mol Pharmacol.* **57**, 2-12.
- Carujo, S., Estanyol, J.M., Ejarque, A., Agell, N., Bachs, O., Pujol, M.J. (2006). Glyceraldehyde 3-phosphate dehydrogenase is a SET-binding protein and regulates cyclin B-cdk1 activity. *Oncogene.* **25**, 4033-4042.
- DeSesso, J.M., Jacobson, C.F., Scialli, A.R., Goeringer, G.C. (2000). Hydroxylamine moiety of developmental toxicants is associated with early cell death: a structure-activity analysis. *Teratology.* **62**, 346-355.
- DeSesso, J.M., Scialli, A.R., Goeringer, G.C. (1994). D-mannitol, a specific hydroxyl free radical scavenger, reduces the developmental toxicity of hydroxyurea in rabbits. *Teratology.* **49**, 248-259.
- Diez, J.A., Maderdrut, J.L. (1977). Development of multiple forms of mouse brain monoamine oxidase in vivo and in vitro. *Brain Res.* **128**, 187-192.
- Esterbauer, H., Schaur, R.J., Zollner, H. (1991). Chemistry and biochemistry of 4-hydroxynonenal, malonaldehyde and related aldehydes. *Free Radic. Biol.* **11**, 81-128.

Hara, M.R., Snyder, S.H. (2006a). Nitric oxide-GAPDH-Siah: a novel cell death cascade. *Cell Mol. Neurobiol.* **26**, 527-538.

Hara, M.R., Thomas, B., Cascio, M.B., Bae, B.I., Hester, L.D., Dawson, V.L., Dawson, T.M., Sawa, A., Snyder, S.H. (2006b). Neuroprotection by pharmacologic blockade of the GAPDH death cascade. *Proc. Natl. Acad. Sci. U. S. A.* **103**, 3887-3889.

Huang, J., Yakubu, M., Kim-Shapiro, D.B., King, S.B. (2006). Rat liver-mediated metabolism of hydroxyurea to nitric oxide. *Free Radic. Biol. Med.* **40**, 1675-1681.

Human prescription drug label; Eldepryl (selegiline hydrochloride) capsule. Somerset Pharmaceuticals Inc. 2009.

Jiang, Z.L., Fletcher, N.M., Diamond, M.P., Abu-Soud, H.M., Saed, G.M. (2009) S-nitrosylation of caspase-3 is the mechanism by which adhesion fibroblasts manifest lower apoptosis. *Wound Repair Regen.* **17**, 224-229.

Kornberg, M.D., Sen, N., Hara, M.R., Juluri, K.R., Nguyen, J.V., Snowman, A.M., Law, L., Hester, L.D., Snyder, S.H. (2010). GAPDH mediates nitrosylation of nuclear proteins. *Nat. Cell Biol.* **12**, 1094-1100.

Kovacic, P. (2011). Hydroxyurea (therapeutics and mechanism): Metabolism, carbamoyl nitroso, nitroxyl, radicals, cell signaling and clinical applications. *Med. Hypo.* **76**, 24-31.

Kusner, L.L., Sarthy, V.P., Mohr, S. (2004). Nuclear translocation of glyceraldehyde-3-phosphate dehydrogenase: a role in high glucose-induced apoptosis in retinal Müller cells. *Invest. Ophthalmol. Vis. Sci.* **45**, 1553-1561.

Le, W., Jankovic, J., Xie, W., Kong, R., Appel, S.H. (1997). (-)-Deprenyl protection of 1-methyl-4 phenylpyridium ion (MPP⁺)-induced apoptosis independent of MAO-B inhibition. *Neurosci. Lett.* **224**, 197-200.

Magyar, K., Szende, B. (2004). (-)-Deprenyl, A Selective MAO-B inhibitor, with apoptotic and anti-apoptotic properties. *Neurotox.* **25**, 233-242.

Meyer-Siegler, K., Mauro, D.J., Seal, G., Wurzer, J., deRiel, J.K., Sirover, M.A. (1991). A human nuclear uracil DNA glycosylase is the 37-kDa subunit of glyceraldehyde-3-phosphate dehydrogenase. *Proc. Nat. Acad. Sci.* **88**, 8460-8464.

Nicotra, A., Pierucci, F., Parvez, H., Senatori, O. (2004). Monoamine oxidase expression during development and aging. *Neurotox.* **25**, 155-165.

Olanow, C.W. (1993). A rationale for monoamine oxidase inhibition as neuroprotective therapy for Parkinson's disease. *Mov. Disord.* **8 Suppl 1**, S1-7.

Ornoy, A. (2007). Embryonic oxidative stress as a mechanism of teratogenesis with special emphasis on diabetic embryopathy. *Repro. Tox.* **24**, 31-41.

Ortiz-Ortiz, M.A., Morán, J.M., Ruiz-Mesa, L.M., Bravo-San Pedro, J.M., Fuentes, J.M. (2010). Paraquat exposure induces nuclear translocation of glyceraldehyde-3-phosphate dehydrogenase (GAPDH) and the activation of the nitric oxide-GAPDH-Siah cell death cascade. *Toxicol. Sci.* **116**, 614-622.

Sen, N., Hara, M.R., Kornberg, M.D., Cascio, M.B., Bae, B.I., Shahani, N., Thomas, B., Dawson, T.M., Dawson, V.L., Snyder, S.H., Sawa, A. (2008). Nitric oxide-induced nuclear GAPDH activates p300/CBP and mediates apoptosis. *Nat. Cell Biol.* **10**, 866-873.

Schardein, J.L. (2000). *Chemically Induced Birth Defects*, 3rd ed., pp. 566-574. Marcel Dekker, Inc, New York, NY.

Schlisser, A., Yan, J., Hales, B.F. (2010). Teratogen-induced oxidative stress targets glyceraldehyde-3-phosphate dehydrogenase in the organogenesis stage mouse embryo. *Toxicol. Sci.* **118**, 686-695.

Szende, B., Bökönyi, G., Bocsi, J., Kéri, G., Timár, F., Magyar, K. (2001). Anti-apoptotic and apoptotic action of (-)-deprenyl and its metabolites. *J. Neural Transm.* **108**, 25-33.

Tatton, W.G., Wadia, J.S., Ju, W.Y., Chalmers-Redman, R.M., Tatton, N.A. (1996). (-)-Deprenyl reduces neuronal apoptosis and facilitates neuronal outgrowth by altering protein synthesis without inhibiting monoamine oxidase. *J. Neural Transm. Suppl.* **48**, 45-59.

Thangima Zannat, M., Bhattacharjee, R.B., Bag, J. (2011). In the absence of cellular poly (A) binding protein, the glycolytic enzyme GAPDH translocated to the cell nucleus and activated the GAPDH mediated apoptotic pathway by enhancing acetylation and serine 46 phosphorylation of p53. *Biochem. Biophys. Res. Commun.* **409**, 171-176.

Tristan, C., Shahani, N., Sedlak, T.W., Sawa, A. (2011). The diverse functions of GAPDH: views from different subcellular compartments. *Cell Signal.* **23**, 317-323.

Wells, P.G., Bhuller, Y., Chen, C.S., Jeng, W., Kasapinovic, S., Kennedy, J.C., Kim, P.M., Laposa, R.R., McCallum, G.P., Nicol, C.J., Parman, T., Wiley, M.J., Wong, A.W. (2005). Molecular and biochemical mechanisms in teratogenesis involving reactive oxygen species. *Toxicol. Appl. Pharmacol.* **207**, 354-366.

Xiao, H., Lv, F., Xu, W., Zhang, L., Jing, P., Cao, X. (2011). Deprenyl prevents MPP(+)-induced oxidative damage in PC12 cells by the upregulation of Nrf2-mediated NQO1 expression through the activation of PI3K/Akt and Erk. *Toxicology.* **290**, 286-294.

Yan, J., Hales, B.F. (2005). Activator protein-1 (AP-1) DNA binding activity is induced by hydroxyurea in organogenesis stage mouse embryos. *Toxicol. Sci.* **85**, 1013-1023.

Yan, J., Hales, B.F. (2006). Depletion of glutathione induces 4-hydroxynonenal protein adducts and hydroxyurea teratogenicity in the organogenesis stage mouse embryo. *J. Pharmacol. Exp. Ther.* **319**, 613-621.

Zheng, L., Roeder, R.G., Luo, Y. (2003). S phase activation of the histone H2B promoter by OCA-S, a coactivator complex that contains GAPDH as a key component. *Cell.* **114**, 255–266.

CONNECTING TEXT

In chapter III we determined that deprenyl enhanced caudal malformations in embryos exposed to hydroxyurea despite the inhibition of the nuclear translocation of GAPDH. Thus, contrary to the literature, GAPDH plays a protective role in the nucleus in organogenesis stage embryos. To have a broader understanding of the nuclear changes occurring in the embryo following hydroxyurea, in chapter IV, we sought out to determine the gene expression changes occurring in the embryos. In addition, ROS seems to play a very important role in the gene expression changes ensuing. Experiments using microarray technology, qRT-PCR and redox western blots were carried out to elucidate early stress response mechanisms in response to hydroxyurea.

Chapter IV

**The Effects of Hydroxyurea on Redox Status and Gene Expression in Organogenesis Stage
Mouse Embryos**

Ava Schlisser, Barbara F. Hales

Submitted Manuscript

ABSTRACT

The exposure of embryos to drugs and environmental contaminants can generate reactive oxygen species (ROS), cause oxidative stress and perturb the cellular redox status. We hypothesized that redox dysregulation and subsequent changes in gene expression determine the fate of organogenesis-stage embryos after exposure. To test this hypothesis, CD1 mice were exposed to a model teratogen, hydroxyurea, on gestation day 9. Hydroxyurea exposure dysregulated redox homeostasis as indicated by a dose-dependent increase in the oxidation of thioredoxin 1 (TRX1) and glyceraldehyde-3-phosphate dehydrogenase (GAPDH). Microarray analysis revealed that hydroxyurea exposure upregulated the expression of 503 genes whereas the expression of 358 was downregulated. Among these, nuclear factor (erythroid-derived 2)-like 2 (*Nrf2*), a redox-sensitive transcription factor, was significantly upregulated. Hydroxyurea also significantly upregulated the expression of peroxiredoxin (*Prdx1*), a downstream target of NRF2, and thioredoxin interacting protein (*Txnip*), a protein involved in regulating the activity of TRX1 and triggering apoptosis. Pathway analysis revealed that a large network of cell cycle genes was downregulated while genes in the intrinsic and extrinsic apoptotic pathways were significantly upregulated; both of these pathways contain genes that respond to oxidative stress. Poly (ADP-ribose) polymerase 1 (PARP1) cleavage, a marker of apoptosis, was dose dependently increased following hydroxyurea insult. Together, our studies indicate that teratogenic doses of hydroxyurea trigger the oxidation of redox regulated proteins and perturb the expression of redox-sensitive genes, affecting critical pathways in the embryo. Understanding the pathways that mediate the embryonic stress response may help in the development of strategies to prevent teratogenic insult.

HIGHLIGHTS: Dysregulation of redox signaling in the embryo by teratogenic doses of hydroxyurea

KEYWORDS: Redox regulation, thioredoxin, microarray, embryonic stress response, oxidative stress, teratogen

INTRODUCTION

A number of known teratogens act mechanistically through pathways that generate reactive oxygen species (ROS) (Harris and Hansen, 2012a). Thalidomide embryotoxicity is associated with oxidative stress by increasing glutathione disulfide and shifting redox homeostasis (Hansen and Harris, 2013). Phenytoin, a widely-used anticonvulsant, leads to oxidative DNA damage that is reversible by antioxidants (Dennery, 2007). Antioxidants also provide partial protection against the embryotoxicity of hydroxyurea, suggesting that this toxicity is related to the rapid generation of ROS rather than to the inhibition of DNA synthesis (DeSesso *et al.*, 2000). These studies and others support the central role of antioxidants and redox signaling in determining embryotoxicity.

Embryonic development is a period of dynamic change and complex programmed processes that require tight regulation of ROS and redox status to drive normal morphogenesis and function. Dysregulation of ROS, leading to oxidative stress and redox changes, can lead to the development of malformations (Hansen, 2006). Alterations in redox status can perturb enzyme activity, DNA synthesis, signal transduction, gene expression and cell cycle, leading to cell death (Hansen, 2006). The response to redox changes occurs as individual signaling and controlled events through discrete redox pathways; however, high levels of oxidants are not selective in oxidation (Jones, 2006). The two central cellular antioxidant and redox-regulating systems, glutathione (GSH) and thioredoxin (TRX1), complement each other in maintaining protein thiol/disulfide redox states (Watson and Jones, 2003); they also possess roles in redox signaling (Lu and Holmgren, 2012). During oxidative stress conditions, GSH has an essential role in Fas-mediated apoptosis and the induction of thioredoxin interacting protein (TXNIP),

eicosanoid metabolism, regulation of the cell cycle and gene expression (Arrigo, 1999). In the presence of oxidized TRX1, TXNIP is thought to be involved in the activation of apoptosis signal-regulating kinase 1 (ASK1), MAPKKs and JNK, signaling apoptosis (Zhou and Chng, 2013). The redox state of TRX1 in the cytoplasm and nucleus regulates cell death and survival signaling by controlling interactions with TRX1-binding proteins (Fratelli *et al.*, 2005; Go and Jones, 2010).

Oxidants stimulate the phosphorylation and translocation of transcription-factor proteins (e.g. AP-1, NRF2, NF- κ B, and P53). AP-1 family members play important roles in normal embryogenesis and activate the transcription of gene products that protect the embryo against teratogenic insult. In previous studies, we found that in utero exposure to hydroxyurea disturbs skeletal development, depletes GSH, increases the formation of 4-hydroxynonenal protein adducts, and induces AP-1 DNA-binding activity in embryos (Yan and Hales, 2005; Yan and Hales, 2006). Changes in redox status also compromise cell cycle progression, especially during GSH depletion (Reddy *et al.*, 2008). AP-1 proteins, mostly those that belong to the JUN group, control cell cycle and death through their ability to regulate the expression and function of cell cycle regulators such as CYCLIN D1, P53, and P21 (Shaulian and Karin, 2001). The transcription factor nuclear factor erythroid 2-related factor 2 (NRF2), the major regulator of the antioxidant response element (ARE), induces the expression of genes encoding antioxidant proteins and phase 2 detoxifying enzymes, playing a significant role in controlling oxidative stress (Dennery, 2007). NRF2 directly interacts with cyclin-dependent kinase inhibitor 1 (P21) mediating NRF2 protection against oxidative stress (Chen *et al.*, 2009). A potent inducer of NRF2, 3H-1, 2 dithiole-3-thione (D3T), strongly increases *Nrf2* expression and NRF2-ARE binding, inducing NRF2 downstream target genes. Studies in ethanol-exposed mouse embryos

pretreated with D3T resulted in a significant decrease in ethanol-induced ROS generation and apoptosis in the embryos (Chen, 2012).

In the organogenesis stage mouse embryo, gestation day 9 is a time of high susceptibility to insult, especially in caudal structures. The redox status of the caudal region during the highly proliferative state differs from regions that are differentiating or undergoing programmed cell death (Hansen and Harris, 2013). More negative potential (E_h) values (more highly reduced redox states) are associated with cell proliferation, and less negative E_h values (more highly oxidized redox states) are associated with differentiation and apoptosis (Hansen and Harris, 2013). ROS generated by teratogens may target areas of highly reduced states because the potential for oxidation is greater. Hydroxyurea exposure on gestation day 9 increases GSH depletion, the caudal-specific generation of 4-hydroxynonenal, a lipid peroxidation end product and mediator of oxidative stress, and defects of the lumbosacral vertebrae, hindlimbs, and tail (Schlisser and Hales, 2013; Yan and Hales, 2006). We hypothesize that teratogen-induced abnormal development in organogenesis stage mouse embryos is determined by the extent to which the insult induces redox perturbations and disturbances in gene expression profiles. We used hydroxyurea as a model teratogen to investigate the role of oxidative stress in mediating redox dysfunction and gene expression changes in the organogenesis stage mouse embryos.

METHODS AND MATERIALS

Animal experiments were approved by McGill University under protocol number 4456 and were conducted in accordance with the guidelines outlined in the Canadian Council on

Animal Care Guide to the Care and Use of Experimental Animals. Timed-pregnant CD1 mice, mated between 8:00 am and 10:00 am (gestation day 0), were purchased from Charles River Canada Ltd. (St. Constant, QC, Canada) and housed in the McIntyre Animal Resource Centre (McGill University, Montreal, QC, Canada). On gestation day 9 at 9:00 am, mice were treated with hydroxyurea (400 or 600 mg/kg, Sigma-Aldrich Canada Ltd. ON, Canada) or vehicle, by intraperitoneal injection. Dams were euthanized by CO₂ overdose and cervical dislocation on gestation day 9 at 12:00 pm. The uteri were removed and embryos were explanted into Hank's balanced salt solution (Life Technologies Inc., Burlington, ON, Canada). Embryos were washed with filtered 1X PBS and flash frozen in liquid nitrogen and then stored at -80°C for redox western blots, or immediately immersed in RNeasy Lysis Reagent (Qiagen, Mississauga, ON, Canada) and stored at -80C for microarray and qRT-PCR analysis.

Redox and classic western blots

TRX1 and GAPDH redox status assessments were done as previously described by (Hansen, 2012). Briefly, embryos were explanted and surrounding tissue was removed. Embryos from one litter were pooled and placed in ice-cold 10% trichloroacetic acid (TCA) and incubated on ice for 30 min. Samples were sonicated in 5 bursts of 3 seconds, 5 seconds apart, and centrifuged for 10 min at room temperature to pellet precipitated protein. TCA was removed and the pellet was washed with acetone and sonicated once again, then placed on ice for 30 min. Acetone was removed and acetoamidomaleimidylstilbenedisulphonic acid (AMS) (Invitrogen, Carlsbad, CA) was added to the samples and incubated in the dark for 1 h. Samples were subjected to SDS-PAGE electrophoresis and a non-reducing loading buffer was added in a 1:1 ratio with sample. The gel was transferred to a nitrocellulose membrane then the membrane was

blocked with Odyssey blocking solution (Mandel Scientific Company, INC, Guelph, ON, Canada) and incubated with TRX1 antibody (1:5,000; Abcam, Cambridge, MA, Catalog # ab26320) or GAPDH antibody (1:1000; Abcam, Cambridge, MA, Catalog # ab9485) for 1.5 h and 2 h, respectively. Membranes were incubated with horseradish peroxidase-conjugated secondary antibodies (1:10,000; GE Healthcare, Buckinghamshire, UK) for 2 h at room temperature. After 6 washes of 5 min and incubation with enhanced chemiluminescence (GE Healthcare), for 5 min in the dark, the membranes were visualized with CL-Xposure film (Fisher Scientific, Ottawa, ON). Quantification of western blot data was done using a ChemiImager 4000 imaging system (Alpha Inotech, San Leandro, CA) with AlphaEase 3.3b software. Bands of interest were outlined and a densitometry value was obtained for the upper (reduced) and lower (oxidized) bands. The densitometry values were converted into a potential with the Nernst equation ($E_h = E_a + 30 \cdot \ln(\text{RFU}_{\text{lower band}}/\text{RFU}_{\text{upper band}})$), expressed in mV. E_h : redox potential; E_a : midpoint potential; RFU: relative fluorescence unit. Each experiment was replicated 3 times and separate litters were used for each group.

Classic western blots were used to quantify cleaved poly (ADP-ribose) polymerase 1 (PARP1), as previously described (Schlisser and Hales, 2013). Membranes were probed using primary antibodies against cleaved PARP1 (1:1,000; Cell Signaling Technology, Inc., Danvers, MA, Catalog # 9544) or β -ACTIN (1:5,000; Santa Cruz Biotechnology, Inc., Santa Cruz, CA, Catalog # sc-2056), overnight at 4°C. Membranes were incubated with horseradish peroxidase-conjugated secondary antibodies (1:10,000; GE Healthcare) for 2 h at room temperature and proteins were detected by enhanced chemiluminescence (Amersham Biosciences). Protein bands were visualized using a ChemiDoc MP (Bio-Rad, Hercules, CA) according to the manufacturer's specifications to maximize dynamic range.

RNA extraction, microarray probe preparation and hybridization

The Agilent (Agilent Technologies, Mississauga, ON, Canada) SurePrint G3 Mouse GE 8x60k Microarray kit was used to probe embryonic gene expression. Microarrays were used to measure gene expression in control or 400 mg/kg of hydroxyurea-treated embryos at 3 h post treatment. Total RNA was extracted using Rneasy[®] Plus Mini Kit (Qiagen, Mississauga, ON, Canada). The RNA concentration and purity of each sample were assessed by spectrophotometry using a NanoDrop1000 spectrophotometer (Fisher Scientific) and Agilent 2100 BioAnalyzer (Agilent Technologies). For each sample, 600 ng of Cy3 labeled cDNA was used for the single-color microarray. After 17 h of hybridization at 65°C, the microarray slides were washed as per the recommendations for the Agilent hybridization kit. Arrays were scanned with Agilent DNA Microarray Scanner. Whole litters were pooled for each sample and each experiment was replicated 6 times.

Bioinformatic and statistical analysis

Analysis of the scanned microarrays was done using Agilent's Feature Extraction software. Statistical analysis, clustering and principle component analysis (PCA), and visualizations were done using GeneSpring Gx (Agilent Technologies). Background correction and quantile normalization was done on all probe sets. Student t-test using p -value <0.05 was used to compare groups, and those probe sets that were significantly altered were further filtered with a minimum of 1.5-fold difference. In addition, probe sets were filtered using error with a standard deviation <0.1 . Probe sets were converted into a gene list by filtering out controls, blanks, and multiple probes per genes. Pathway analysis was done using Pathway Studio 7.1 (Ariadne Genomics, Rockville, MD). Redox and classical western blotting were analyzed

statistically using GraphPad Prism Software version 4 (Graph Pad Software Inc., La Jolla, CA). Student t-test and one-way ANOVA were used, as appropriate, to compare all groups with control followed by a Bonferroni correction. The level of significance was $P < 0.05$.

Real-time qRT-PCR validation

To validate the microarray results, qRT-PCR was done for selected genes identified as being affected in the microarray analyses. The samples were diluted to a working solution of 2 ng/ μ l of RNA and transcripts were quantified using Power SYBR Green RNA-to- C_T 1-Step Kit (Applied Biosystems, Foster City, CA) and StepOnePlus Real-Time PCR System (Applied Biosystems). Primer sets were purchased from Qiagen: thioredoxin interacting protein (*Txnip*, QT00296513); nuclear factor (erythroid-derived 2)-like 2 (*Nfe2l2*, QT00095270); peroxiredoxin 1 (*Prdx1*, QT00124460). The reactions were done in a final volume of 20 μ l composed of 10 μ l SYBR Green Master Mix, 2 μ l of forward/reverse primer, 0.16 μ l Reverse Transcriptase mix, 2.84 μ l Rnase-Dnase-free water, and 5 μ l sample. PCR was done under the following conditions: 48°C for 30 min, 95°C for 10 min followed by 40 cycles of 94°C for 15s, 60°C for 58s and melting curve at 95°C for 15s, and 60°C for 15s. Serial dilutions of non-treated maternal liver were used to create a standard curve. Each reaction was done in triplicate, averaged and normalized to the amount of *18S* rRNA transcripts. Each experiment was replicated 5-7 times. All real-time qRT-PCR data were analyzed statistically using GraphPad Prism Software version 4 (Graph Pad Software Inc.). Student t-test and one-way ANOVA were used to compare all groups with control followed by a Bonferroni correction. The level of significance was $P < 0.05$.

RESULTS

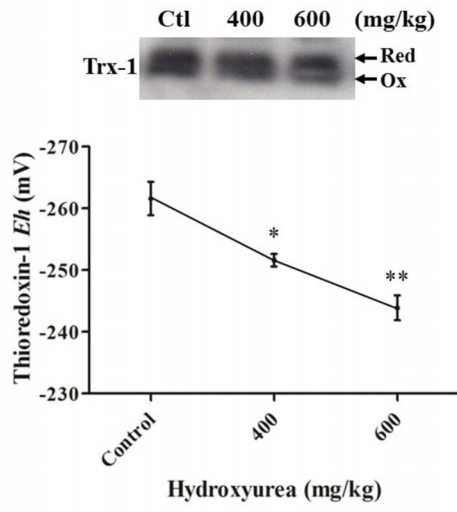
Alterations in Redox Status

Changes in embryonic redox status after hydroxyurea treatment were assessed using redox western blots to analyze the extent to which TRX1 and GAPDH were oxidized in the embryo. Results from these experiments revealed that oxidized and reduced TRX1 were found in control embryos; hydroxyurea treatment caused a significant dose-dependent increase in the potential of TRX1, indicating that TRX1 oxidation was increased by drug treatment (Fig. 4.1A). Similarly, oxidized and reduced GAPDH were present during normal embryonic development; however, after hydroxyurea treatment, the GAPDH potential was increased significantly, demonstrating that hydroxyurea exposure oxidized the sulfhydryl groups of GAPDH (Fig. 4.1B). These results suggest that redox homeostasis was perturbed in hydroxyurea-exposed embryos.

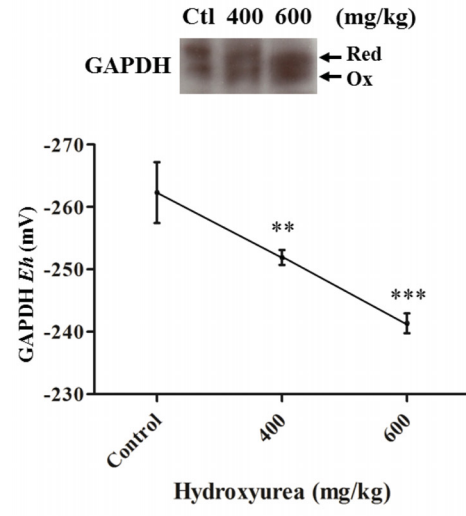
Fig. 4.1 Redox status in embryos following 3 h exposure to 400 or 600 mg/kg hydroxyurea.

(A) Top panel: TRX1 redox state were determined by redox western blotting to separate oxidized and reduced TRX1. Bottom panel: using band densitometry, TRX1 redox potentials were determined and expressed as millivolts (mV). (B) Top panel: GAPDH redox state was determined in the same manner as TRX1. Bottom panel: GAPDH redox potentials were determined and expressed as millivolts (mV). Data represent 8-15 embryos per group from four separately performed experiments. Asterisks (*), (**), (***) denote a statistically significant difference (* = $P < 0.05$, ** = $P < 0.01$, *** = $P < 0.001$) from control.

a.



b.

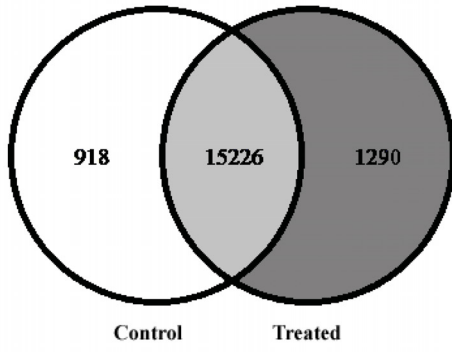


Microarray Analysis of Gene Expression

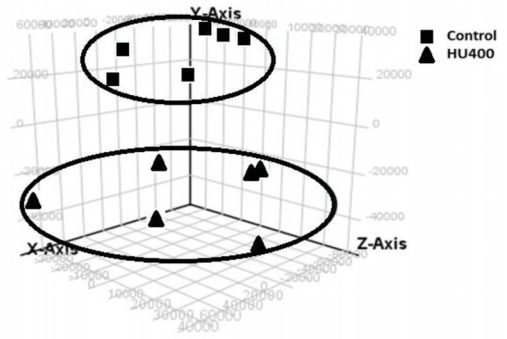
Whole genome microarrays were done to elucidate the impact on the gene expression profiles of embryos exposed to 400 mg/kg of hydroxyurea, a dose that was teratogenic but not highly embryolethal. While 15,226 probe sets were expressed in both control and hydroxyurea-treated embryos, 918 were expressed only in the control embryos and 1290 were expressed only in treated embryos (Fig. 4.2A; all data have been deposited in GEO, study GSE54579, <http://www.ncbi.nlm.nih.gov/geo/query/acc.cgi?acc=GSE54579>). Filtration of the gene expression data, as described, followed by a principle component analysis showed that the gene expression profile in hydroxyurea treated embryos differed significantly from that in control embryos (Fig. 4.2B). We identified 503 genes that were significantly upregulated and 358 genes that were significantly downregulated by hydroxyurea (Fig. 4.2C). A list of the genes that were most significantly altered (fold change ≥ 1.5) is provided in Table 4.1.

Fig. 4.2 Number of probe sets and genes that are significantly altered (by at least 1.5-fold) in embryos exposed to hydroxyurea. (A) Venn diagram of probe sets expressed in control and hydroxyurea exposed embryos exclusively and those that are expressed in both groups. (B) Principle component analysis of probe sets in control and treated group. (C) Number of genes altered by hydroxyurea exposure. Data represent 8-15 embryos per group from six separately performed experiments.

a.



b.



c.

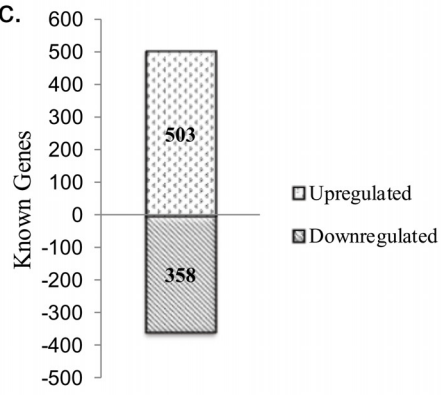


Table 4.1. Upregulated and downregulated genes in embryos exposed to 400 mg/kg hydroxyurea, filtered by fold change >1.5 and p value < 0.05, sorted by descending fold change.

Genes	Description	Fold	
		Change	P value
Upregulated			
<i>Pmaip1</i>	phorbol-12-myristate-13-acetate-induced protein 1	16.916	0.000
<i>1700007K13Rik</i>	RIKEN cDNA 1700007K13 gene	14.324	0.000
<i>Cdkn1a</i>	cyclin-dependent kinase inhibitor 1A (P21)	11.983	0.001
<i>Fas</i>	Fas (TNF receptor superfamily member 6)	11.894	0.001
<i>Trp53inp1</i>	transformation related protein 53 inducible protein 1	11.480	0.000
<i>Zfp365</i>	zinc finger protein 365	10.517	0.000
<i>Svop</i>	SV2 related protein	9.187	0.000
<i>Agtr1b</i>	angiotensin II receptor, type 1b	8.761	0.001
<i>Mab21l3</i>	mab-21-like 3 (C. elegans)	8.565	0.003
<i>Slc19a2</i>	solute carrier family 19 , member 2	7.770	0.004
<i>Phlda3</i>	pleckstrin homology-like domain, family A, member 3	7.382	0.000
<i>Dcxr</i>	dicarbonyl L-xylulose reductase	7.239	0.011
<i>Eva1c</i>	eva-1 homolog C (C. elegans)	6.599	0.000
<i>Tap1</i>	transporter 1, ATP-binding cassette, sub-family B	6.458	0.001
<i>Ddit4l</i>	DNA-damage-inducible transcript 4-like	6.237	0.000
<i>Egr1</i>	early growth response 1	6.064	0.015
<i>Ptprv</i>	protein tyrosine phosphatase, receptor type, V	5.965	0.016
<i>Tnfrsf10b</i>	tumor necrosis factor receptor superfamily,member10b	5.763	0.000
<i>Kcnj4</i>	potassium inwardly-rectifying channel, member 4	5.087	0.021
<i>Anxa8</i>	annexin A8	5.047	0.002
Downregulated			
<i>Syt10</i>	synaptotagmin X	30.286	0.007

<i>Mirg</i>	miRNA containing gene	26.057	0.008
<i>Slc12a5</i>	solute carrier family 12, member 5	19.634	0.007
<i>LOC100862627</i>	uncharacterized LOC100862627	17.616	0.006
<i>Gm5106</i>	predicted gene 5106	15.656	0.045
<i>Tox4</i>	TOX high mobility group box family member 4	9.418	0.013
<i>Hist2h2bb</i>	histone cluster 2, H2bb	9.294	0.000
<i>1700061117Rik</i>	RIKEN cDNA 1700061117 gene	8.928	0.005
<i>Hist1h2ab</i>	histone cluster 1, H2ab	7.929	0.001
<i>Inpp5e</i>	inositol polyphosphate-5-phosphatase E	7.875	0.012
<i>Dnm1</i>	dynamin 1	7.093	0.008
<i>AW413774</i>	expressed sequence AW413774	5.695	0.002
<i>Pon2</i>	paraoxonase 2	5.409	0.018
<i>Amt</i>	aminomethyltransferase	5.338	0.008
<i>Hist1h1a</i>	histone cluster 1, H1a	5.261	0.000

Major families/GO terms

GeneSpring gene ontology analysis revealed that the expression of several families of genes was significantly enriched by hydroxyurea treatment (Table 4.2). The nucleotide binding group included 489 genes with altered expression after hydroxyurea treatment. Nucleotide binding is an umbrella term for any gene encoding a protein interacting selectively and non-covalently with a nucleotide, any compound consisting of a nucleoside that is esterified with (ortho)phosphate, or an oligophosphate at any hydroxyl group on the ribose or deoxyribose. Interestingly, 299 genes found to be altered were involved in cell cycle and 188 in apoptosis, two critical events dysregulated in hydroxyurea teratogenesis. Other contributing events, such as DNA damage response, oxidative stress and DNA repair gene ontologies, were also enriched with genes altered by hydroxyurea treatment.

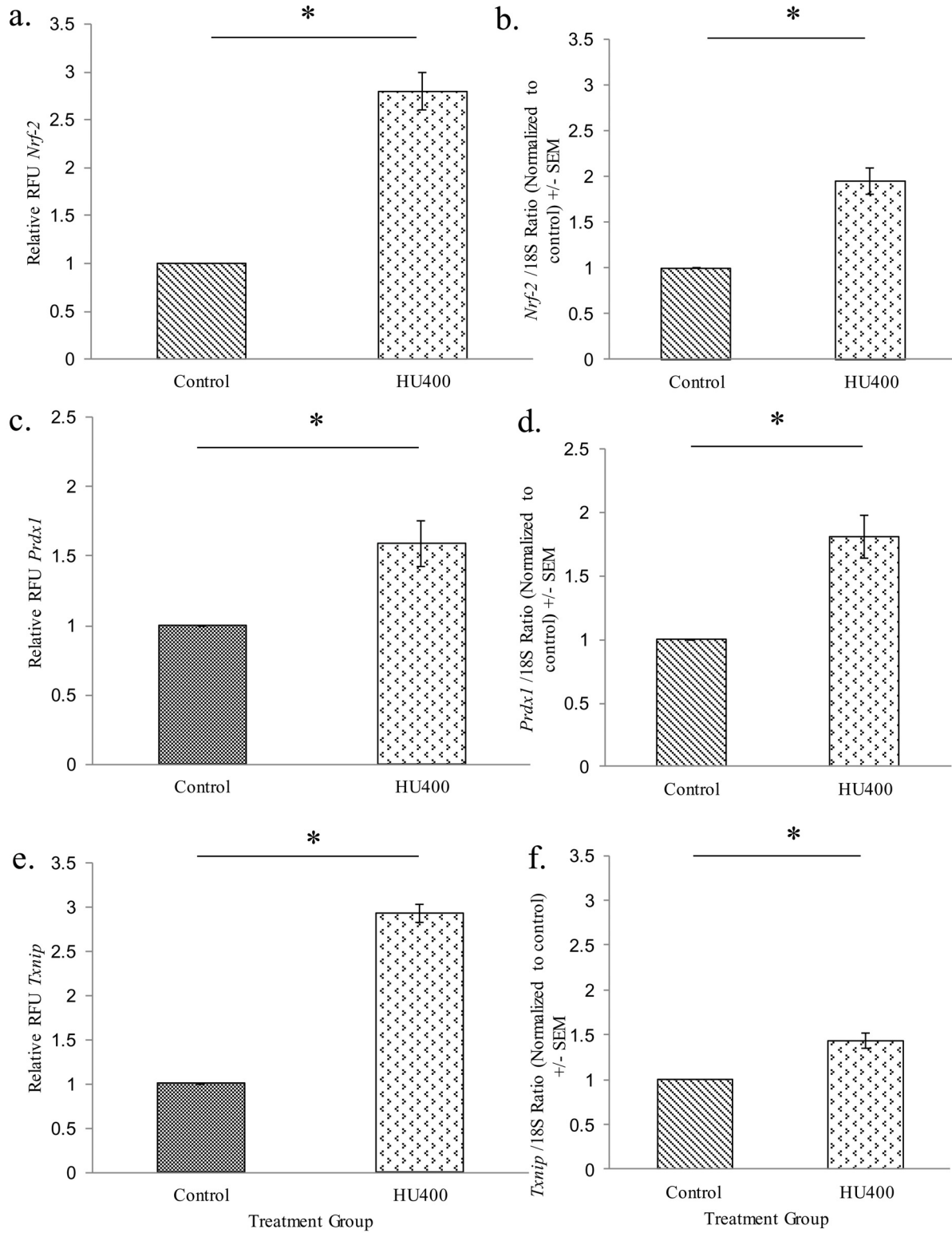
Table 4.2. Functional grouping of genes up- or downregulated in embryos by exposure to hydroxyurea, filtered on fold change > 1.5 and p value < 0.05.

Gene Ontology	Gene Count
Nucleotide Binding	489
Cell Cycle	299
Apoptosis	188
Embryonic Development	80
DNA Damage Response	71
Transcription Regulation	61
Cell Adhesion Processes	51
Oxidative Stress Response	27
DNA Repair	25

Role of oxidative stress regulated genes

Some of the genes that were significantly altered by hydroxyurea treatment are regulated by oxidative stress. *Nrf2*, the primary defense mechanism against cytotoxic effects of oxidative stress and the major regulator of the antioxidant response element (ARE), was found in low levels in control embryos. Following exposure to 400 mg/kg hydroxyurea, *Nrf2* was significantly upregulated in our microarray analysis (Fig. 4.3A); qRT-PCR validation also revealed significant upregulation of *Nrf2* expression (Fig. 4.3B). One of the downstream target genes of *Nrf2* is peroxiredoxin 1 (*Prdx1*), an antioxidant gene involved in reducing hydrogen peroxide and alkyl hydroperoxides, intermediate products derived from ROS. The relative expression of *Prdx1* was increased significantly from control both in our microarray analysis and by qRT-PCR (Fig. 4.3C, D). Another gene involved in the response to oxidative stress is *Txnip*; *Txnip* expression was increased significantly from control both in our microarray analysis and in the qRT-PCR analysis (Fig. 4.3E, F).

Fig. 4.3 Microarray analysis and real-time qRT-PCR of genes involved in oxidative stress. Left panel: microarray analysis, right panel: qRT-PCR. *Nrf2* (A), *Prdx1* (B), *Txnip* (C). qRT-PCR transcripts were normalized to the *18S* rRNA transcript and represent 8-15 embryos per group from five-seven separately performed experiments. Asterisks (*) denote a statistically significant difference (* = $p < 0.05$) from control.



Pathway Analysis

The genes involved in several biological processes were mapped to known pathways. Eight pathways were enriched with genes significantly altered by hydroxyurea treatment (Table 4.3). Many genes described as having functions in cell cycle regulation also have roles in apoptosis or DNA damage repair, thus the components in the pathways overlap. It was not surprising that the cell cycle pathway was downregulated by hydroxyurea, as it halts cells in S phase (Liebelt *et al.*, 2007): 140 genes were enriched in the cell cycle pathway and several of these are directly involved in cell cycle arrest. For example, cyclin-dependent kinase inhibitor 1a (*p21*) was found to be dramatically upregulated by 12-fold (Table 4.1), while cyclin-dependent kinase 1 (*Cdk1*) was downregulated by 1.5-fold in our microarray and 7-fold by qRT-PCR. Another gene involved in cell cycle arrest, tumor protein p53-inducible nuclear protein 1 (*Tp53inp1*), referred to as SIP or “stress inducible protein” (Tomasini *et al.*, 2002), was upregulated by 11.4-fold.

Hydroxyurea exposure also altered the pyrimidine metabolism pathway. Essential for the synthesis of uridine monophosphate (UMP) and uridine triphosphate (UTP), building blocks of RNA, the pyrimidine metabolism pathway is tightly regulated by folate metabolism. Gene expression changes in this pathway included a 1.6-fold increase in *Nme7* (Non-Metastatic Cells 7) that has a major role in the synthesis of nucleoside triphosphates other than ATP. Thymidine Kinase 1 (*Tk1*), catalyzing the production of deoxythymidine monophosphate, was upregulated by 1.5-fold, and deoxythymidylate kinase (*Dtym1*), an enzyme involved in the production of dTMP (thymidine monophosphate), a nucleotide monomer in DNA, was upregulated by 1.5-fold.

Table 4.3. Pathway analysis of genes that were significantly altered (>1.5-fold) in embryos exposed to hydroxyurea, filtered by ascending P-value (<0.05).

Name	Total Entities	Expanded # of Entities	P-value
Cell cycle	140	585	0.000
Pyrimidine metabolism	105	184	0.018
Apoptosis	93	186	0.015
mRNA Transcription and Processing	49	391	0.000
Histone and DNA Methylation	37	352	0.000
Double Strand DNA Non-Homologous Repair	32	136	0.009
TNFR -> NF-kB signaling	32	40	0.033
SWI/SNF BRG1/BAF Chromatin Remodeling	25	284	0.000

Effects of hydroxyurea on apoptosis pathway genes

Despite the stress response/repair efforts of the embryo that are triggered by hydroxyurea exposure, cell death is a common outcome. Many genes involved in apoptosis were highly upregulated; these included *Noxa* (phorbol-12-myristate-13-acetate-induced protein 1), *Fas* (TNF receptor superfamily member 6), *Apaf1* (apoptotic peptidase activating factor 1), and *Bcl10* (B-cell leukemia/lymphoma 10) (Table 4.4). Pathway analysis revealed that the extrinsic and intrinsic pathways of apoptosis were activated by hydroxyurea (Fig. 4.4). The cleavage of PARP1 is commonly used as a marker of apoptosis: PARP1 is one of several known cellular substrates of caspases. The immunoreactivity of cleaved PARP1 was barely detected in control embryos; hydroxyurea exposure led to a significant dose-dependent increase in cleaved PARP1 immunoreactivity (400 mg/kg: 1.7-fold increase; 600 mg/kg: 2.9-fold increase (Fig. 4.5).

Table 4.4. Upregulated genes involved in apoptosis, filtered by fold change > 1.5 and P value < 0.05.

Gene	Gene Name	Fold Change
<i>Noxa</i>	phorbol-12-myristate-13-acetate-induced protein 1	16.916
<i>Fas</i>	Fas (TNF receptor superfamily member 6)	11.894
<i>Trp53inp1</i>	transformation related protein 53 inducible nuclear protein 1	11.480
<i>Phlda3</i>	pleckstrin homology-like domain, family A, member 3	7.382
<i>Ptprv</i>	protein tyrosine phosphatase, receptor type, V	5.964
<i>Apaf1</i>	apoptotic peptidase activating factor 1	4.599
<i>Klf10</i>	Kruppel-like factor 10	2.676
<i>Bbc3</i>	BCL2 binding component 3	2.455
<i>Parp10</i>	Mus musculus poly (ADP-ribose) polymerase family, member 10	2.404
<i>Nr4a1</i>	nuclear receptor subfamily 4, group A, member 1	2.280
<i>Cebpb</i>	CCAAT/enhancer binding protein (C/EBP), beta	2.091
<i>Dapk1</i>	death associated protein kinase 1	1.973
<i>Sh3glb1</i>	SH3-domain GRB2-like B1 (endophilin)	1.857
<i>Aen</i>	apoptosis enhancing nuclease	1.838
<i>Bcl10</i>	B-cell leukemia/lymphoma 10; predicted gene 6141	1.751
<i>Perp</i>	PERP, TP53 apoptosis effector	1.718
<i>Msh6</i>	mutS homolog 6 (E. coli)	1.629
<i>Brca2</i>	breast cancer 2	1.604
<i>Pml</i>	promyelocytic leukemia	1.570

Fig. 4.4 Pathway analysis of apoptotic genes expressed in embryos following hydroxyurea exposure. Intrinsic and extrinsic apoptotic pathways are upregulated and include several genes that respond to oxidative stress. Statistical significance of pathways were determined by gene enrichment and include those for which P values are <0.05 .

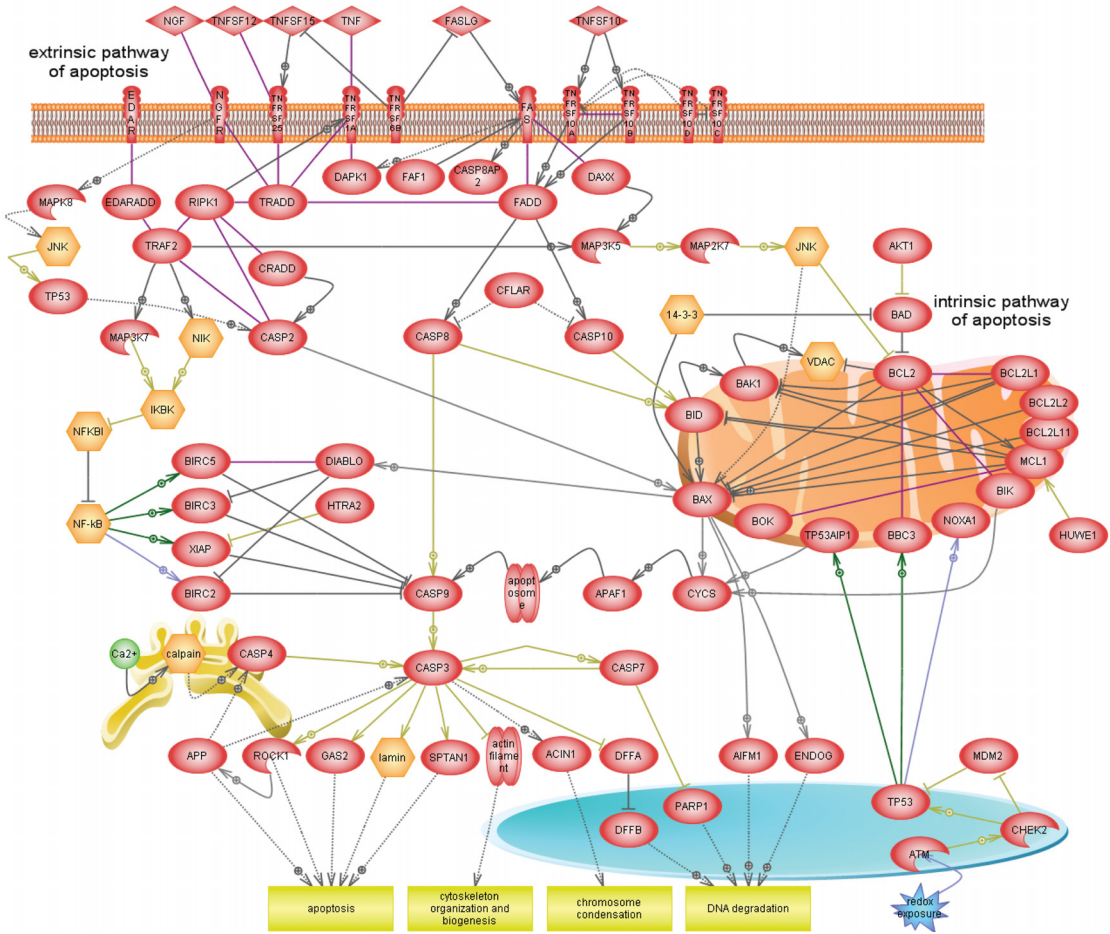
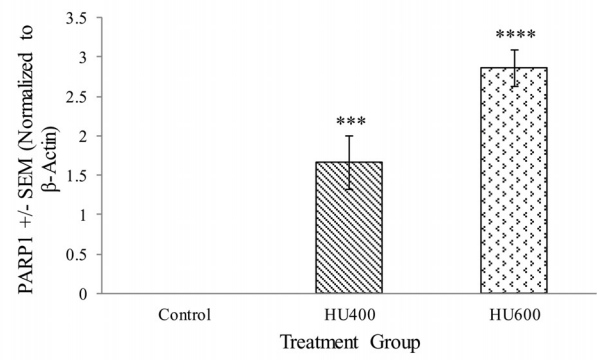
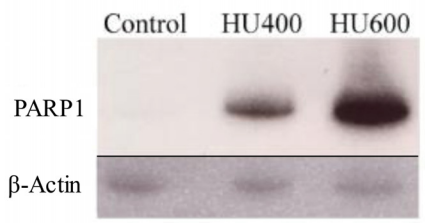


Fig. 4.5 Cleaved PARP1 immunoreactivity in embryos 3 h following hydroxyurea exposure. Top panel: western blot of cleaved PARP1, bottom panel: densitometry quantification of cleaved PARP1 immunoreactivity. Data represent 8-15 embryos per group from four separately performed experiments. Asterisks (***) or (****) denote a statistically significant difference (***) = $P < 0.001$, (****) = $P < 0.00001$) from control.



DISCUSSION

Antioxidant response to hydroxyurea

Hydroxyurea exposure triggered the oxidation of TRX1 within 3 h, concomitantly with GSH depletion (Schlisser and Hales, 2013). TRX1 is a critical oxidoreductase that participates in the regulation of critical cysteine residues in many proteins, in the cytoplasm and nucleus, including transcription factors, such as AP-1 (Mitomo *et al.*, 1994). Hydroxyurea exposure increased AP-1 DNA binding activity in the embryo (Yan and Hales, 2005). TRX1 oxidation may play a role in the activation of AP-1 since reduced TRX1 is required to regenerate redox factor-1 (REF-1), a nuclear protein that functions to repair DNA and interact with transcription factors such as AP-1 to regulate their redox states and activities (Yamawaki *et al.*, 2003). Studies in mouse embryos on gestation day 8 have shown that after H₂O₂ treatment TRX1 does not rebound quickly but rather remains oxidized for 120 min (Harris and Hansen, 2012b). In our model system, hydroxyurea provoked a prolonged (>3 h) period of TRX1 oxidation. If sustained oxidation of TRX1 occurs, TRX1-dependent processes, such as activation of REF-1, remain disrupted (Nishi *et al.*, 2002).

TXNIP, an endogenous inhibitor of TRX1, is involved in apoptosis and was upregulated by 1.5-fold at the transcript level following hydroxyurea exposure. Various stress stimuli, including oxidative stress, stimulate TXNIP expression (Lu and Holmgren, 2012). TRX1 blocks apoptosis signal-regulating kinase 1 (ASK1) activity and the subsequent ASK1-dependent apoptosis, and this TRX1-mediated inhibitory effect is abolished by TXNIP (Chen *et al.*, 2008). ASK1 can then mediate JNK activation, including C-JUN (Turpaev, 2002).

Hydroxyurea exposure oxidized embryonic GAPDH in addition to its effects on TRX1. In previous studies we showed that hydroxyurea treatment reduced GAPDH enzymatic activity and its translocation into the nucleus in the embryo in a region-specific manner (Schlisser *et al.*, 2010). The protective role of nuclear GAPDH in the embryo is likely to be mediated by its redox sensitivity (Schlisser and Hales, 2013; Schlisser, Yan and Hales, 2010). GAPDH has been linked to apoptosis by enhancing acetylation and serine 46 phosphorylation of P53 in the nucleus. As a result, P53 translocated to the mitochondria to initiate Bax mediated apoptosis (Thangima Zannat *et al.*, 2011). P53 may also play a role in DNA repair and survival in the embryo (Adimoolam and Ford, 2003).

Redox regulation at the gene level may be mediated by the ARE that possesses structural and biological features characterizing its unique responsiveness to oxidative stress (Rushmore *et al.*, 1991). NRF2, the main regulator of the ARE, is a transcription factor stabilized during stress conditions; NRF2 binds to the ARE, leading to the induction of antioxidant enzymes important in maintaining cellular redox homeostasis (Harris and Hansen, 2012b). NRF2 deficiency enhances oxidative stress and toxicity during development, suggesting that NRF2 may protect the conceptus from developmental toxicants (Ramkissoon and Wells, 2013). Our microarray data revealed a significant increase in the expression of *Nrf2* and its downstream target, *Prdx1*, in hydroxyurea-treated embryos. Interestingly, the expression of NRF2 downstream antioxidant genes, including *Gclc*, *heme oxygenase-1*, *glutathione S-transferase*, and *UDP-glucuronosyltransferase*, was not significantly altered by hydroxyurea treatment. Glutathione pathway genes were also not upregulated with our treatment, even in areas of high susceptibility, such as the tail region (Suppl. Fig. 4.1). NRF2 was found to bind to the ARE in the TRX1 promoter in response to oxidative stress stimuli (Hawkes *et al.*, 2014); however, *Trx1* genes were

not altered by hydroxyurea in our experiments (Suppl. Fig. 4.2). Since NRF2-regulated gene products were limited in expression, it was not surprising that the expression of *Trx1* genes were not changed.

Cell cycle and apoptosis pathway analysis

Pathway analysis identified several pathways that are significantly altered by hydroxyurea. The regulation of the cell cycle pathway, leading to cell survival or death, depends on the balance between the transcription of proapoptotic and antiapoptotic genes and may be further regulated by P53 and P21 through their cell-cycle regulatory activities (Trachootham *et al.*, 2008). Cyclin-dependent kinase inhibitors (CDKIs) are proteins that play important roles regulating proliferation during development and differentiation and after genotoxic stress (Gartel and Tyner, 2002). Interestingly, in our microarray analysis, we identified *p21* to be highly expressed after hydroxyurea exposure; *p21* may have a dual role in mediating cell cycle arrest and *Nrf2* induced ARE activation (Chen *et al.*, 2009). We have also shown that hydroxyurea exposure activates the AP-1 family of transcription factors (Yan and Hales, 2008). In our pathway analysis, G1/S-specific CYCLIN D1 is a target of C-JUN and C-FOS, inhibiting the cell cycle; however, C-JUN also seems to play a role in mediating apoptosis.

The balance between proapoptotic and antiapoptotic genes that is induced may determine cell fate (Trachootham *et al.*, 2008). Cell cycle arrest leading to cell death has a dramatic impact on the growth and development of the conceptus; teratogen exposure induced unscheduled cell death may either lead to malformations or to a loss of viability of the conceptus (Vinson and Hales, 2002). Several critical genes involved in the initiation or activation of the intrinsic or extrinsic apoptotic signaling pathways were significantly upregulated following hydroxyurea

treatment. *Noxa* and MAP kinase genes have been shown to be involved in oxidative stress-dependent apoptosis (Mao *et al.*, 2010). *Mek3*, *Mek6*, and *c-Jun* are involved in apoptosis as a response to oxidative stress. We have previously reported that MEK3 and 6 are phosphorylated at the protein level and signal phosphorylation of P38 (Banh and Hales, 2013). Oxidative stress leading to unscheduled apoptosis in developing organs on gestation day 9, accompanied by the lack of antioxidant response, may mediate the caudal malformations associated with hydroxyurea exposure.

DNA damage and repair pathways in the embryo

The ability of the embryo to repair DNA damage is an important determinant of its fate after exposure to teratogenic doses of hydroxyurea. Hydroxyurea induces DNA damage, both by increased oxidative stress and by inhibiting ribonucleotide reductase, causing replication fork arrest and subsequent DNA breaks (Banh and Hales, 2013; Desesso *et al.*, 1994). Indeed, in previous studies we have shown that immunoreactivity to γ -H2AX, a marker of DNA double-strand breaks (DSBs), was increased in embryos 3 h after exposure to hydroxyurea (Banh and Hales, 2013). DSBs are among the most dangerous inducers of genotoxic damage and cell death via apoptosis (Henrique Barreta *et al.*, 2012). . In cleavage-stage bovine embryos, the two main pathways involved in repair of DSBs are homologous repair (HR) and non-homologous end-joining repair (NHEJ) (Henrique Barreta *et al.*, 2012). Here, we report that pathway analysis revealed that 32 genes involved in NHEJ were upregulated in hydroxyurea-exposed embryos; this was the only DNA damage repair pathway significantly upregulated by hydroxyurea. The NHEJ repair pathway genes included *Rad50*, *Mre11A*, *PolB*, and *Parp1*. It is likely that hydroxyurea also causes single-strand breaks (SSB); however, the *Xrcc1* gene product that plays

a major role in SSB repair was not upregulated following hydroxyurea. Our results suggests that an early response to DNA damage is limited to NHEJ repair; however, the need for DNA repair during organogenesis, coincident with ongoing rapid cell proliferation and the switch from anaerobic metabolism to an oxidative one may underlie the susceptibility of the embryo to genotoxic stress.

In response to the inhibition of *de novo* synthesis of DNA, hydroxyurea also caused the upregulation of the pyrimidine pathway. The pyrimidine pathway may be a way to respond to depletion in DNA building blocks. The dysregulation of the normal embryonic pyrimidine pathway may have an impact on folate metabolism and the development of neural tube defects.

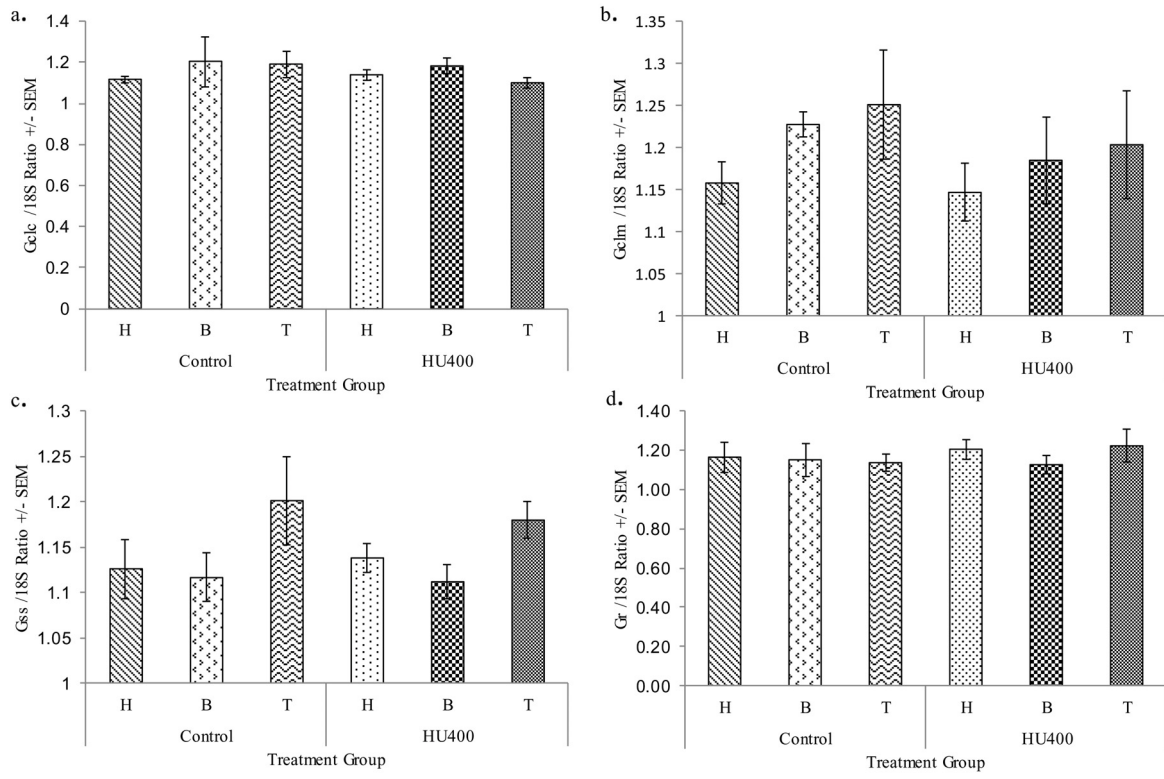
Conclusion

These studies demonstrate that hydroxyurea exposure during organogenesis elicits an early oxidative stress response. The redox homeostasis dysregulation of oxidoreductases such as TRX1 and GAPDH triggers changes their function and localization. TRX1 oxidation may be involved in mediating an AP-1-mediated stress response, while oxidized GAPDH may protect the conceptus against oxidative stress. Hydroxyurea drives the regulation of some antioxidant and DNA repair pathway genes, coincident with cell cycle arrest and the activation of two major apoptosis pathways. Disruption of redox-regulating proteins and redox-sensitive signal transduction, especially in regions of high susceptibility to oxidative stress such as the caudal area, together with the induction of cell cycle arrest and apoptosis during a critical time when the organs are developing, mediate the developmental toxicity of hydroxyurea. Induction of the NRF2-mediated antioxidant response and/or antioxidant supplementation may reduce the susceptibility of the conceptus to oxidant insult.

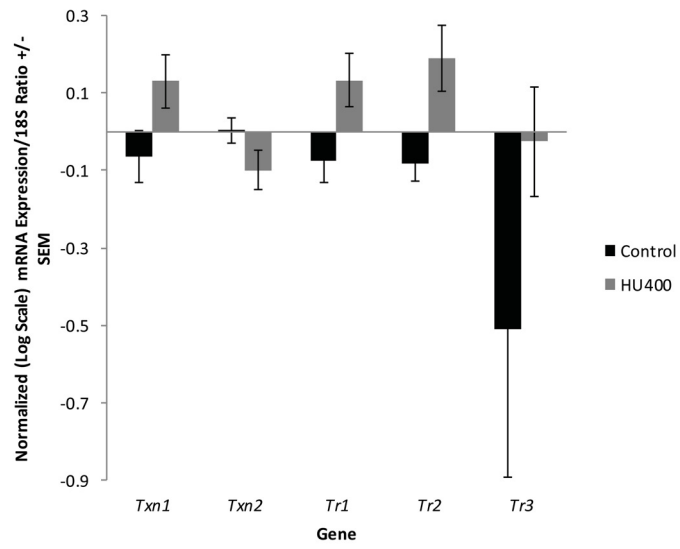
SUPPLEMENTAL DATA DESCRIPTION

The effects of hydroxyurea exposure on the expression of glutathione (Suppl. Fig. 4.1) and thioredoxin pathway (Suppl. Fig. 4.2) genes in the embryo are provided as supplementary data. Microarray data have been deposited in GEO (study GSE54579, <http://www.ncbi.nlm.nih.gov/geo/query/acc.cgi?acc=GSE54579>).

S 4.1.



S 4.2.



ACKNOWLEDGEMENTS

We are grateful to Claudia Lalancette for her expertise and help with the microarray protocol and analyses. We also thank Jason M. Hansen for his valuable input in TRX1 and GAPDH redox western blots. This research is funded by the Canadian Institutes of Health Research (FRN 57867).

REFERENCES

- Adimoolam, S., and Ford, J. M. (2003). p53 and regulation of DNA damage recognition during nucleotide excision repair. *DNA Repair* **2**, 947-954.
- Arrigo, A. P. (1999). Gene expression and the thiol redox state. *Free Radical Biol. Med.* **27**, 936-944.
- Azam, S., Jouvet, N., Jilani, A., Vongsamphanh, R., Yang, X., Yang, S., and Ramotar, D. (2008). Human glyceraldehyde-3-phosphate dehydrogenase plays a direct role in reactivating oxidized forms of the DNA repair enzyme APE1. *J. Biol. Chem.* **283**, 30632-30641.
- Banh, S., and Hales, B. F. (2013). Hydroxyurea exposure triggers tissue-specific activation of p38 mitogen-activated protein kinase signaling and the DNA damage response in organogenesis-stage mouse embryos. *Toxicol. Sci.* **133**, 298-308.
- Chen, C. L., Lin, C. F., Chang, W. T., Huang, W. C., Teng, C. F., and Lin, Y. S. (2008). Ceramide induces p38 MAPK and JNK activation through a mechanism involving a thioredoxin-interacting protein-mediated pathway. *Blood* **111**, 4365-4374.
- Chen, S. Y. (2012). Analysis of Nrf2-mediated transcriptional induction of antioxidant response in early embryos. *Methods Mol. Biol.* **889**, 277-290.
- Chen, W., Sun, Z., Wang, X. J., Jiang, T., Huang, Z., Fang, D., and Zhang, D. D. (2009). Direct interaction between Nrf2 and p21(Cip1/WAF1) upregulates the Nrf2-mediated antioxidant response. *Mol. Cell* **34**, 663-673.
- Dennery, P. A. (2007). Effects of oxidative stress on embryonic development. *Birth Defects Res. C* **81**, 155-162.

DeSesso, J. M., Jacobson, C. F., Scialli, A. R., and Goeringer, G. C. (2000). Hydroxylamine moiety of developmental toxicants is associated with early cell death: a structure-activity analysis. *Teratology* **62**, 346-355.

Desesso, J. M., Scialli, A. R., and Goeringer, G. C. (1994). D-mannitol, a specific hydroxyl free radical scavenger, reduces the developmental toxicity of hydroxyurea in rabbits. *Teratology* **49**, 248-259.

Fratelli, M., Goodwin, L. O., Orom, U. A., Lombardi, S., Tonelli, R., Mengozzi, M., and Ghezzi, P. (2005). Gene expression profiling reveals a signaling role of glutathione in redox regulation. *Proc. Natl. Acad. Sci. U.S.A.* **102**, 13998-14003.

Gartel, A. L., and Tyner, A. L. (2002). The role of the cyclin-dependent kinase inhibitor p21 in apoptosis. *Mol. Cancer Ther.* **1**, 639-649.

Go, Y. M., and Jones, D. P. (2010). Redox control systems in the nucleus: mechanisms and functions. *Antioxid. Redox Signal.* **13**, 489-509.

Hansen, J. M. (2006). Oxidative stress as a mechanism of teratogenesis. *Birth Defects Res. C* **78**, 293-307.

Hansen, J. M. (2012). Thioredoxin redox status assessment during embryonic development: the redox Western. *Methods Mol. Biol.* **889**, 305-313.

Hansen, J. M., and Harris, C. (2013). Redox control of teratogenesis. *Reprod. Toxicol.* **35**, 165-179.

Harris, C., and Hansen, J. M. (2012a). Oxidative stress, thiols, and redox profiles. *Methods Mol. Biol.* **889**, 325-346.

Harris, C., and Hansen, J. M. (2012b). Nrf2-mediated resistance to oxidant-induced redox disruption in embryos. *Birth Defects Res. B* **95**, 213-218.

Hawkes, H. J., Karlenius, T. C., and Tonissen, K. F. (2014). Regulation of the human thioredoxin gene promoter and its key substrates: A study of functional and putative regulatory elements. *Biochim. Biophys. Acta* **1840**, 303-314.

Henrique Barreta, M., Garziera Gasperin, B., Braga Rissi, V., de Cesaro, M. P., Ferreira, R., de Oliveira JF, Gonçalves PB, and Bordignon V. (2012). Homologous recombination and non-homologous end-joining repair pathways in bovine embryos with different developmental competence. *Exp. Cell Res.* **318**, 2049-2058.

Jones, D. P. (2006). Redefining oxidative stress. *Antioxid. Redox Signal.* **8**, 1865-1879.

Liebelt, E. L., Balk, S. J., Faber, W., Fisher, J. W., Hughes, C. L., Lanzkron, S. M., Lewis, K. M., Marchetti, F., Mehendale, H. M., Rogers, J. M., Shad, A. T., Skalko, R. G., and Stanek, E. J. (2007). NTP-CERHR expert panel report on the reproductive and developmental toxicity of hydroxyurea. *Birth Defects Res. B* **80**, 259-366.

Lu, J., and Holmgren, A. (2012). Thioredoxin system in cell death progression. *Antioxid. Redox Signal.* **17**, 1738-1747.

Mao, X. W., Green, L. M., Mekonnen, T., Lindsey, N., and Gridley, D. S. (2010). Gene expression analysis of oxidative stress and apoptosis in proton-irradiated rat retina. *In vivo* **24**, 425-430.

Mitomo, K., Nakayama, K., Fujimoto, K., Sun, X., Seki, S., and Yamamoto, K. (1994). Two different cellular redox systems regulate the DNA-binding activity of the p50 subunit of NF-kappa B in vitro. *Gene* **145**, 197-203.

Nishi, T., Shimizu, N., Hiramoto, M., Sato, I., Yamaguchi, Y., Hasegawa, M., Aizawa, S., Tanaka, H., Kataoka, K., Watanabe, H., and Handa, H. (2002). Spatial redox regulation of a critical cysteine residue of NF-kappa B in vivo. *J Biol. Chem.* **277**, 44548-44556.

Ramkisson, A., and Wells, P. G. (2013). Developmental role of nuclear factor E2-related factor 2 in mitigating methamphetamine fetal toxicity and postnatal neurodevelopmental deficits. *Free Radical Biol. Med.* **65**, 620-631.

Reddy, N. M., Kleeberger, S. R., Bream, J. H., Fallon, P. G., Kensler, T. W., Yamamoto, M., and Reddy, S. P. (2008). Genetic disruption of the Nrf2 compromises cell-cycle progression by impairing GSH-induced redox signaling. *Oncogene* **27**, 5821-5832.

Rushmore, T. H., Morton, M. R., and Pickett, C. B. (1991). The antioxidant responsive element. Activation by oxidative stress and identification of the DNA consensus sequence required for functional activity. *J Biol. Chem.* **266**, 11632-11639.

Schlisser, A. E., and Hales, B. F. (2013). Deprenyl enhances the teratogenicity of hydroxyurea in organogenesis stage mouse embryos. *Toxicol. Sci.* **134**, 391-399.

Schlisser, A. E., Yan, J., and Hales, B. F. (2010). Teratogen-induced oxidative stress targets glyceraldehyde-3-phosphate dehydrogenase in the organogenesis stage mouse embryo. *Toxicol. Sci.* **118**, 686-695.

Shaulian, E., and Karin, M. (2001). AP-1 in cell proliferation and survival. *Oncogene* **20**, 2390-2400.

Thangima Zannat, M., Bhattacharjee, R. B., and Bag, J. (2011). In the absence of cellular poly (A) binding protein, the glycolytic enzyme GAPDH translocated to the cell nucleus and activated the GAPDH mediated apoptotic pathway by enhancing acetylation and serine 46 phosphorylation of p53. *Biochem. Biophys. Res. Commun.* **409**, 171-176.

- Tomasini, R., Samir, A. A., Pebusque, M. J., Calvo, E. L., Totaro, S., Dagorn, J. C., Dusetti, N. J., and Iovanna, J. L. (2002). P53-dependent expression of the stress-induced protein (SIP). *Eur. J Cell Biol.* **81**, 294-301.
- Trachootham, D., Lu, W., Ogasawara, M. A., Nilsa, R. D., and Huang, P. (2008). Redox regulation of cell survival. *Antioxid. Redox Signal.* **10**, 1343-1374.
- Turpaev, K. T. (2002). Reactive oxygen species and regulation of gene expression. *Biochem.* **67**, 281-292.
- Vinson, R. K., and Hales, B. F. (2002). DNA repair during organogenesis. *Mut. Res.* **509**, 79-91.
- Watson, W. H., and Jones, D. P. (2003). Oxidation of nuclear thioredoxin during oxidative stress. *FEBS lett.* **543**, 144-147.
- Yamawaki, H., Haendeler, J., and Berk, B. C. (2003). Thioredoxin: a key regulator of cardiovascular homeostasis. *Circ. Res.* **93**, 1029-1033.
- Yan, J., and Hales, B. F. (2005). Activator protein-1 (AP-1) DNA binding activity is induced by hydroxyurea in organogenesis stage mouse embryos. *Toxicol. Sci.* **85**, 1013-1023.
- Yan, J., and Hales, B. F. (2006). Depletion of glutathione induces 4-hydroxynonenal protein adducts and hydroxyurea teratogenicity in the organogenesis stage mouse embryo. *J Pharmacol. Exp. Ther.* **319**, 613-621.
- Yan, J., and Hales, B. F. (2008). p38 and c-Jun N-terminal kinase mitogen-activated protein kinase signaling pathways play distinct roles in the response of organogenesis-stage embryos to a teratogen. *J Pharmacol. Exp. Ther.* **326**, 764-772.
- Zhou, J., and Chng, W. J. (2013). Roles of thioredoxin binding protein (TXNIP) in oxidative stress, apoptosis and cancer. *Mitochondrion* **13**, 163-169.

Chapter V

DISCUSSION

5.1 Summary

The goals of these studies were to better understand the developmental toxicity of hydroxyurea and the impact of oxidative stress-mediated insult on the organogenesis stage mouse embryo. Hydroxyurea exposure of GD 9 CD1 mice caused lipid peroxidation and increases in 4-HNE-protein adducts. One of the protein targets of 4-HNE was the multifunctional protein GAPDH, decreasing its enzymatic activity and causing its nuclear translocation in areas of high susceptibility to insult. Furthermore, hydroxyurea caused GSH depletion. Blocking the nuclear translocation of GAPDH led to the enhancement of hydroxyurea-induced caudal malformations without further depleting GSH. Hydroxyurea also disrupted redox homeostasis and caused gene expression changes that are redox dependent. Major pathways activated by hydroxyurea are apoptosis and cell cycle arrest. These findings suggest that oxidative stress plays a major role in the induction of specific malformations and triggering a stress response in the embryo that may involve nuclear GAPDH and dysregulation in gene expression.

5.2 The role of oxidative stress in hydroxyurea-induced developmental toxicity

Hydroxyurea exposure to GD 9 embryos induced dose-dependent developmental toxicity. Exposure to 400 mg/kg resulted in decreased fetal weight and few external and skeletal malformations, whereas exposure to 600 mg/kg greatly increased the incidence of fetal resorptions, reduced body weight, and external and skeletal malformations (Schlisser and Hales, 2013). Malformations observed at this gestational time were concentrated in caudal tissues, including the hindlimb, lumbosacral vertebrae, and tail. We observed an increase in lipid peroxidation specifically in the affected areas of the embryo within 3 h following hydroxyurea exposure (Schlisser *et al.*, 2010). Furthermore, GSH was depleted coincident with increased apoptosis. Supporting these results, hydroxyurea exposure caused an early episode of cell death in the limb mesenchyme within 2-4 h that was delayed to 4-6 h with co-administration of propyl gallate, a phenolic antioxidant (DeSesso and Goeringer, 1990). Redox status, determined by assessing the ratio of oxidized to reduced redox-sensitive proteins, was altered as revealed by an early significant and dramatic increase in oxidation, of two specific proteins, TRX1 and GAPDH. Redox-signaling pathways involving GSH/GSSH and TRX1_{red}/TRX1_{ox} seem to occur through discrete compartments rather than working together in equilibrium (Jones, 2006). Experiments using NADPH-oxidase-1 (NOX-1) transfected cells generating high amounts of

H₂O₂ activated the ARE and was quenched by catalase without detectable oxidation of either GSH or TRX1 (Go *et al.*, 2004). In contrast to experiments with NOX-1-derived H₂O₂ generation, addition of H₂O₂ results in extensive and parallel oxidation of both GSH and TRX1 (Watson and Jones, 2003). A similar outcome in hydroxyurea-exposed embryos leads to extensive and dose-dependent oxidation of GSH, TRX1 and GAPDH. 4-HNE immunoreactivity experiments revealed that 4-HNE-adducts accumulate in malformation-sensitive areas of the embryo, suggesting that cellular oxidation may be region specific or compartmentalized (Schlisser *et al.*, 2010). Investigating compartmentalized redox status in the embryo may provide insight into region-specific susceptibility to oxidative stress. Changes in redox homeostasis during organogenesis following thalidomide exposure appear to cause misregulation of developmental events involved in limb bud outgrowth that lead to phocomelia, but also include effects on other systems, such as nervous, gastrointestinal, cardiac and respiratory systems. The severity of thalidomide's effects and the organ systems affected are dependent upon the gestational day of exposure (Hansen and Harris, 2013). The consequences of GSH and TRX1 oxidation after exposure to hydroxyurea and other teratogens are diverse and complex. The teratogenic endpoint may not be merely the result of unscheduled cell death but untimely dysregulation of critical cellular signaling occurring in specific organs at specific times.

ROS/RNS can induce several protein modifications that are either reversible or non-reversible. Cysteine modifications including *S*-sulfenylation, *S*-nitrosylation, *S*-glutathionylation, and disulfide formation are all reversible, however, carbonylation and 3-nitrotyrosine modifications are not (Cai and Yan, 2013). Misfolded proteins due to oxidative modifications can cause aggregates or are shuttled to the endoplasmic reticulum where they are degraded (Narayan, 2012). Certain oxidative posttranslational modifications, for example to P53 or FOXO, can cause cytoplasmic mislocalization leading to various types of cancer (Hung and Link, 2011). *S*-nitrosylation of GAPDH following nitric oxide stimulation inhibits its enzymatic activity and causes its nuclear translocation (Hara *et al.*, 2005). 4-HNE is also a posttranslational oxidative modification that has the potential to affect the function, folding and localization of proteins, other than GAPDH. Heat shock protein 60 kDa (HSP60), aldolase 1, A isoform (ALDOA1), glutamate oxaloacetate transaminase 2 (GOT2) and heterogeneous nuclear ribonucleoprotein isoform A1-A (HNRNP A1A) are also identified as protein targets of 4-HNE

and thus investigating the consequences of posttranslational modifications of proteins could further elucidate oxidative stress mechanisms.

5.3 The role of GAPDH in hydroxyurea-induced developmental toxicity

We have shown that the caudal region of the embryo is susceptible to oxidative stress and protein modifications such as 4-HNE. Proteins modified by 4-HNE in the tail region were identified. Among the eight proteins identified, three are involved in energy metabolism; these are GAPDH, GOT2, and ALDOA1 (Schlisser *et al.*, 2010). This finding indicates that oxidative stress may affect embryonic energy metabolism. Analysis of 4-HNE- GAPDH protein adducts revealed that the increase in 4-HNE conjugation led to a decrease in the amount of GAPDH detected (to 50% of control) and altered its electrophoretic mobility, indicating a conformational change. Further investigation reported a decrease in the enzymatic activity of GAPDH. Parallel to the enzymatic assay carried out to determine the activity of GAPDH, NADH was also measured. Hydroxyurea caused a steady and dose-dependent decrease in the production of NADH, suggesting that reducing equivalents, such as NAD⁺, are depleted in hydroxyurea insult (Schlisser *et al.*, 2010). Glycolysis is the main fuel-producing pathway activated during early embryo development and organogenesis (Hunter and Sadler, 1988). The pentose pathway and Krebs cycle are activated after GD 9 and increase with gestational age (Hunter and Sadler, 1988). Glucose utilization and lactate formation are critical during organogenesis and are increased by 18-fold and 36-fold, respectively (Neubert, 1970). Lactate measurements in the embryo revealed a dose-dependent decrease in lactate production. In addition to 4-HNE-GAPDH protein modifications, GAPDH is also modified by PAR modifications. During oxidative stress conditions, PARP1 becomes cleaved and oxidizes NAD⁺ to NADH and ADP-ribose and polymerizes the latter on cytoplasmic proteins, nuclear acceptor proteins such as GAPDH, histones, transcription factors, and PARP itself (Wang *et al.*, 1997). In chapter IV, cleaved PARP1 was measured as a marker of apoptosis; however, PARP1 is also involved in DNA damage, repair, and energy status. The transfer of ADP(ribose) to acceptor proteins utilizes NAD⁺, and ATP in the process (Heeres and Hergenrother, 2007). Extensive DNA damage and PARP1 activation depletes the cell of NAD⁺ and ATP energy stores. The depletion of energy and inhibition of glycolysis in the embryo is correlated with GSH oxidation and changes in thiol/disulfide status (Hiranruengchock and Harris, 1995). Other glycolytic enzymes, such as

ALDOA1 and phosphofruktokinase, are also modified by oxidative stress (Schlisser *et al.*, 2010; Hiranruengchock and Harris, 1995). Together, these studies indicate that oxidative stress depletes energy status that may have detrimental effects on developmental processes, cellular function and signal transduction that depend on energy homeostasis.

With the advent of confocal microscopy and 3D image analysis, more accurate localization of GAPDH was possible as opposed to classical cytoplasmic/nuclear fractionation. Lumbosacral assessments of GAPDH localization indicated a dose-dependent increase in the nuclear content of GAPDH following hydroxyurea exposure. Blocking the nuclear translocation of GAPDH with deprenyl allowed us to better understand the role it plays in the nucleus. The literature strongly suggests that GAPDH plays a detrimental role in the nucleus in patients suffering from Parkinson's disease and that blocking its nuclear translocation improves the state of neuronal cells and prevents cell death (Sen *et al.*, 2008). Interestingly, the preadministration of deprenyl following hydroxyurea exposure led to an enhancement in fetal death, fetal weight, external and skeletal malformations, specifically those of the hindlimbs, lumbosacral vertebrae, and tail. The increases in malformations were not accompanied by an increase in GSH depletion or GSSG increase, indicating that the malformations were not a result of an increase in oxidative stress. Deprenyl and hydroxyurea did not further deplete lactate production. Because GAPDH is susceptible to oxidative modifications, it seems likely that its nuclear translocation is associated with a stress response and is a redox sensor of the cell. The activities within the nucleus following hydroxyurea exposure indicate a protective role; by inhibiting its translocation, detrimental processes ensue. Cleaved caspase-3 immunoreactivity as a marker of apoptosis was also enhanced with deprenyl, indicating that it did not delay cell death by blocking the nuclear translocation of GAPDH, which are mechanisms described in the literature for the action deprenyl. Clearly there is a dichotomy occurring in the embryo and the adult, where GAPDH does not play similar roles during a stress response. Perhaps experiments overexpressing GAPDH in the embryo during organogenesis, with or without mutations at the NAD⁺ binding site to abolish the glycolytic activity (Tyr42Gly, Tyr45Gly, Tyr49Gly, and Ser51Gly (Nicholls *et al.*, 2012), would provide a better understanding of the protective properties of GAPDH. Immunoprecipitation of GAPDH and its binding partner in the nucleus will also help better understand its role that deviates from glycolysis.

Despite the diverse roles of GAPDH in the cytoplasm and in the nucleus, it is commonly used as an intracellular control for PCR and Western/Northern blot techniques. The frequent use of GAPDH as an internal control is based on the regulation of its cellular levels. The GAPDH promoter region contains HREs and IREs (Hypoxia- and Iron- Responsive Elements, respectively). Upregulation of GAPDH expression involves iron deficiency, P53, C-JUN/AP-1 and HIF-1 α transcription factors that interact with upstream elements. GAPDH is expressed from mRNA in the cytoplasm, where it exists with a half-life of about 5 days. GAPDH is degraded by a process known as chaperone-mediated autophagy (Isenman and Dice, 1989; Cuervo *et al.*, 1994; Shen *et al.*, 2006). The constitutive expression of GAPDH and its major role in bioenergetics is the very feature that has made this gene a suitable choice as a control. However, I would argue that GAPDH not be used as a control in techniques, such as qRT-PCR or Western and Northern blots, when using cell lines, tissues or organs *in vivo* or *in vitro* to model diseases and/or insult that involve ROS or hypoxia, as the levels become very variable following hydroxyurea insult. Furthermore, in neurodegenerative disorders, specifically Parkinson's disease, GAPDH mRNA and protein levels rise as dopaminergic cells approach apoptosis (Shashidharan *et al.*, 1999). Finally, GAPDH should not be used as a cytoplasmic marker regardless of its directed expression since it can translocate into the nucleus during oxidative stress or stress produced during experimental preparations.

5.4 The role of the embryonic stress response

Exposure to hydroxyurea at a dose of 400 mg/kg triggered a major change in gene regulation. Many genes identified respond to changes in redox homeostasis, such as *Nrf2*, the major regulator of the ARE, its downstream target *Prdx1* and an endogenous inhibitor of TRX1, *Txnip*. Surprisingly, other genes under the control of the ARE, such as glutathione-related genes, were not changed by hydroxyurea exposure, despite the depletion in GSH. In human developmental toxicology studies of the phenytoin exposure of second trimester aborted fetuses a significant depletion of GSH and increased GSSG with the induction of *hGSTA1*, but not of other glutathione-related genes, were observed (Gallagher and Sheehy, 2000). Perhaps the gene regulation response to GSH depletion is time specific and the windows of upregulation were not captured in these studies. Mouse embryos treated with H₂O₂ displayed GSH depletion within 120 minutes of exposure; however, NRF2-dependent gene expression changes were apparent only

after 14 h of D3T and H₂O₂ treatment (Harris and Hansen, 2012). In our studies, the redox-sensitive signaling occurs shortly after insult; however, GSH may only be restored over a longer period of time. Once GSH is depleted, the restoration occurs by one of two pathways. The first involves direct transport of extracellular GSH into the cells; however, this pathway occurs in a limited number of cells types such as those of the small intestine and kidney proximal tubules (Lash and Jones, 1983). Direct transport has not been shown to contribute significantly to GSH restoration in the development rodent conceptus (Harris *et al.*, 1995). The most important means of restoring GSH status is through *de novo* synthesis. GCL, the rate-limiting step in the production of GSH synthesis, catalyzes the first step in the pathway forming γ -glutamyl cysteine (Harris *et al.*, 1995). Experiments using diethyl maleate (DEM) to deplete GSH, demonstrated that the visceral yolk sac synthesized sufficient GSH to exceed the initial levels by 3 h; however, no evidence of restoration was seen in the tissues of the embryo proper (Harris *et al.*, 1995). This result underlies the susceptibilities of the embryo to oxidative stress and its delayed response to upregulate an antioxidant pathway. Enhancing the response to oxidative stress could be done using transgenic mice overexpressing GCL, GS, or supplementation with compounds that activate the ARE, such as n-acetylcysteine, D3T, lycopene, β -carotene, or *tert*-butylhydroquinone, thus improving the tolerance to hydroxyurea (Ben-Dor *et al.*, 2005).

5.5 The role of apoptotic gene regulation

In addition to redox-dependent gene responses, several critical genes involved in the initiation or activation of apoptotic signaling pathways, intrinsic or extrinsic, were significantly upregulated following hydroxyurea. The genes identified include *Noxa1*, *Bax*, *Fas*, *MAPK*, *Trp53inp1*, and *Apaf1*. P53-dependent genes such as *Noxa*, *Bax*, and *Trp53inp1* were found to be upregulated following hydroxyurea. Increased P53 immunoreactivity and enhanced mRNA levels of pro-apoptotic genes, *p21*, *Bax*, and *Cyclin G*, were reported in a hydroxyurea target tissues (Woo *et al.*, 2003). Pathway analysis revealed a network of these genes in addition to several others that crosstalk to initiate the extrinsic and intrinsic apoptotic pathways. The abnormal and unscheduled cell death, determined by cleaved caspase-3 and PARP1, occurs simultaneously to the expression of gene products involved in apoptosis. *Noxa* and MAP kinase genes have been shown to be involved in oxidative stress-dependent apoptosis (Mao *et al.*, 2010). *Mek3*, *Mek6*, and *c-Jun* are genes involved in apoptosis in response to oxidative stress.

We have previously reported that MEK3 and 6 are phosphorylated at the protein level and signal phosphorylation of P38 following hydroxyurea exposure (Banh and Hales, 2013). C-JUN N-terminal kinase (JNKs) pathways were found to protect the conceptus against oxidative stress (Yan and Hales, 2008). Oxidative stress may stimulate JNKs mainly through activation of ASK1, a MAP3K (Matsuzawa and Ichijo, 2008). Inhibiting JNK pathways specifically enhanced the hindlimb defects induced by hydroxyurea (Yan and Hales, 2008). C-JUN has been suggested to induce apoptosis in limbs during normal development and as a consequence of the stress induced by thalidomide, H₂O₂, or UV irradiation (Grotewold and Ruther, 2002b). How JNKs might mediate a region-specific protective effect on the hindlimbs is unclear. Perhaps spatiotemporal gene expression of JNKs plays a critical role in limb pattern development and alterations during stress trigger a region-specific effect. Activation of JNKs was accompanied by changes in FGF8 expression during chemical-induced ameloblast differentiation (Abe *et al.*, 2007). The anterior part of the limb is highly sensitive to changes in the levels of FGF8. A decrease in FGF8 was detected in the caudal region of the embryo after hydroxyurea treatment (Yan and Hales, 2008). Interestingly, FGFR3 was decreased following hydroxyurea exposure in our microarray analysis and has been associated with skeletal dysplasias (Ohbayashi *et al.*, 2002). FGFR3 inhibition or mutations have been associated with apoptosis and decreased proliferation of chondrocytes (Iwata *et al.*, 2000). Oxidative stress was reported to have an impact on the expression of FGF-8/FGF-10 through the inability of NF-κB to bind to its DNA promoter, specifically in the apical ectodermal ridge during limb outgrowth (Hansen and Harris, 2004). Investigating the consequences of altering FGF signaling may provide insight into the mechanisms of limb malformations following oxidative stress.

5.6 The role of cell cycle gene regulation

In addition to the apoptotic pathways, the cell cycle pathway was greatly affected by hydroxyurea. Hydroxyurea exposure prevented the expansion of dNTP pools when cells enter S phase and arrested the cell cycle at the G1-S boundary (Kurose *et al.*, 2006). AP-1-dependent *Cyclin D1* was downregulated and *p21* was upregulated following hydroxyurea exposure. 4-HNE may be responsible for regulating *p21* and *cyclin D1* genes (Calonghi *et al.*, 2002; Barrera *et al.*, 2004). These genes crosstalk with a large network of other genes involved in diverse roles, including apoptosis, DNA damage, G1/S transition, and transcription. The pathway analysis

demonstrates an upregulation in cell cycle arrest gene expression; however, the depletion of dNTPs also has an impact on the progression of the cell cycle since mechanically, the DNA is not able to expand. Thus, both the dysregulation of these genes and depletion of DNA building blocks following hydroxyurea insult cause cell cycle arrest that contributes to the teratogenicity of hydroxyurea.

5.7 The role of DNA repair pathways

Another interesting pathway that was altered in our microarray experiment was the DNA damage/repair pathway. Pathway analysis revealed 32 upregulated genes involved in double strand non-homologous end-joining repair (NHEJ); they include, *Rad50*, *Mre11a*, *PolB* and *Parp1*. Perhaps the DNA repair capabilities following DNA damage maintain the viability of the embryo despite the detrimental impact of hydroxyurea on its growth and development. It appears as though not all the critical gene products involved in DNA repair are upregulated; AP endonuclease (*Apex*), DNA ligase 1 (*Lig1*), uracil-DNA glycosylase (*UNG*), XRCC1 and XRCC4 protein (*Xrcc1* and *Xrcc14*), ataxia telangiectasia mutated/related (*ATM/ATR*), and P53 protein (*p53*), were not changed following hydroxyurea exposure. Experiments with null mutation mice suggest that DNA repair gene products that contribute to, the base excision repair (BER), nucleotide excision repair (NER), mismatch repair (MMR), non-homologous end-joining (NHEJ), and checkpoint pathways are present during development. Our data suggest that NHEJ is the early repair pathway activated following hydroxyurea insult; however, the limitation in the repair process, considering only one repair pathway was activated, reveals critical windows of susceptibility to genotoxic and oxidative stress producing agents.

It has been suggested that the early onset of apoptosis associated with hydroxyurea is not mediated by its ability to cause DNA damage but rather by the rapid onset of oxidative stress (DeSesso *et al.*, 1991). Hydroxyurea-induced oxidative stress and its mechanism of action to inhibit DNA replication is known to stall replication forks causing DNA replication stress, triggering the formation of γ -H2AX foci at the collapsed forks (Ward and Chen, 2001). Γ -H2AX immunoreactivity in GD 9 embryos exposed to hydroxyurea was enhanced in malformation-sensitive tissues (Banh and Hales, 2013). Exposure to other DNA synthesis inhibitors, such as methotrexate, induced γ -H2AX phosphorylation and cell death, preferentially affecting S-phase cells (Kurose *et al.*, 2006). However, methotrexate is associated with oxidative stress-induced

DNA damage and apoptosis (Elango *et al.*, 2013). Treatment with high concentrations of thymidine also inhibits DNA replication and synchronizes cells in S-phase but does not trigger γ -H2AX phosphorylation or cell death (Kurose *et al.*, 2006). It is intriguing to consider the role of DNA damage during organogenesis without the confounding complication of oxidative stress-induced DNA damage. DNA synthesis inhibitors that do not produce oxidative stress, such as treatment with high concentrations of deoxyadenosine, deoxyguanosine, or thymidine, generating a negative feedback and blocking the progression through S-phase, may provide insight into teratogenic mechanisms of oxidative stress-induced DNA damage. Separating the effects of oxidatively-modified targets and redox-sensitive gene regulation from DNA damage and repair during organogenesis will help to elucidate the mechanisms of hydroxyurea teratogenesis.

5.8 Conclusions

1) Hydroxyurea exposure during early organogenesis induced ROS leading to GSH depletion. The products of lipid peroxidation were concentrated in tissues particularly sensitive to hydroxyurea-induced malformations. Lipid peroxides, specifically 4-HNE, were adducted with several proteins, including the multifunctional GAPDH. 4-HNE-GAPDH protein adducts led to the decrease in GAPDH enzymatic activity and glycolysis. Furthermore, GAPDH translocated from the cytoplasm to the nucleus in the lumbosacral region, an area of high susceptibility to defects. Thus, region-specific enhanced oxidative stress and affected proteins may be the basis for the susceptibility of the caudal region of the embryo to hydroxyurea-induced teratogenesis.

2) The roles of GAPDH in the nucleus may be essential in the protection of the conceptus against insult. The susceptibility of GAPDH to oxidation and 4-HNE protein adducts suggests that it may act as a redox sensor in the cell. Since GAPDH is a major target of hydroxyurea-induced oxidative stress and glycolysis is the major source of energy in the embryo during organogenesis, the depletion in energy may be a significant aspect to hydroxyurea teratogenesis.

3) Exposure to hydroxyurea shifted the redox homeostasis to an oxidized state, severely oxidizing important redox-regulating proteins like TRX1 and GAPDH, and most likely many more. Dysregulation of redox-sensitive proteins during organogenesis, especially in regions of high susceptibility to oxidative stress, such as the caudal region that depends on oxidoreductase

activities, renders the conceptus vulnerable to oxidative damage and perturbations of important developmental redox signaling. The extent to which proteins are posttranslationally modified by hydroxyurea-induced oxidative stress and the changes in their folding, function and localization need to be further elucidated.

4) Hydroxyurea caused a dramatic change in gene regulation. Specific antioxidant gene products were upregulated, protecting the conceptus against oxidative stress, albeit a limited response. The redox-sensitive signaling, such as AP-1, that was activated following hydroxyurea exposure is likely to be involved in triggering apoptosis. Many other genes that respond to oxidative stress were involved in activating apoptosis and cell cycle arrest, causing the cessation of developmental programming that is likely to lead to malformations or embryonic death. Among the many genes found to be involved in apoptosis and cell cycle, a significant decrease in FGFR3 was found in the embryo after hydroxyurea treatment. FGFR3 is expressed in the long bones and vertebrae at the time of hydroxyurea exposure and is essential for chondrogenesis. The lumbosacral vertebrae column and hindlimb defects may indicate cell death or disruption of the tail bud and hindlimb growth that is partly dependent on FGFR3 levels.

ORIGINAL CONTRIBUTIONS

1. GAPDH is a major target of 4-HNE-protein adducts in malformation-sensitive regions of the embryo. GAPDH is also a target of PAR and oxidative modifications regulating the functional versatility of this enzyme.
2. Following hydroxyurea exposure, the enzymatic activity of GAPDH, responsible for its catalytic actions in glycolysis, is attenuated. The final step in glycolysis is the production of lactate, an important source of energy during early organogenesis; lactate was also decreased with hydroxyurea treatment. The demand for energy at this critical stage of rapid cell proliferation plays a role in the development of hydroxyurea-induced malformations.
3. Upon hydroxyurea exposure, GAPDH translocates into the nucleus in lumbosacral somites, an area of high susceptibility to malformations. Inhibition of the nuclear translocation of GAPDH increased the incidence of malformations in caudal structures. GAPDH appears to play a protective role in the nucleus and is regulated by redox-dependent posttranslational modifications.
4. A single exposure to hydroxyurea perturbed the redox potential of TRX1 and GAPDH simultaneously with GSH depletion. These studies provide evidence that embryos exposed to hydroxyurea cannot maintain redox homeostasis by the network of reducing equivalents present. The limited antioxidant capacity renders the embryo susceptible to high oxidation and major dysregulation of redox sensitive targets.
5. Hydroxyurea exposure induced a limited number of antioxidant gene products; analysis of the differences in gene expression between control and hydroxyurea-exposed embryos revealed that apoptosis, cell cycle arrest and DNA damage response were highly activated in the embryo. Many components of these pathways are redox sensitive and respond to oxidative stress. Our studies demonstrate that the response at the gene level to counter oxidative stress is very limited and coincidentally initiates a stress response that contributes to the detriment of the embryo.

REFERENCES

- Abe, K., Miyoshi, K., Muto, T., Ruspita, I., Horiguchi, T., Nagata, T., and Noma, T. (2007). Establishment and characterization of rat dental epithelial derived ameloblast-lineage clones. *J Biosci. Bioeng.* **103**, 479-85.
- Akhondzadeh, S., Tavakolian, R., Davari-Ashtiani, R., Arabgol, F., and Amini, H. (2003). Selegiline in the treatment of attention deficit hyperactivity disorder in children: a double blind and randomized trial. *Prog. Neuropsychopharmacol. Biol. Psychiatry* **27**, 841-845.
- Alderton, A. L., Faustman, C., Liebler, D. C., and Hill, D. W. (2003). Induction of redox instability of bovine myoglobin by adduction with 4-hydroxy-2-nonenal. *Biochem.* **42**, 4398-4405.
- Aldini, G., Gamberoni, L., Orioli, M., Beretta, G., Regazzoni, L., Maffei Facino, R., and Carini, M. (2006). Mass spectrometric characterization of covalent modification of human serum albumin by 4-hydroxy-trans-2-nonenal. *J Mass Spec.* **41**, 1149-1161.
- Allison, W. S. (1968). Structure and evolution of triose phosphate and lactate dehydrogenases. *Ann. N. Y. Acad. Sci.* **151**, 180-199.
- Arcari, P., Martinelli, R., and Salvatore, F. (1989). Human glyceraldehyde-3-phosphate dehydrogenase pseudogenes: molecular evolution and a possible mechanism for amplification. *Biochem. Genet.* **27**, 439-450.
- Awasthi, Y. C., Sharma, R., Sharma, A., Yadav, S., Singhal, S. S., Chaudhary, P., Awasthi, S. (2008). Self-regulatory role of 4-hydroxynonenal in signaling for stress-induced programmed cell death. *Free Radic Biol Med.* **45**:111-118.

Bacot, S., Bernoud-Hubac, N., Baddas, N., Chantegrel, B., Deshayes, C., Doutheau, A., Lagarde, M., Guichardant, M. (2003). Covalent binding of hydroxy-alkenals 4-HDDE, 4-HHE, and 4-HNE to ethanolamine phospholipid subclasses. *J Lipid Res.* **44**:917-926.

Bailey, J., Knight, A., Balcombe, J. (2005). The future of teratology research is *in vitro*. *Biogen. Amines* **19**, 97-145.

Banh, S., and Hales, B. F. (2013). Hydroxyurea exposure triggers tissue-specific activation of p38 mitogen-activated protein kinase signaling and the DNA damage response in organogenesis-stage mouse embryos. *Toxicol. Sci.* **133**, 298-308.

Bar-Am, O., Amit, T., Weinreb, O., Youdim, M. B., and Mandel, S. (2010). Propargylamine containing compounds as modulators of proteolytic cleavage of amyloid-beta protein precursor: involvement of MAPK and PKC activation. *J Alzheimer's Dis.* **21**, 361-371.

Barrett, J. S., Hochadel, T. J., Morales, R. J., Rohatagi, S., DeWitt, K. E., Watson, S. K., and DiSanto, A. R. (1996). Pharmacokinetics and safety of a selegiline transdermal system relative to single-dose oral administration in the elderly. *Am. J Ther.* **3**, 688-698.

Barrera, G., Di Mauro, C., Muraca, R., Ferrero, D., Cavalli, G., Fazio, VM., Paradisi, L., Dianzani, M. U. (1991). Induction of differentiation in human HL-60 cells by 4-hydroxynonenal, a product of lipid peroxidation. *Exp Cell Res.* **197**:148-152.

Ben-Dor, A., Steiner, M., Gheber, L., Danilenko, M., Dubi, N., Linnewiel, K., Zick, A., Sharoni, Y., and Levy, J. (2005). Carotenoids activate the antioxidant response element transcription system. *Mol. Cancer Ther.* **4**, 177-186.

Botzen, D., and Grune, T. (2007). Degradation of HNE-modified proteins--possible role of ubiquitin. *Redox Rep.* **12**, 63-67.

Buko, V. U., Artsukevich, A. A., and Ignatenko, K. V. (1999). Aldehydic products of lipid peroxidation inactivate cytochrome P-450. *Exp. Toxicol. Path.* **51**, 294-298.

Butterfield, D. A., Hardas, S. S., and Lange, M. L. (2010). Oxidatively modified glyceraldehyde-3-phosphate dehydrogenase (GAPDH) and Alzheimer's disease: many pathways to neurodegeneration. *J Alzheimer's Dis.* **20**, 369-393.

Cai, Z., and Yan, L. J. (2013). Protein oxidative modifications: beneficial roles in disease and health. *J Biochem. Pharmacol. Res.* **1**, 15-26.

Calonghi, N., Boga, C., Cappadone, C., Pagnotta, E, Bertucci, C, Fiori, J, Masotti, L. (2002). Cytotoxic and cytostatic effects induced by 4-hydroxynonenal in human osteosarcoma cells. *Biochem. Biophys Res Commun.* **293**:1502-1507.

Campion, S. N., Davenport, S. J., Nowland, W. S., Cappon, G. D., Bowman, C. J., and Hurtt, M. E. (2012). Sensitive windows of skeletal development in rabbits determined by hydroxyurea exposure at different times throughout gestation. *Birth Defects Res. B Dev. Reprod. Toxicol.* **95**, 238-249.

Carbone, D. L., Doorn, J. A., and Petersen, D. R. (2004). 4-Hydroxynonenal regulates 26S proteasomal degradation of alcohol dehydrogenase. *Free Radic. Biol Med.* **37**, 1430-1439.

Carlile, G. W., Chalmers-Redman, R. M., Tatton, N. A., Pong, A., Borden, K. E., and Tatton, W. G. (2000). Reduced apoptosis after nerve growth factor and serum withdrawal: conversion of tetrameric glyceraldehyde-3-phosphate dehydrogenase to a dimer. *Molec. Pharmacol.* **57**, 2-12.

Chiarpotto, E., Domenicotti, C., Paola, D., Vitali, A., Nitti, M., Pronzato, M. A., Biasi, F., Cottalasso, D., Marinari, U. M., Dragonetti, A., Cesaro, P., Isidoro, C., and Poli, G. (1999). Regulation of rat hepatocyte protein kinase C beta isoenzymes by the lipid peroxidation product

4-hydroxy-2,3-nonenal: A signaling pathway to modulate vesicular transport of glycoproteins. *Hepatology* **29**, 1565-1572.

Choe, H., Hansen, J. M., and Harris, C. (2001). Spatial and temporal ontogenies of glutathione peroxidase and glutathione disulfide reductase during development of the prenatal rat. *J Biochem. Mol. Toxicol.* **15**, 197-206.

Cool, B. L., and Sirover, M. A. (1989). Immunocytochemical localization of the base excision repair enzyme uracil DNA glycosylase in quiescent and proliferating normal human cells. *Cancer Res.* **49**, 3029-3036.

Cuervo, A. M., Terlecky, S. R., Dice, J. F., and Knecht, E. (1994). Selective binding and uptake of ribonuclease A and glyceraldehyde-3-phosphate dehydrogenase by isolated rat liver lysosomes. *J Biol. Chem.* **269**, 26374-26380.

Dalleau, S., Baradat, M., Gueraud, F., and Huc, L. (2013). Cell death and diseases related to oxidative stress: 4-hydroxynonenal (HNE) in the balance. *Cell Death Differ.* **20**, 1615-1630.

Dennery, P. A. (2007). Effects of oxidative stress on embryonic development. *Birth Defects Res. C Embryo Today* **81**, 155-162.

DeSesso, J. M. (2011). Comparative gestational milestones in vertebrate development. In *Developmental and Reproductive Toxicology: A Practical Approach* (R. D. Hood, Ed.), 3rd ed., pp. 93-138. CRC Press. Boca Raton, Florida.

DeSesso, J. M. (1981a). Amelioration of teratogenesis. I. Modification of hydroxyurea-induced teratogenesis by the antioxidant propyl gallate. *Teratology* **24**, 19-35.

DeSesso, J. M. (1981b). Comparative ultrastructural alterations in rabbit limb-buds after a teratogenic dose of either hydroxyurea or methotrexate. *Teratology* **23**, 197-215.

DeSesso, J. M., and Goeringer, G. C. (1990a). Ethoxyquin and nordihydroguaiaretic acid reduce hydroxyurea developmental toxicity. *Reprod. Toxicol.* **4**, 267-275.

DeSesso, J. M., and Goeringer, G. C. (1990b). The nature of the embryo-protective interaction of propyl gallate with hydroxyurea. *Reprod. Toxicol.* **4**, 145-152.

DeSesso, J. M., Jacobson, C. F., Scialli, A. R., and Goeringer, G. C. (2000). Hydroxylamine moiety of developmental toxicants is associated with early cell death: a structure-activity analysis. *Teratology* **62**, 346-355.

Desesso, J. M., Scialli, A. R., and Goeringer, G. C. (1994). D-mannitol, a specific hydroxyl free radical scavenger, reduces the developmental toxicity of hydroxyurea in rabbits. *Teratology* **49**, 248-259.

Dickinson, D. A., Iles, K. E., Watanabe, N., Iwamoto, T., Zhang, H., Krzywanski, D. M., Forman, H. J. (2002). 4-Hydroxynonenal induces glutamate cysteine ligase through JNK in HBE1 cells. *Free Radic Biol Med.* **33**:974.

Diez, J. A., and Maderdrut, J. L. (1977). Development of multiple forms of mouse brain monoamine oxidase in vivo and in vitro. *Brain Res.* **128**, 187-192.

Doorn, J. A., and Petersen, D. R. (2002). Covalent modification of amino acid nucleophiles by the lipid peroxidation products 4-hydroxy-2-nonenal and 4-oxo-2-nonenal. *Chem. Res. Toxicol.* **15**, 1445-1450.

Dreosti, I. E. (1987). Micronutrients, superoxide and the fetus. *Neurotoxicology* **8**, 445-449.

Dumollard, R., Carroll, J., Duchon, M. R., Campbell, K., Swann, K. (2009). Mitochondrial function and redox state in mammalian embryos. *Semin Cell Dev Biol.* **20**:346-353.

Elango, T., Dayalan, H., Gnanaraj, P., Malligarjunan, H., and Subramanian, S. (2013). Impact of methotrexate on oxidative stress and apoptosis markers in psoriatic patients. *Clin. Exp. Med.* [Epub ahead of print] PMID: 23949337.

Esterbauer, H., and Cheeseman, K. H. (1990). Determination of aldehydic lipid peroxidation products: malonaldehyde and 4-hydroxynonenal. *Methods Enzymol.* **186**, 407-421.

Esterbauer, H., Cheeseman, K. H., Dianzani, M. U., Poli, G., and Slater, T. F. (1982). Separation and characterization of the aldehydic products of lipid peroxidation stimulated by ADP-Fe²⁺ in rat liver microsomes. *Biochem. J* **208**, 129-140.

Ferrington, D. A., and Kapphahn, R. J. (2004). Catalytic site-specific inhibition of the 20S proteasome by 4-hydroxynonenal. *FEBS Lett.* **578**, 217-223.

Finkelstein, E. I., Ruben, J., Koot, C. W., Hristova, M., and van der Vliet, A. (2005). Regulation of constitutive neutrophil apoptosis by the alpha,beta-unsaturated aldehydes acrolein and 4-hydroxynonenal. *Am. J Physiol. Lung Cell. Mol. Physiol.* **289**, L1019-1028.

Gallagher, E. P., and Sheehy, K. M. (2001). Effects of phenytoin on glutathione status and oxidative stress biomarker gene mRNA levels in cultured precision human liver slices. *Toxicol. Sci.* **59**, 118-126.

Glover, V., Gibb, C., and Sandler, M. (1986). The role of MAO in MPTP toxicity--a review. *J Neural Transm. Suppl.* **20**, 65-76.

Go, Y. M., Gipp, J. J., Mulcahy, R. T., and Jones, D. P. (2004). H₂O₂-dependent activation of GCLC-ARE4 reporter occurs by mitogen-activated protein kinase pathways without oxidation of cellular glutathione or thioredoxin-1. *J Biol. Chem.* **279**, 5837-5845.

Grady, M. M., and Stahl, S. M. (2012). Practical guide for prescribing MAOIs: debunking myths and removing barriers. *CNS Spectr.* **17**, 2-10.

Grotewold, L., and Ruther, U. (2002). The wnt antagonist dickkopf-1 is regulated by Bmp signaling and c-Jun and modulates programmed cell death. *EMBO J* **21**, 966-975.

Guerin, P., El Mouatassim, S., and Menezo, Y. (2001). Oxidative stress and protection against reactive oxygen species in the pre-implantation embryo and its surroundings. *Hum. Reprod. Update* **7**, 175-189.

Gwilt, P. R., and Tracewell, W. G. (1998). Pharmacokinetics and pharmacodynamics of hydroxyurea. *Clin. Pharmacokinet.* **34**, 347-358.

Hagell, P., Odin, P., and Vinge, E. (1998). Pregnancy in Parkinson's disease: a review of the literature and a case report. *Mov. Disord.* **13**, 34-38.

Halliwell, B. Gutteridge, J.M. (1989). The use of HPLC with electrochemical detection. In *Neurochemical Markers of Degenerative Nervous Diseases and Drug Addiction* (G.A. Qureshi, H. Parvez, P. Caudy, S. Parvez, Eds), 1 ed., pp. 13-14. VSP BV, Netherlands.

Hansen, J. M. (2006). Oxidative stress as a mechanism of teratogenesis. *Birth Defects Res. C Embryo Today* **78**, 293-307.

Hansen, J. M., Carney, E. W., and Harris, C. (1999). Differential alteration by thalidomide of the glutathione content of rat vs. rabbit conceptuses in vitro. *Reprod. Toxicol.* **13**, 547-554.

Hansen, J. M., and Harris, C. (2004). A novel hypothesis for thalidomide-induced limb teratogenesis: redox misregulation of the NF-kappaB pathway. *Antioxid. Redox Signal.* **6**, 1-14.

Hansen, J. M., and Harris, C. (2013). Redox control of teratogenesis. *Reprod. Toxicol.* **35**, 165-179.

Hansen, J. M., Lee, E., and Harris, C. (2004). Spatial activities and induction of glutamate-cysteine ligase (GCL) in the postimplantation rat embryo and visceral yolk sac. *Toxicol. Sci.* **81**, 371-378.

Hara, M. R., Thomas, B., Cascio, M. B., Bae, B. I., Hester, L. D., Dawson, V. L., Dawson, T. M., Sawa, A., and Snyder, S. H. (2006). Neuroprotection by pharmacologic blockade of the GAPDH death cascade. *Proc. Natl. Acad. Sci. U.S.A.* **103**, 3887-3889.

Harris, C., and Hansen, J. M. (2012). Nrf2-mediated resistance to oxidant-induced redox disruption in embryos. *Birth Defects Res. B Devel. Reprod. Toxicol.* **95**, 213-218.

Heeres, J. T., and Hergenrother, P. J. (2007). Poly(ADP-ribose) makes a date with death. *Curr. Opin. Chem. Biol.* **11**, 644-653.

Hiranruengchok, R., and Harris, C. (1995). Diamide-induced alterations of intracellular thiol status and the regulation of glucose metabolism in the developing rat conceptus in vitro. *Teratology* **52**, 205-214.

Hirota, K., Matsui, M., Iwata, S., Nishiyama, A., Mori, K., and Yodoi, J. (1997). AP-1 transcriptional activity is regulated by a direct association between thioredoxin and Ref-1. *Proc. Natl. Acad. Sci. U.S.A.* **94**, 3633-3638.

Holmgren, A. (1985). Thioredoxin. *Ann. Rev. Biochem.* **54**, 237-271.

Holmgren, A., and Lu, J. (2010). Thioredoxin and thioredoxin reductase: current research with special reference to human disease. *Biochem. Biophys. Res. Commun.* **396**, 120-124.

Hornykiewicz, O. (2001). Dopamine and Parkinson's disease. A personal view of the past, the present, and the future. *Adv. Neurol.* **86**, 1-11.

Human prescription drug label; Eldepryl (selegiline hydrochloride) capsule. Somerset Pharmaceuticals Inc. 2009.

Hung, M. C., and Link, W. (2011). Protein localization in disease and therapy. *J Cell Sci.* **124**, 3381-3392.

Hunter, E. S., 3rd, and Sadler, T. W. (1988). Embryonic metabolism of foetal fuels in whole-embryo culture. *Toxicol. In Vitro* **2**, 163-167.

Hunter, E. S., 3rd, and Tugman, J. A. (1995). Inhibitors of glycolytic metabolism affect neurulation-staged mouse conceptuses in vitro. *Teratology* **52**, 317-323.

Hussain, S. N., Matar, G., Barreiro, E., Florian, M., Divangahi, M., and Vassilakopoulos, T. (2006). Modifications of proteins by 4-hydroxy-2-nonenal in the ventilatory muscles of rats. *Am. J Physiol. Lung Cell. Mol. Physiol.* **290**, L996-1003.

Hwang, N. R., Yim, S. H., Kim, Y. M., Jeong, J., Song, E. J., Lee, Y., Lee, J. H., Choi, S., and Lee, K. J. (2009). Oxidative modifications of glyceraldehyde-3-phosphate dehydrogenase play a key role in its multiple cellular functions. *Biochem. J* **423**, 253-264.

Isenman, L. D., and Dice, J. F. (1989). Secretion of intact proteins and peptide fragments by lysosomal pathways of protein degradation. *J Biol. Chem.* **264**, 21591-21596.

Ishii, T., Tatsuda, E., Kumazawa, S., Nakayama, T., and Uchida, K. (2003). Molecular basis of enzyme inactivation by an endogenous electrophile 4-hydroxy-2-nonenal: identification of modification sites in glyceraldehyde-3-phosphate dehydrogenase. *Biochemistry* **42**, 3474-3480.

Iwata, T., Chen, L., Li, C., Ovchinnikov, D. A., Behringer, R. R., Francomano, C. A., and Deng, C. X. (2000). A neonatal lethal mutation in FGFR3 uncouples proliferation and differentiation of growth plate chondrocytes in embryos. *Hum. Mol. Genet.* **9**, 1603-1613.

Jacobs, A. T., and Marnett, L. J. (2010). Systems analysis of protein modification and cellular responses induced by electrophile stress. *Acc. Chem. Res.* **43**, 673-683.

Jones, D. P. (2006). Redefining oxidative stress. *Antioxid. Redox Signal.* **8**, 1865-1879.

Kim, J. H., and Scialli, A. R. (2011). Thalidomide: the tragedy of birth defects and the effective treatment of disease. *Toxicol. Sci.* **122**, 1-6.

Knobloch, J., Jungck, D., and Koch, A. (2011). Apoptosis induction by thalidomide: critical for limb teratogenicity but therapeutic potential in idiopathic pulmonary fibrosis? *Curr. Mol. Pharmacol.* **4**, 26-61.

Knoll, J. (1983). Deprenyl (selegiline): the history of its development and pharmacological action. *Acta Neurol. Scand. Suppl.* **95**, 57-80.

Knoll, J. (1986). The pharmacology of (-)deprenyl. *J Neural Transm. Suppl.* **22**, 75-89.

Kruszewski, M., and Iwanenko, T. (2003). Labile iron pool correlates with iron content in the nucleus and the formation of oxidative DNA damage in mouse lymphoma L5178Y cell lines. *Acta Biochim. Pol.* **50**, 211-215.

Kurose, A., Tanaka, T., Huang, X., Traganos, F., and Darzynkiewicz, Z. (2006). Synchronization in the cell cycle by inhibitors of DNA replication induces histone H2AX phosphorylation: an indication of DNA damage. *Cell Prolif.* **39**, 231-240.

Langston, J. W. (1990). Selegiline as neuroprotective therapy in Parkinson's disease: concepts and controversies. *Neurology* **40**, 61-66.

Larouche, G., and Hales, B. F. (2009). The impact of human superoxide dismutase 1 expression in a mouse model on the embryotoxicity of hydroxyurea. *Birth Defects Res. A Clin. Mol. Teratol.* **85**, 800-807.

Liebelt, E. L., Balk, S. J., Faber, W., Fisher, J. W., Hughes, C. L., Lanzkron, S. M., Lewis, K. M., Marchetti, F., Mehendale, H. M., Rogers, J. M., Shad, A. T., Skalko, R. G., and Stanek, E. J. (2007). NTP-CERHR expert panel report on the reproductive and developmental toxicity of hydroxyurea. *Birth Defects Res. B Dev. Reprod. Toxicol.* **80**, 259-366.

- Lillig, C. H., and Holmgren, A. (2007). Thioredoxin and related molecules--from biology to health and disease. *Antioxid. Redox Signal.* **9**, 25-47.
- Lipton, J. W., Gyawali, S., Borys, E. D., Koprach, J. B., Ptaszny, M., and McGuire, S. O. (2003). Prenatal cocaine administration increases glutathione and alpha-tocopherol oxidation in fetal rat brain. *Brain Res. Dev. Brain Res.* **147**, 77-84.
- Liu, W., Akhand, A. A., Kato, M., Yokoyama, I., Miyata, T., Kurokawa, K., Uchida, K., and Nakashima, I. (1999). 4-hydroxynonenal triggers an epidermal growth factor receptor-linked signal pathway for growth inhibition. *J Cell Sci.* **112**, 2409-2417.
- Lori, F., Kelly, L. M., Foli, A., and Lisziewicz, J. (2004). Safety of hydroxyurea in the treatment of HIV infection. *Expert Opin. Drug Saf.* **3**, 279-288.
- Lu, J., and Holmgren, A. (2012). Thioredoxin system in cell death progression. *Antioxid. Redox Signal.* **17**, 1738-1747.
- Lu, S. C. (2013). Glutathione synthesis. *Biochim. Biophys. Acta* **1830**, 3143-3153.
- Mackler, B., Grace, R., Haynes, B., Bargman, G. J., and Shepard, T. H. (1973). Studies of mitochondrial energy systems during embryogenesis in the rat. *Arch. Biochem. Biophys.* **158**, 662-666.
- Magyar, K. (2011). The pharmacology of selegiline. *Int. Rev. Neurobiol.* **100**, 65-84.
- Magyar, K., Szende, B., Jenei, V., Tabi, T., Palfi, M., and Szoko, E. (2010). R-deprenyl: pharmacological spectrum of its activity. *Neurochem. Res.* **35**, 1922-1932.
- Mao, X. W., Green, L. M., Mekonnen, T., Lindsey, N., and Gridley, D. S. (2010). Gene expression analysis of oxidative stress and apoptosis in proton-irradiated rat retina. *In vivo* **24**, 425-430.

Maruyama, W., Akao, Y., Youdim, M. B., Davis, B. A., and Naoi, M. (2001). Transfection-enforced Bcl-2 overexpression and an anti-Parkinson drug, rasagiline, prevent nuclear accumulation of glyceraldehyde-3-phosphate dehydrogenase induced by an endogenous dopaminergic neurotoxin, N-methyl(R)salsolinol. *J Neurochem.* **78**, 727-735.

Matsui, M., Oshima, M., Oshima, H., Takaku, K., Maruyama, T., Yodoi, J., and Taketo, M. M. (1996). Early embryonic lethality caused by targeted disruption of the mouse thioredoxin gene. *Dev. Biol.* **178**, 179-185.

Matsuzawa, A., and Ichijo, H. (2008). Redox control of cell fate by MAP kinase: physiological roles of ASK1-MAP kinase pathway in stress signaling. *Biochim. Biophys. Acta* **1780**, 1325-1336.

McDermott, G. P., Francis, P. S., Holt, K. J., Scott, K. L., Martin, S. D., Stupka, N., Barnett, N. W., and Conlan, X. A. (2011). Determination of intracellular glutathione and glutathione disulfide using high performance liquid chromatography with acidic potassium permanganate chemiluminescence detection. *Analyst* **136**, 2578-2585.

Meister, A., and Anderson, M. E. (1983). Glutathione. *Ann. Rev. Biochem.* **52**, 711-760.

Moore, K. L. Persaud, T. V. N. (1998). *The Developing Human: Clinically Oriented Embryology* (W. Schmitt, Ed), 6th ed, W.B. Saunders Company, Philadelphia.

Morgan, J. S., Creasey, D. C., and Wright, J. A. (1986). Evidence that the antitumor agent hydroxyurea enters mammalian cells by a diffusion mechanism. *Biochem Biophys. Res. Commun.* **134**, 1254-1259.

Nakajima, H., Amano, W., Kubo, T., Fukuhara, A., Ihara, H., Azuma, Y. T., Tajima, H., Inui, T., Sawa, A., and Takeuchi, T. (2009). Glyceraldehyde-3-phosphate dehydrogenase aggregate formation participates in oxidative stress-induced cell death. *J Biol. Chem.* **284**, 34331-34341.

Narayan, M. (2012). Disulfide bonds: protein folding and subcellular protein trafficking. *FEBS J* **279**, 2272-2282.

Neely, M. D., Sidell, K. R., Graham, D. G., and Montine, T. J. (1999). The lipid peroxidation product 4-hydroxynonenal inhibits neurite outgrowth, disrupts neuronal microtubules, and modifies cellular tubulin. *Journal of neurochemistry* **72**(6), 2323-2333.

Neubert, D. (1970). Aerobic glycolysis in mammalian embryos. In *Metabolic Pathways in Mammalian Embryos during Organogenesis and Its Modifications by Drugs* (R. Bass, F. Beck, H. J. Merker, D. Neubert, and Randhahn, Eds), 1st ed., pp. 225-249. FU-Berlin, Berlin, Germany.

Nicotra, A., Pierucci, F., Parvez, H., and Senatori, O. (2004). Monoamine oxidase expression during development and aging. *Neurotoxicol.* **25**, 155-165.

Ohbayashi, N., Shibayama, M., Kurotaki, Y., Imanishi, M., Fujimori, T., Itoh, N., and Takada, S. (2002). FGF18 is required for normal cell proliferation and differentiation during osteogenesis and chondrogenesis. *Genes Dev.* **16**, 870-879.

Okada, K., Wangpoengtrakul, C., Osawa, T., Toyokuni, S., Tanaka, K., and Uchida, K. (1999). 4-Hydroxy-2-nonenal-mediated impairment of intracellular proteolysis during oxidative stress. Identification of proteasomes as target molecules. *J Biol. Chem.* **274**, 23787-23793.

Olanow, C. W. (2006). Rationale for considering that propargylamines might be neuroprotective in Parkinson's disease. *Neurology* **66**, S69-79.

Ornoy, A. (2007). Embryonic oxidative stress as a mechanism of teratogenesis with special emphasis on diabetic embryopathy. *Reprod. Toxicol.* **24**, 31-41.

Ou, X. M., Stockmeier, C. A., Meltzer, H. Y., Overholser, J. C., Jurjus, G. J., Dieter, L., Chen, K., Lu, D., Johnson, C., Youdim, M. B., Austin, M. C., Luo, J., Sawa, A., May, W., and Shih, J.

C. (2010). A novel role for glyceraldehyde-3-phosphate dehydrogenase and monoamine oxidase B cascade in ethanol-induced cellular damage. *Biol. Psychiatry* **67**, 855-863.

Ozeki, M., Miyagawa-Hayashino, A., Akatsuka, S., Shirase, T., Lee, W. H., Uchida, K., and Toyokuni, S. (2005). Susceptibility of actin to modification by 4-hydroxy-2-nonenal. *J Chromatogr. B Analyt. Technol. Biomed. Life Sci.* **827**, 119-126.

Ozolins, T. R., and Hales, B. F. (1997). Oxidative stress regulates the expression and activity of transcription factor activator protein-1 in rat conceptus. *J Pharmacol. Exp. Ther.* **280**, 1085-1093.

Ozolins, T. R., and Hales, B. F. (1999). Tissue-specific regulation of glutathione homeostasis and the activator protein-1 (AP-1) response in the rat conceptus. *Biochem. Pharmacol.* **57**, 1165-1175.

Paniagua-Castro, N., Escalona-Cardoso, G., Madrigal-Bujaidar, E., Martinez-Galero, E., and Chamorro-Cevallos, G. (2008). Protection against cadmium-induced teratogenicity in vitro by glycine. *Toxicol. In Vitro* **22**, 75-79.

Petersen, D. R., and Doorn, J. A. (2004). Reactions of 4-hydroxynonenal with proteins and cellular targets. *Free Radical Biol. Med.* **37**, 937-945.

Poli, G., and Schaur, R. J. (2000). 4-Hydroxynonenal in the pathomechanisms of oxidative stress. *IUBMB Life* **50**, 315-321.

Rancourt, D. E., Tsuzuki, T., and Capecchi, M. R. (1995). Genetic interaction between *hoxb-5* and *hoxb-6* is revealed by nonallelic noncomplementation. *Genes Dev* **9**(1), 108-22.

Robkin, M. A. (1997). Carbon monoxide and the embryo. *Int. J Dev. Biol.* **41**, 283-289.

Rodriguez, G. I., Kuhn, J. G., Weiss, G. R., Hilsenbeck, S. G., Eckardt, J. R., Thurman, A., Rinaldi, D. A., Hodges, S., Von Hoff, D. D., and Rowinsky, E. K. (1998). A bioavailability and pharmacokinetic study of oral and intravenous hydroxyurea. *Blood* **91**, 1533-1541.

Saha, D. T., A (2011). Xenobiotics, oxidative stress, free radicals vs. antioxidants: dance of death to heaven's life. *Asian J. Res. Pharm. Sci.* **1**, 36-38.

Saitoh, M., Nishitoh, H., Fujii, M., Takeda, K., Tobiume, K., Sawada, Y., Kawabata, M., Miyazono, K., and Ichijo, H. (1998). Mammalian thioredoxin is a direct inhibitor of apoptosis signal-regulating kinase (ASK) 1. *EMBO J* **17**, 2596-2606.

Schafer, F. Q., and Buettner, G. R. (2001). Redox environment of the cell as viewed through the redox state of the glutathione disulfide/glutathione couple. *Free Radical Biol. Med.* **30**, 1191-1212.

Schaur, R. J. (2003). Basic aspects of the biochemical reactivity of 4-hydroxynonenal. *Mol. Aspects Med.* **24**, 149-159.

Schlisser, A. E., and Hales, B. F. (2013). Deprenyl enhances the teratogenicity of hydroxyurea in organogenesis stage mouse embryos. *Toxicol. Sci.* **134**, 391-399.

Schneider, C., Boeglin, W. E., Yin, H., Ste, D. F., Hachey, D.L., Porter, N.A., Brash, A. R. (2005). Synthesis of dihydroperoxides of linoleic and linolenic acids and studies on their transformation to 4-hydroperoxynonenal. *Lipids.* **40**:1155-1162.

Schutt, F., Bergmann, M., Holz, F. G., and Kopitz, J. (2003). Proteins modified by malondialdehyde, 4-hydroxynonenal, or advanced glycation end products in lipofuscin of human retinal pigment epithelium. *Invest. Ophthalmol. Vis. Sci.* **44**, 3663-3668.

Seidler, N. W. (2013). GAPDH: Biological properties and diversity. 1st ed. Springer Science+Business Media Dordrecht.

Sen, N., Hara, M. R., Ahmad, A. S., Cascio, M. B., Kamiya, A., Ehmsen, J. T., Agrawal, N., Hester, L., Dore, S., Snyder, S. H., and Sawa, A. (2009). GOSPEL: a neuroprotective protein that binds to GAPDH upon S-nitrosylation. *Neuron* **63**, 81-91.

Sen, N., Hara, M. R., Kornberg, M. D., Cascio, M. B., Bae, B. I., Shahani, N., Thomas, B., Dawson, T. M., Dawson, V. L., Snyder, S. H., and Sawa, A. (2008). Nitric oxide-induced nuclear GAPDH activates p300/CBP and mediates apoptosis. *Nature Cell Biol.* **10**, 866-873.

Shashidharan, P., Chalmers-Redman, R. M., Carlile, G. W., Rodic, V., Gurvich, N., Yuen, T., Tatton, W. G., and Sealfon, S. C. (1999). Nuclear translocation of GAPDH-GFP fusion protein during apoptosis. *Neuroreport* **10**, 1149-1153.

Shen, W., Brown, N. S., Finn, P. F., Dice, J. F., and Franch, H. A. (2006). Akt and Mammalian target of rapamycin regulate separate systems of proteolysis in renal tubular cells. *J Am. Soc. Nephrol.* **17**, 2414-2423.

Shepard, T. H., Muffley, L. A., and Smith, L. T. (1998). Ultrastructural study of mitochondria and their cristae in embryonic rats and primate (*N. nemestrina*). *Anat. Rec.* **252**, 383-392.

Sies, H. (1993). Strategies of antioxidant defense. *Eur. J Biochem.* **215**, 213-219.

Sies, H., and Cadenas, E. (1985). Oxidative stress: damage to intact cells and organs. *Philos. Trans. R. Soc. Lond. B Biol. Sci.* **311**(1152), 617-631.

Soukri, A., Mougin, A., Corbier, C., Wonacott, A., Branlant, C., and Branlant, G. (1989). Role of the histidine 176 residue in glyceraldehyde-3-phosphate dehydrogenase as probed by site-directed mutagenesis. *Biochem.* **28**, 2586-2592.

Spivak, J. L., and Hasselbalch, H. (2011). Hydroxycarbamide: a user's guide for chronic myeloproliferative disorders. *Expert Rev. Anticancer Ther.* **11**, 403-414.

Srivastava, S., Chandra, A., Wang, L. F., Seifert, W. E., Jr., DaGue, B. B., Ansari, N. H., Srivastava, S. K., and Bhatnagar, A. (1998). Metabolism of the lipid peroxidation product, 4-hydroxy-trans-2-nonenal, in isolated perfused rat heart. *J Biol. Chem.* **273**, 10893-10900.

Tarze, A., Deniaud, A., Le Bras, M., Maillier, E., Molle, D., Larochette, N., Zamzami, N., Jan, G., Kroemer, G., and Brenner, C. (2007). GAPDH, a novel regulator of the pro-apoptotic mitochondrial membrane permeabilization. *Oncogene* **26**, 2606-2620.

Tatton, W., Chalmers-Redman, R., and Tatton, N. (2003). Neuroprotection by deprenyl and other propargylamines: glyceraldehyde-3-phosphate dehydrogenase rather than monoamine oxidase B. *J Neural Trans.* **110**, 509-515.

Tatton, W. G., Chalmers-Redman, R. M., Elstner, M., Leesch, W., Jagodzinski, F. B., Stupak, D. P., Sugrue, M. M., and Tatton, N. A. (2000). Glyceraldehyde-3-phosphate dehydrogenase in neurodegeneration and apoptosis signaling. *J Neural Trans. Suppl.* (60), 77-100.

Thauvin-Robinet, C., Maingueneau, C., Robert, E., Elefant, E., Guy, H., Caillot, D., Casasnovas, R. O., Douvier, S., and Nivelon-Chevallier, A. (2001). Exposure to hydroxyurea during pregnancy: a case series. *Leukemia* **15**, 1309-1311.

Therapontos, C., Erskine, L., Gardner, E. R., Figg, W. D., and Vargesson, N. (2009). Thalidomide induces limb defects by preventing angiogenic outgrowth during early limb formation. *Proc. Natl. Acad. Sci. U.S.A.* **106**, 8573-8578.

Thompson, S. A., White, C. C., Krejsa, C. M., Eaton, D. L., and Kavanagh, T. J. (2000). Modulation of glutathione and glutamate-L-cysteine ligase by methylmercury during mouse development. *Toxicol. Sci.* **57**, 141-146.

Tipton, K. F., Boyce, S., O'Sullivan, J., Davey, G. P., and Healy, J. (2004). Monoamine oxidases: certainties and uncertainties. *Curr. Med. Chem.* **11**, 1965-1982.

Tisdale, E. J. (2001). Glyceraldehyde-3-phosphate dehydrogenase is required for vesicular transport in the early secretory pathway. *J Biol. Chem.* **276**, 2480-2486.

Tung, E. W., and Winn, L. M. (2011). Valproic acid increases formation of reactive oxygen species and induces apoptosis in postimplantation embryos: a role for oxidative stress in valproic acid-induced neural tube defects. *Mol. Pharmacol.* **80**, 979-987.

Uchida, K. (2003). 4-Hydroxy-2-nonenal: a product and mediator of oxidative stress. *Prog. Lipid Res.* **42**:318-343.

Uchida, K., and Stadtman, E. R. (1993). Covalent attachment of 4-hydroxynonenal to glyceraldehyde-3-phosphate dehydrogenase. A possible involvement of intra- and intermolecular cross-linking reaction. *J Biol. Chem.* **268**, 6388-6393.

Uchida, K., and Stadtman, E. R. (1992). Modification of histidine residues in proteins by reaction with 4-hydroxynonenal. *Proc. Natl. Acad. Sci. U.S.A.* **89**, 4544-4548.

Uchida, K., and Stadtman, E. R. (2000). Quantitation of 4-hydroxynonenal protein adducts. *Methods Mol. Biol.* **99**, 25-34.

Ufer, C., and Wang, C. C. (2011). The Roles of Glutathione Peroxidases during Embryo Development. *Front. Mol. Neurosci.* **4**, 12.

Vogel, W., Schempp, W., and Sigwarth, I. (1978). Comparison of thymidine, fluorodeoxyuridine, hydroxyurea, and methotrexate blocking at the G1/S phase transition of the cell cycle, studied by replication patterns. *Hum. Genet.* **45**, 193-198.

Wang, Z. Q., Stingl, L., Morrison, C., Jantsch, M., Los, M., Schulze-Osthoff, K., and Wagner, E. F. (1997). PARP is important for genomic stability but dispensable in apoptosis. *Genes Dev.* **11**, 2347-2358.

Ward, I. M., and Chen, J. (2001). Histone H2AX is phosphorylated in an ATR-dependent manner in response to replicational stress. *J Biol. Chem.* **276**, 47759-47762.

Ware, R. E., Despotovic, J. M., Mortier, N. A., Flanagan, J. M., He, J., Smeltzer, M. P., Kimble, A. C., Aygun, B., Wu, S., Howard, T., and Sparreboom, A. (2011). Pharmacokinetics, pharmacodynamics, and pharmacogenetics of hydroxyurea treatment for children with sickle cell anemia. *Blood* **118**, 4985-4991.

Watson, W. H., and Jones, D. P. (2003). Oxidation of nuclear thioredoxin during oxidative stress. *FEBS Lett* **543**, 144-147.

Webster, W. S., and Abela, D. (2007). The effect of hypoxia in development. *Birth Defects Res. C Embryo Today* **81**, 215-228.

Wilson, J. G., Scott, W. J., Ritter, E. J., and Fradkin, R. (1975). Comparative distribution and embryotoxicity of hydroxyurea in pregnant rats and rhesus monkeys. *Teratology* **11**, 169-178.

Wong, M., and Wells, P. G. (1988). Effects of N-acetylcysteine on fetal development and on phenytoin teratogenicity in mice. *Teratog. Carcinog. Mutag.* **8**, 65-79.

Woo, G. H., Katayama, K., Jung, J. Y., Uetsuka, K., Bak, E. J., Nakayama, H., and Doi, K. (2003). Hydroxyurea (HU)-induced apoptosis in the mouse fetal tissues. *Histol. Histopathol.* **18**, 387-392.

Yan, J., and Hales, B. F. (2005). Activator protein-1 (AP-1) DNA binding activity is induced by hydroxyurea in organogenesis stage mouse embryos. *Toxicol. Sci.* **85**, 1013-1023.

Yan, J., and Hales, B. F. (2006). Depletion of glutathione induces 4-hydroxynonenal protein adducts and hydroxyurea teratogenicity in the organogenesis stage mouse embryo. *J Pharmacol. Exp. Ther.* **319**, 613-621.

Yan, J., and Hales, B. F. (2008). p38 and c-Jun N-terminal kinase mitogen-activated protein kinase signaling pathways play distinct roles in the response of organogenesis-stage embryos to a teratogen. *J Pharmacol Exp. Ther.* **326**, 764-772.

Yang, H., Magilnick, N., Lee, C., Kalmaz, D., Ou, X., Chan, J. Y., and Lu, S. C. (2005). Nrf1 and Nrf2 regulate rat glutamate-cysteine ligase catalytic subunit transcription indirectly via NF-kappaB and AP-1. *Mol. Cell. Biol.* **25**, 5933-5946.

Youdim, M. B., Amit, T., Bar-Am, O., Weinreb, O., and Yogev-Falach, M. (2006). Implications of co-morbidity for etiology and treatment of neurodegenerative diseases with multifunctional neuroprotective-neurorescue drugs; lisdostigil. *Neurotox. Res.* **10**, 181-192.

Yu, M. K., Moos, P. J., Cassidy, P., Wade, M., and Fitzpatrick, F. A. (2004). Conditional expression of 15-lipoxygenase-1 inhibits the selenoenzyme thioredoxin reductase: modulation of selenoproteins by lipoxygenase enzymes. *J Biol. Chem.* **279**, 28028-28035.

Zhang, H., Du, Y., Zhang, X., Lu, J., and Holmgren, A. (2013). Glutaredoxin2 Reduces both Thioredoxin2 and Thioredoxin1 and Protects Cells from Apoptosis Induced by Auranofin and 4-Hydroxynonenal. *Antioxid Redox Signal.* [Epub ahead of print]. PMID: 24295294.